



TIM LINDEN

● **THE RISE OF THE LEPTONS**
PULSAR EMISSION DOMINATES THE TEV GAMMA-RAY SKY

Physics and Astronomy Colloquium
University of Utah
November 30, 2018



THE OHIO STATE UNIVERSITY
CENTER FOR COSMOLOGY AND
ASTROPARTICLE PHYSICS

TEV HALOS



Moon (To Scale)

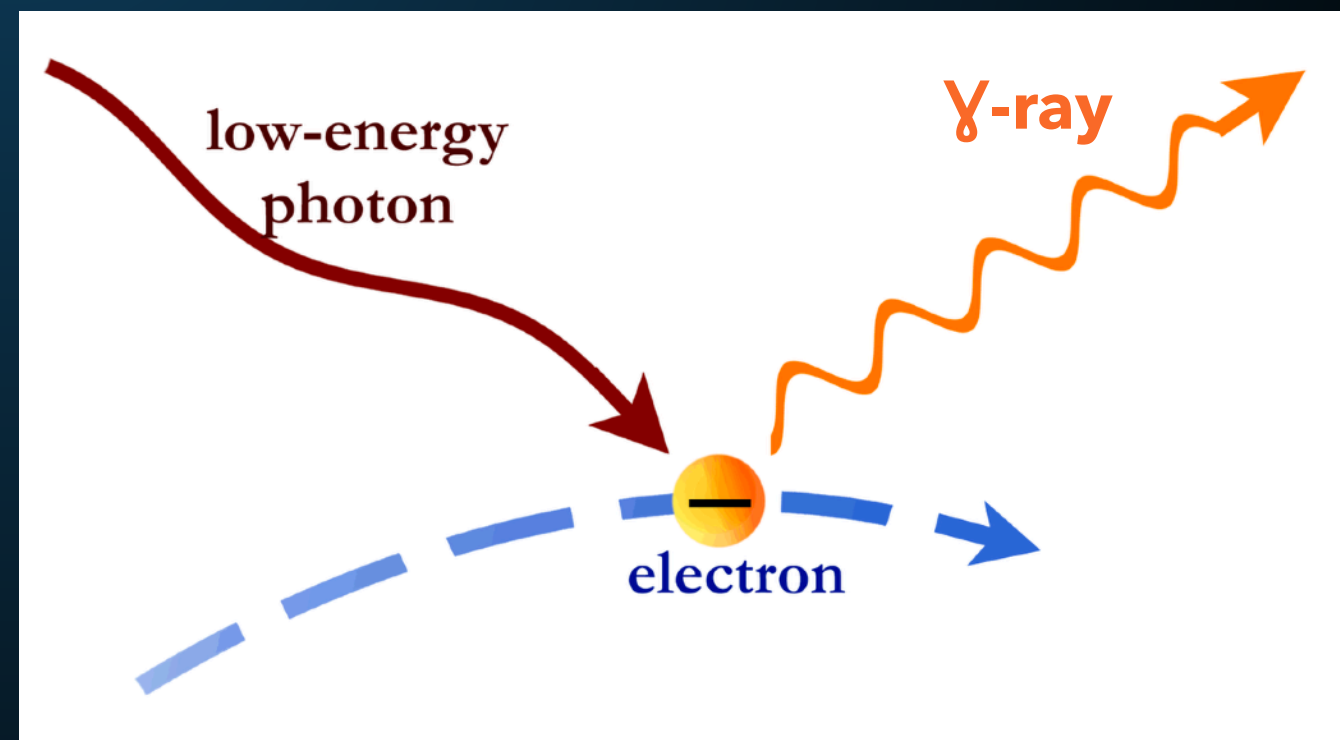
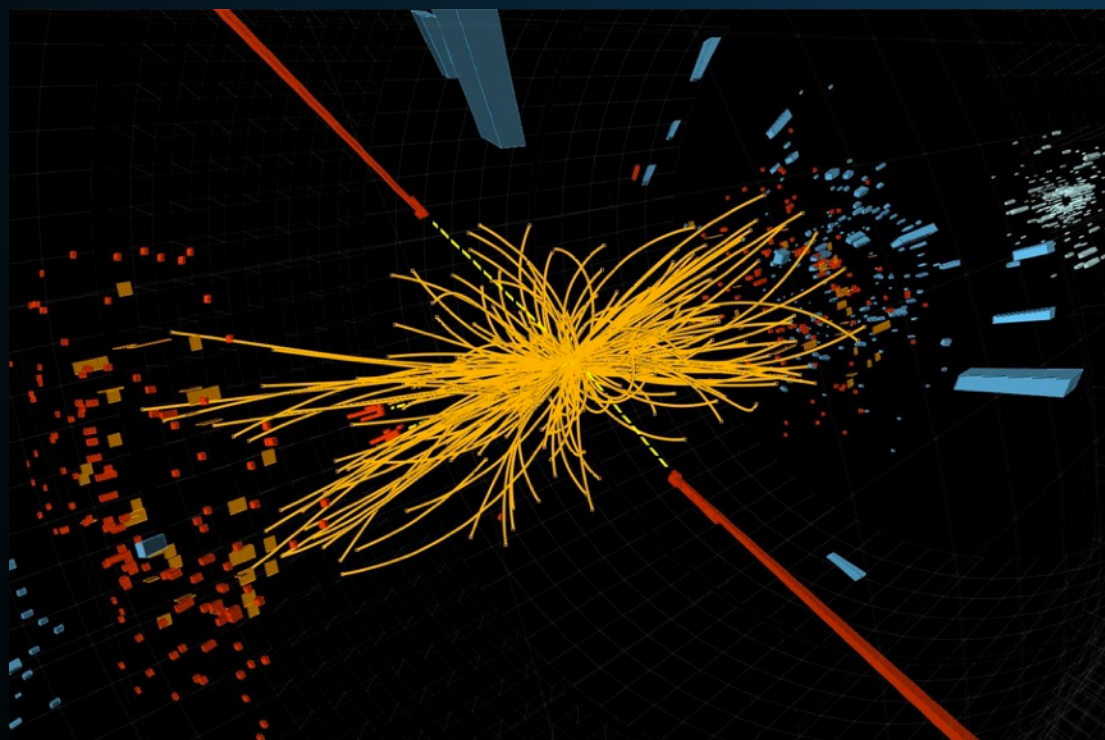
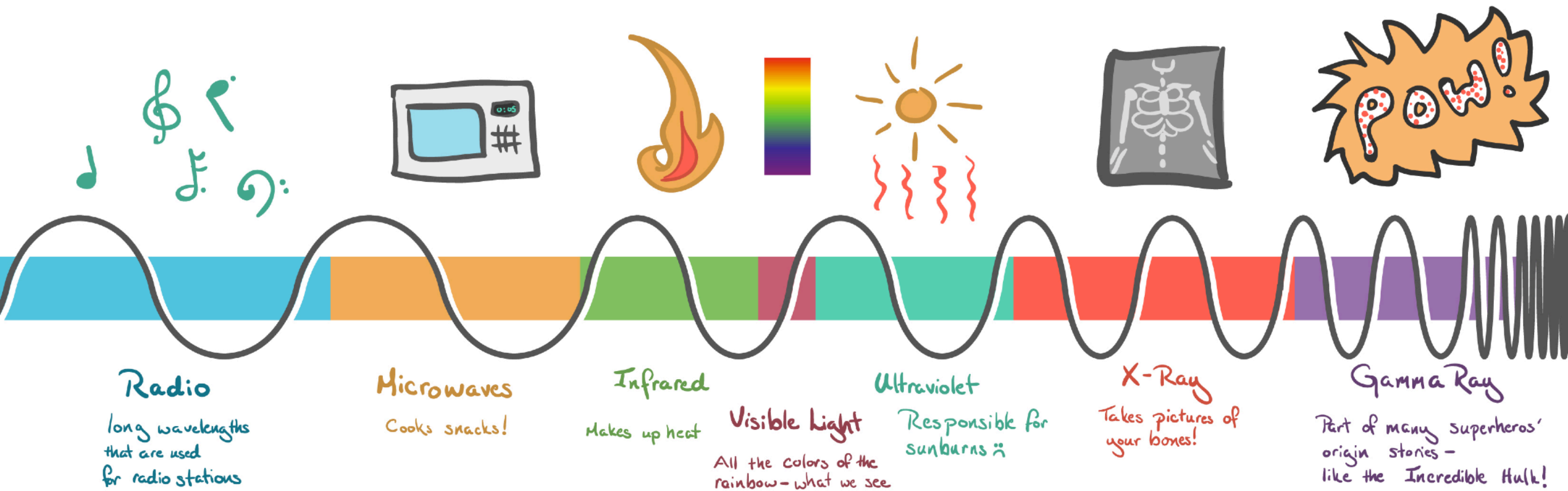
• Angular Resolution

—— 10 pc (Geminga distance)

Geminga

PSR B0656+14
(Monogem)

The Electromagnetic Spectrum









TEV HALOS



Moon (To Scale)

• Angular Resolution

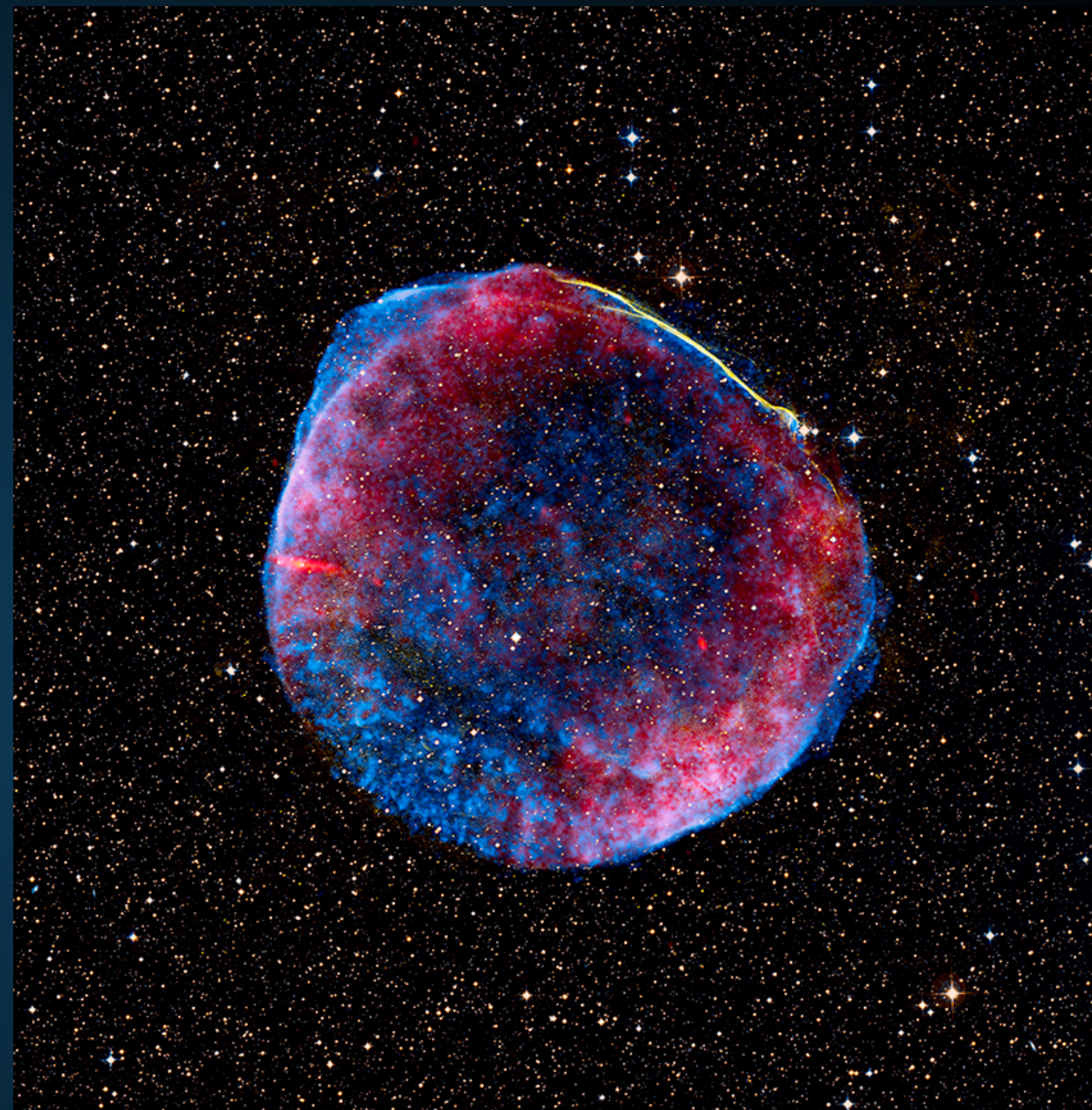
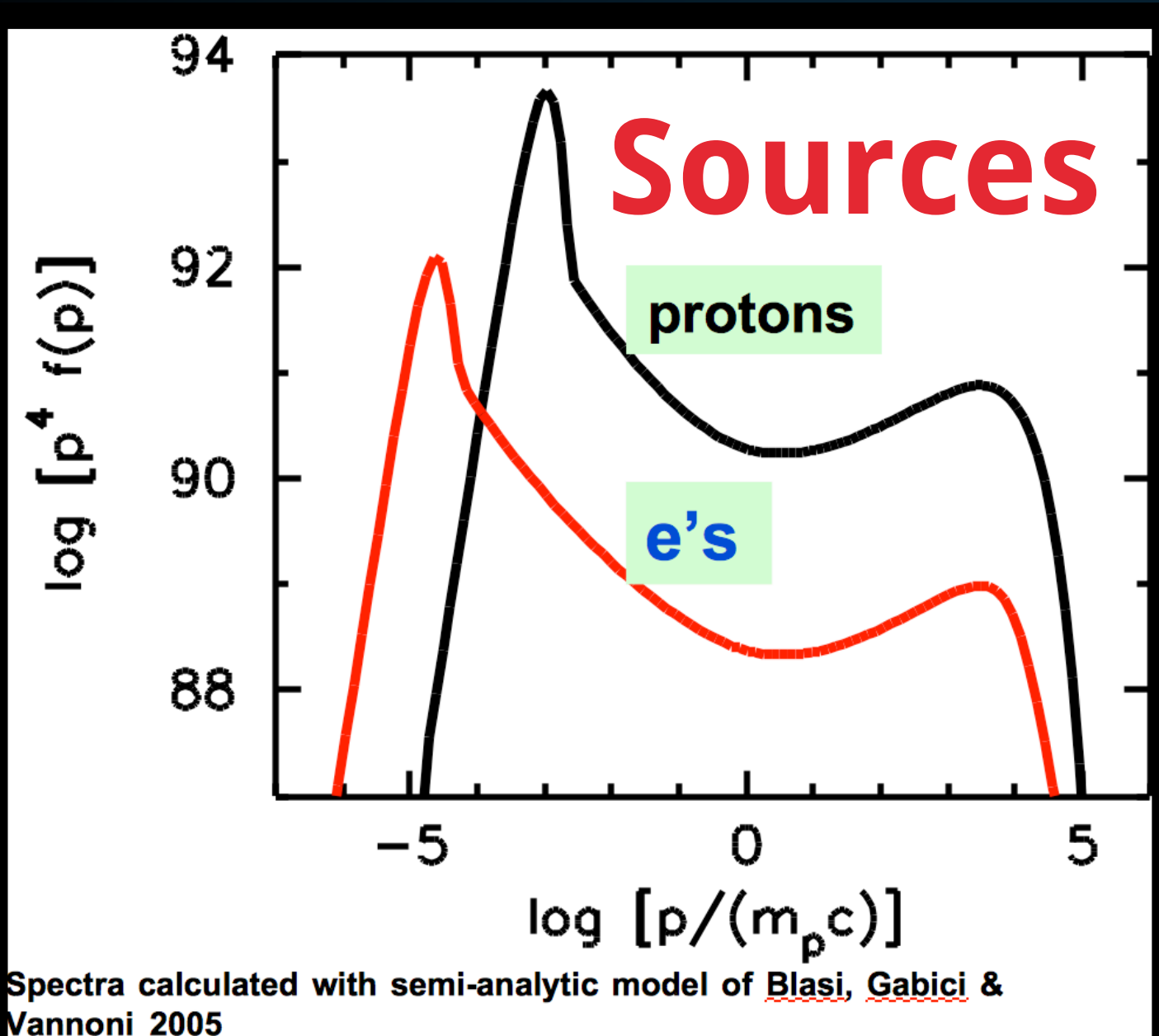
—— 10 pc (Geminga distance)

Geminga

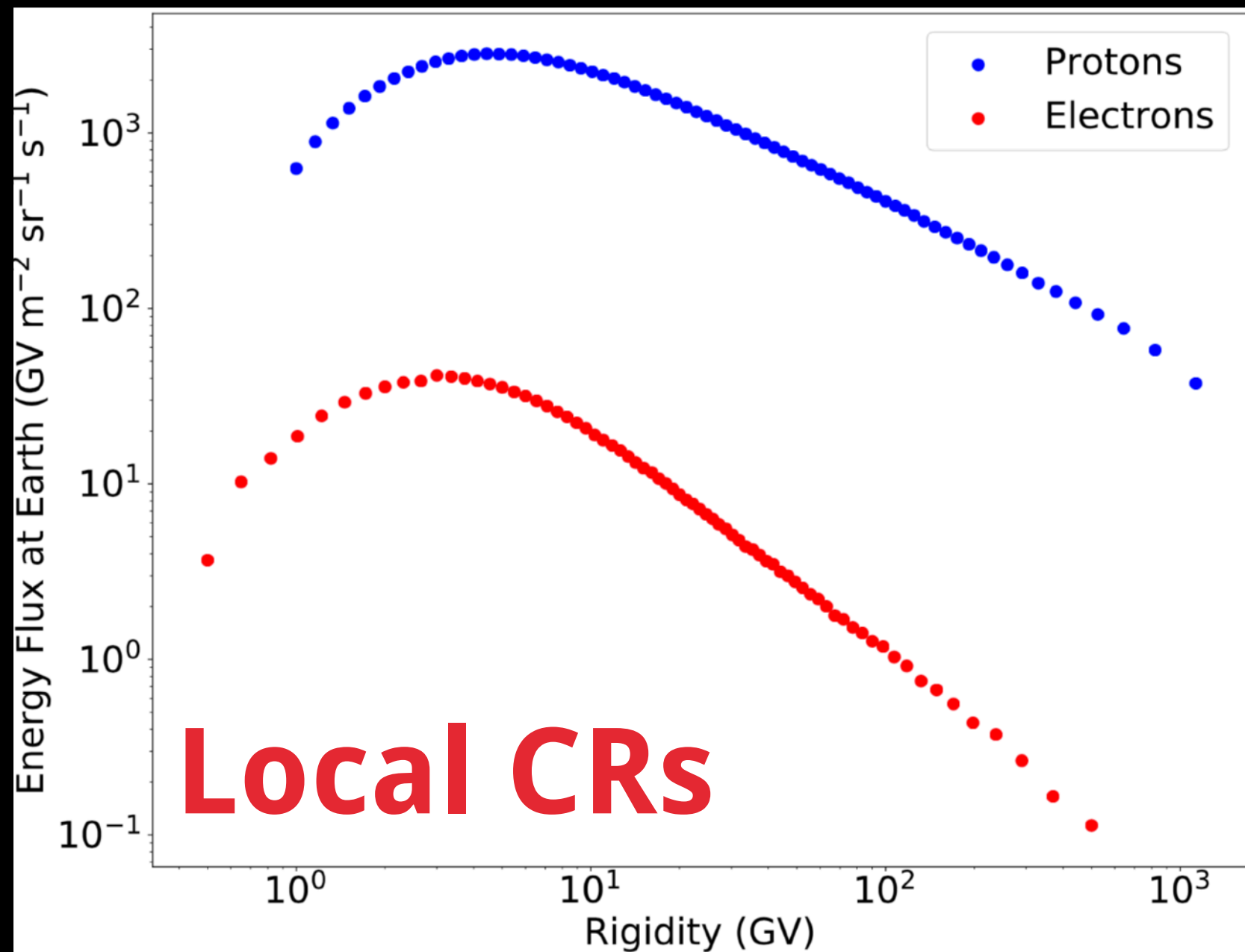
PSR B0656+14
(Monogem)

The Hadronic Fairy Tale

A UNIVERSE DOMINATED BY PROTONS



A UNIVERSE DOMINATED BY PROTONS

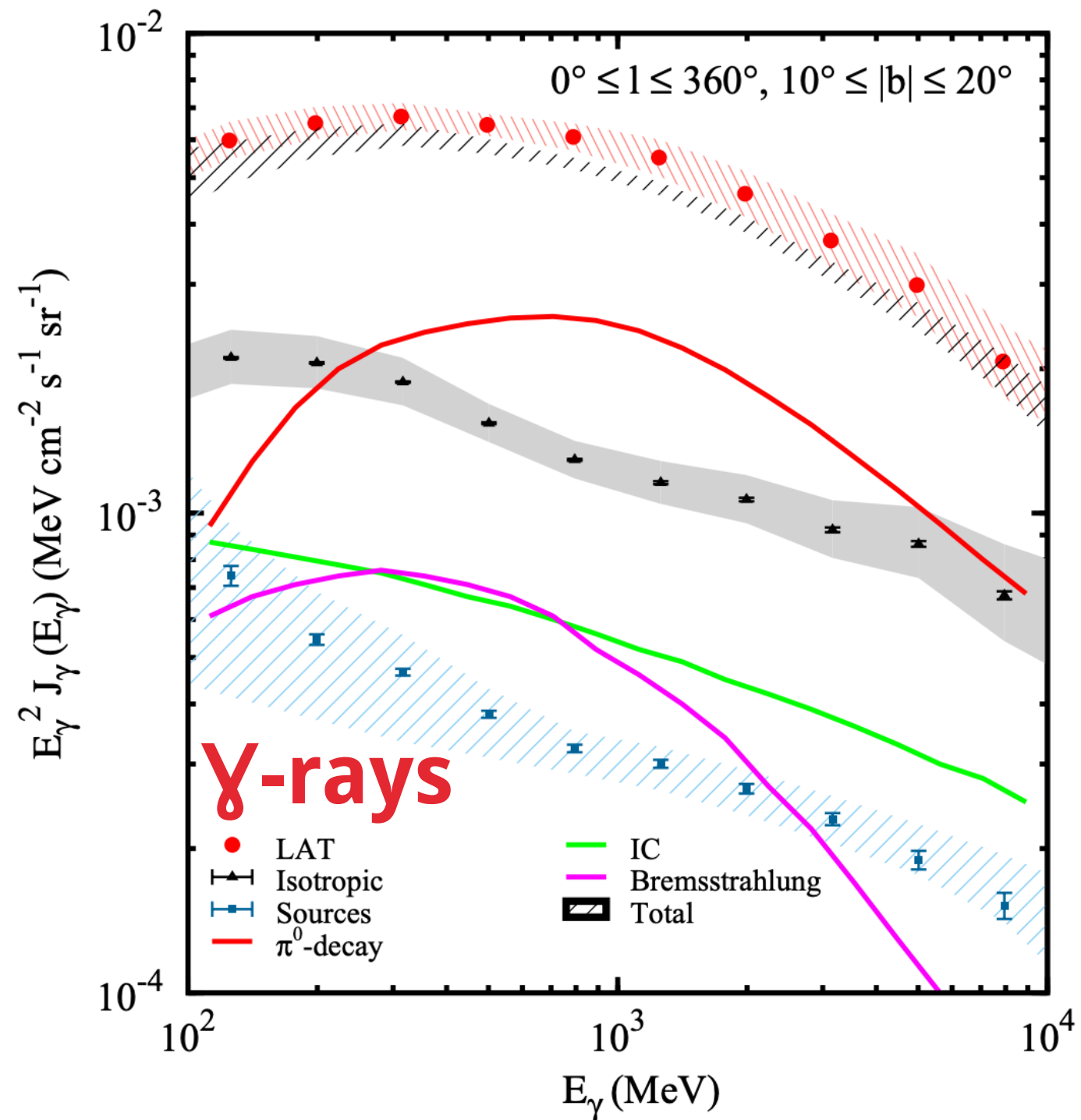


Spectra calculated
Vannoni 2005



A UNIVERSE DOMINATED BY PROTONS

Sources



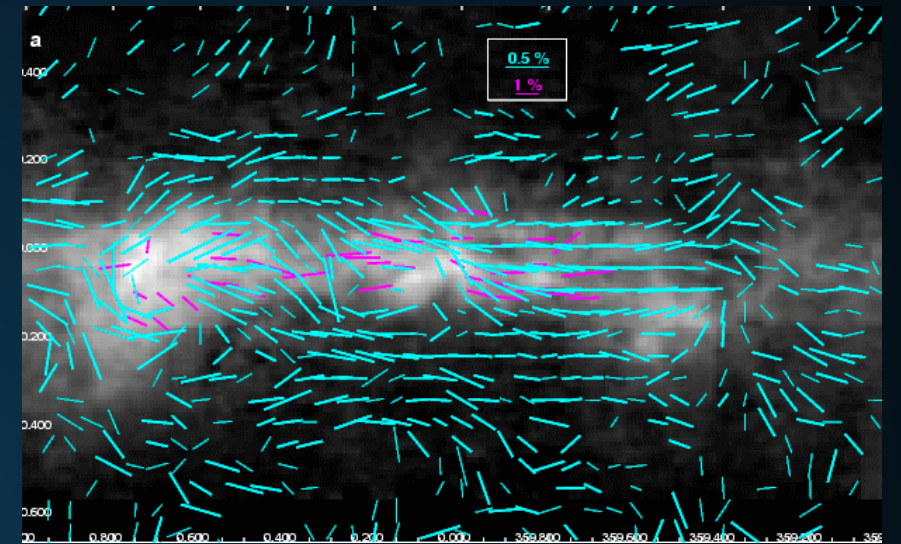
Spectra calculated with semi-analytic model
Vannoni 2005

COSMIC-RAY ACCELERATION AND PROPAGATION



Start with a source of relativistic cosmic-rays

cosmic rays propagate



$$\frac{\partial \psi}{\partial t} = q(\vec{r}, p) + \vec{\nabla} \cdot (D_{xx} \vec{\nabla} \psi - \vec{V} \psi) + \frac{\partial}{\partial p} p^2 D_{pp} \frac{\partial}{\partial p} \frac{1}{p^2} \psi - \frac{\partial}{\partial p} \left[p \psi - \frac{p}{3} (\vec{\nabla} \cdot \vec{V}) \psi \right] - \frac{1}{\tau_f} \psi - \frac{1}{\tau_r} \psi$$

Solved Numerically:
e.g. Galprop

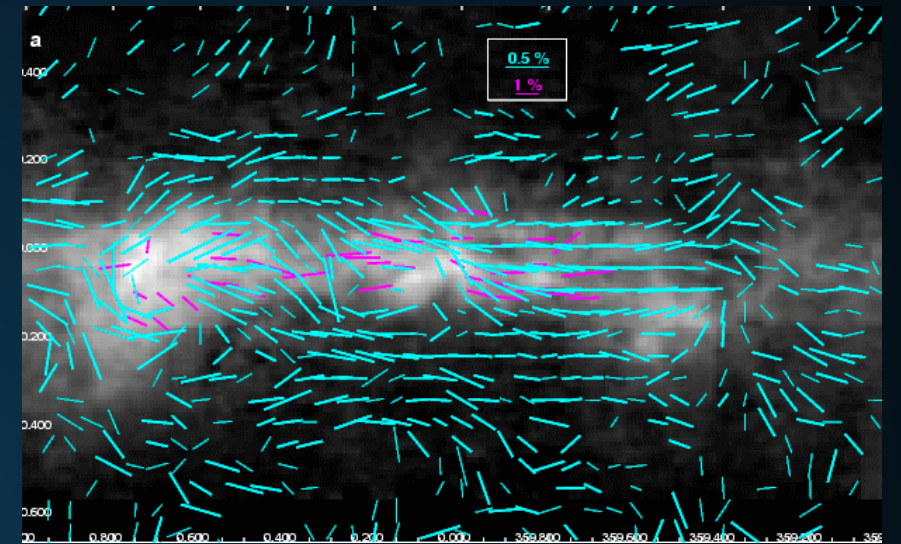
- If they propagate to Earth, can be detected:
 - AMS-02/PAMELA
 - CREAM/HEAT/CAPRICE

COSMIC-RAY ACCELERATION AND PROPAGATION



Start with a source of relativistic cosmic-rays

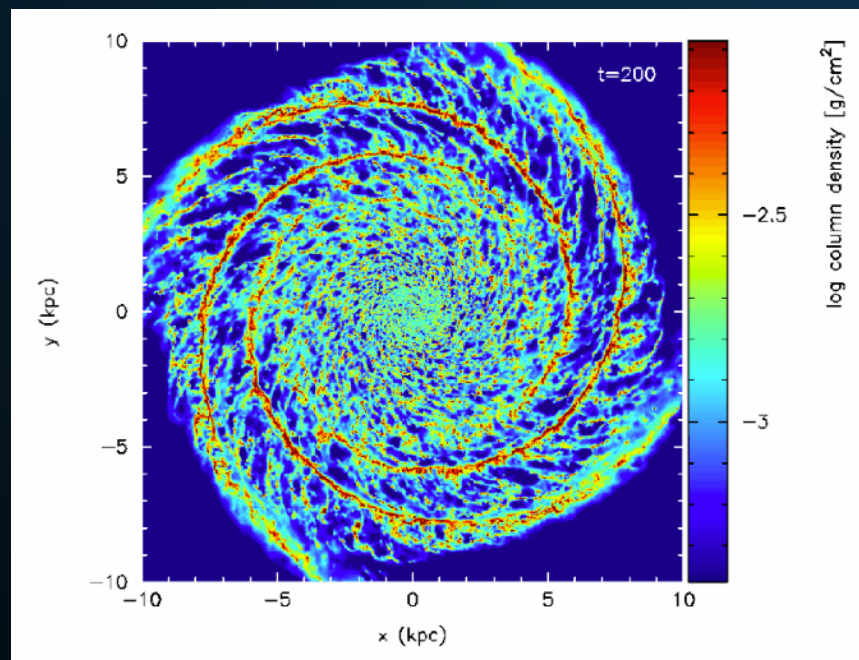
cosmic rays propagate



$$\frac{\partial \psi}{\partial t} = q(\vec{r}, p) + \vec{\nabla} \cdot (D_{xx} \vec{\nabla} \psi - \vec{V} \psi) + \frac{\partial}{\partial p} p^2 D_{pp} \frac{\partial}{\partial p} \frac{1}{p^2} \psi - \frac{\partial}{\partial p} \left[p \psi - \frac{p}{3} (\vec{\nabla} \cdot \vec{V}) \psi \right] - \frac{1}{\tau_f} \psi - \frac{1}{\tau_r} \psi$$

Solved Numerically:
e.g. Galprop

Gas/ISRF



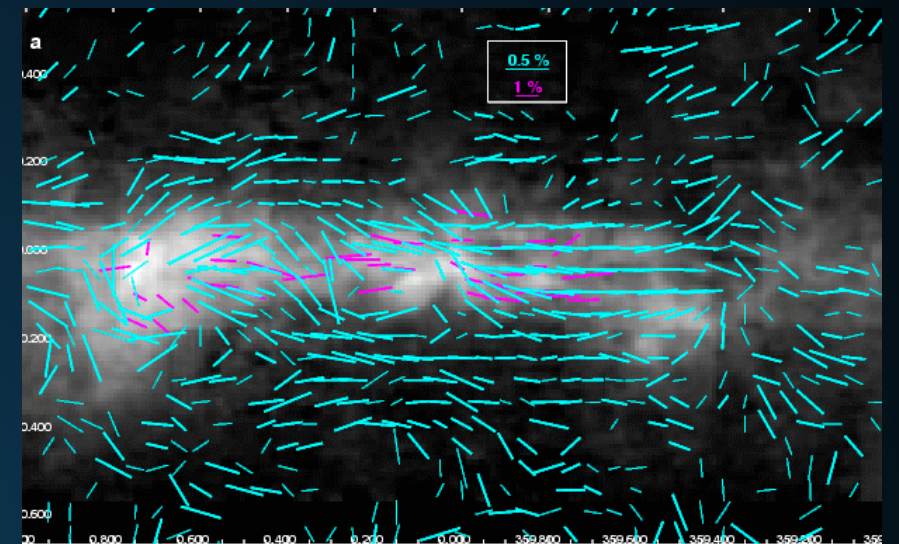
- Alternatively can collide with Galactic gas or the interstellar radiation field.

COSMIC-RAY ACCELERATION AND PROPAGATION



Start with a source of relativistic cosmic-rays

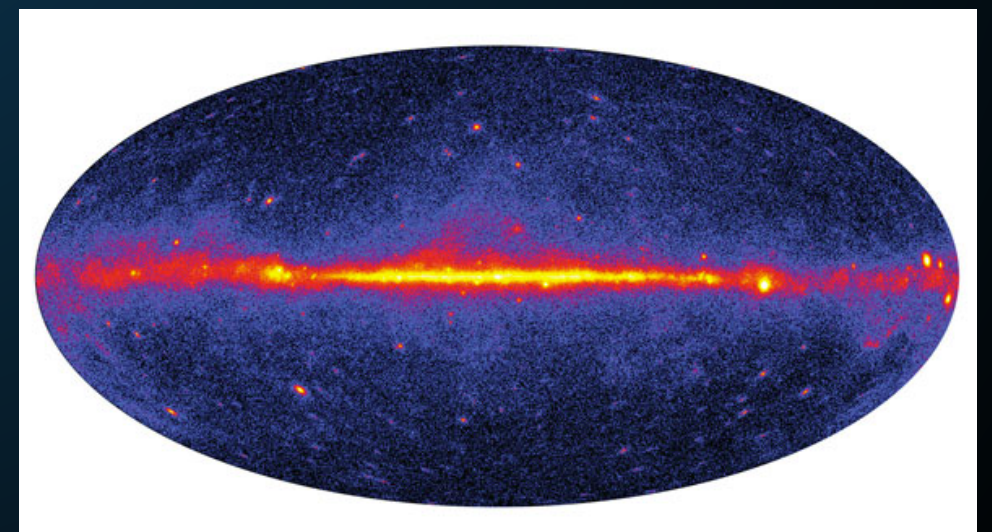
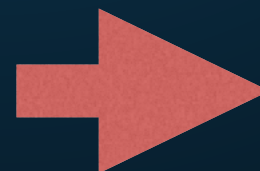
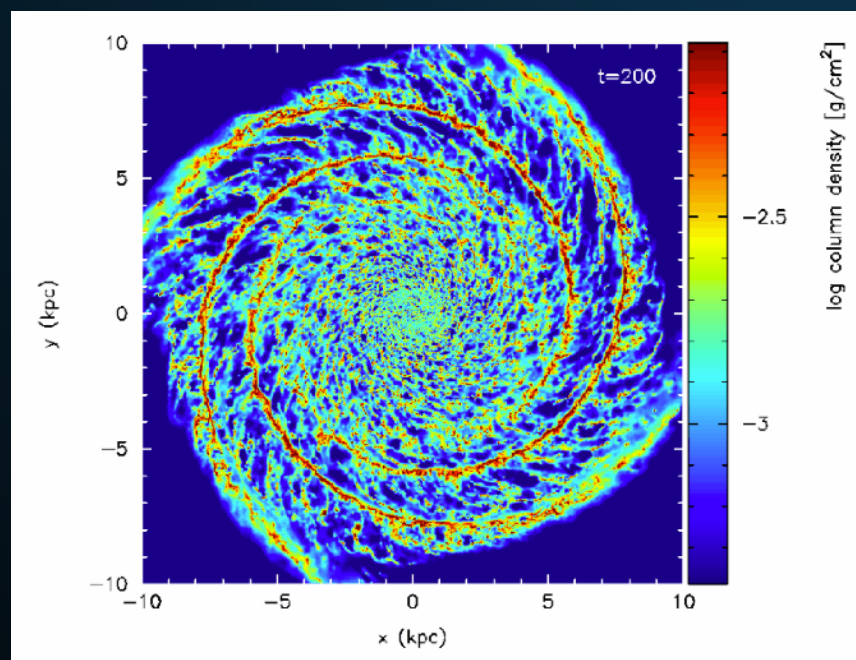
cosmic rays propagate



$$\frac{\partial \psi}{\partial t} = q(\vec{r}, p) + \vec{\nabla} \cdot (D_{xx} \vec{\nabla} \psi - \vec{V} \psi) + \frac{\partial}{\partial p} p^2 D_{pp} \frac{\partial}{\partial p} \frac{1}{p^2} \psi - \frac{\partial}{\partial p} \left[p \psi - \frac{p}{3} (\vec{\nabla} \cdot \vec{V}) \psi \right] - \frac{1}{\tau_f} \psi - \frac{1}{\tau_r} \psi$$

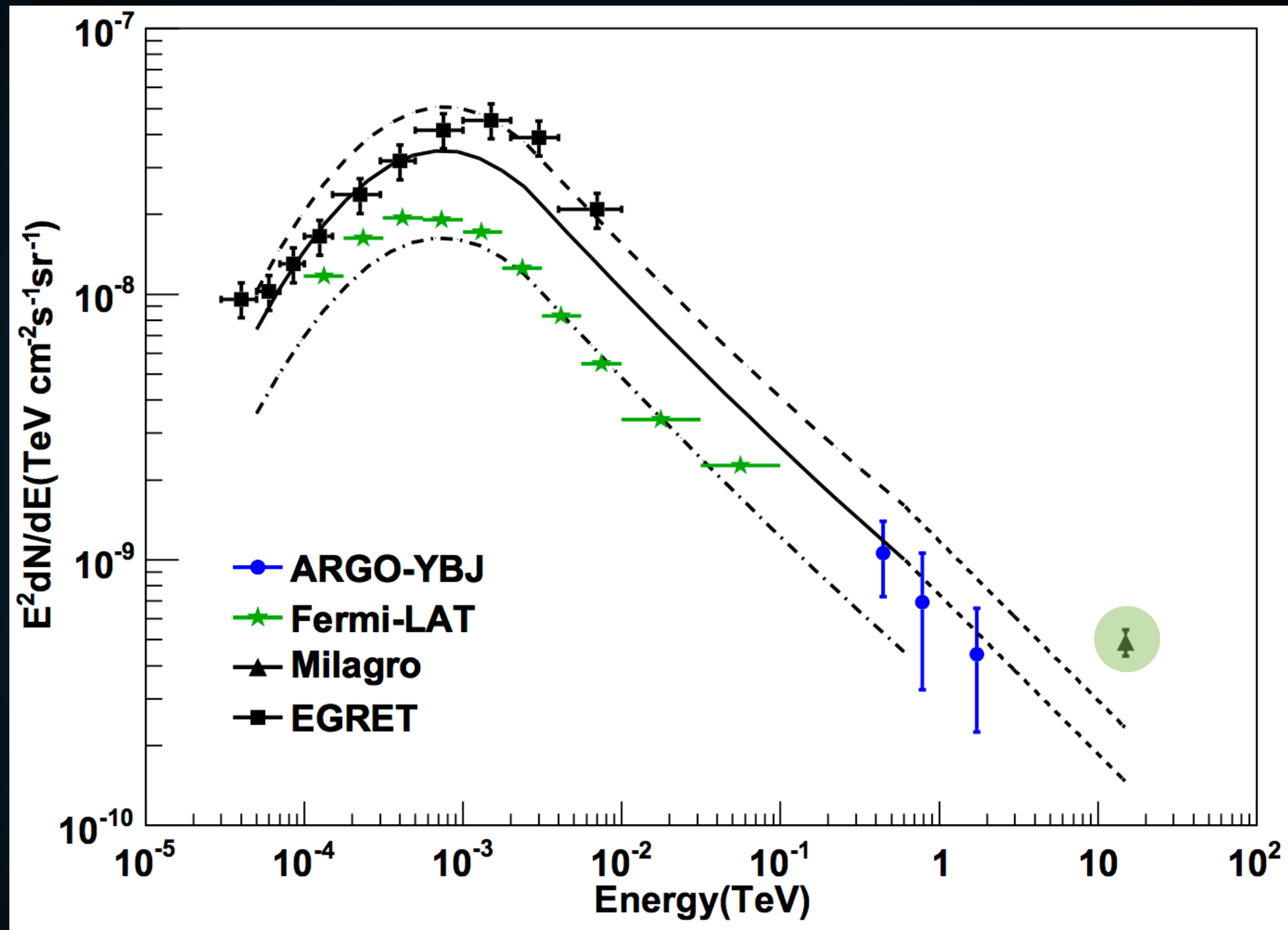
Solved Numerically:
e.g. Galprop

Gas/ISRF



Cracks in the story...

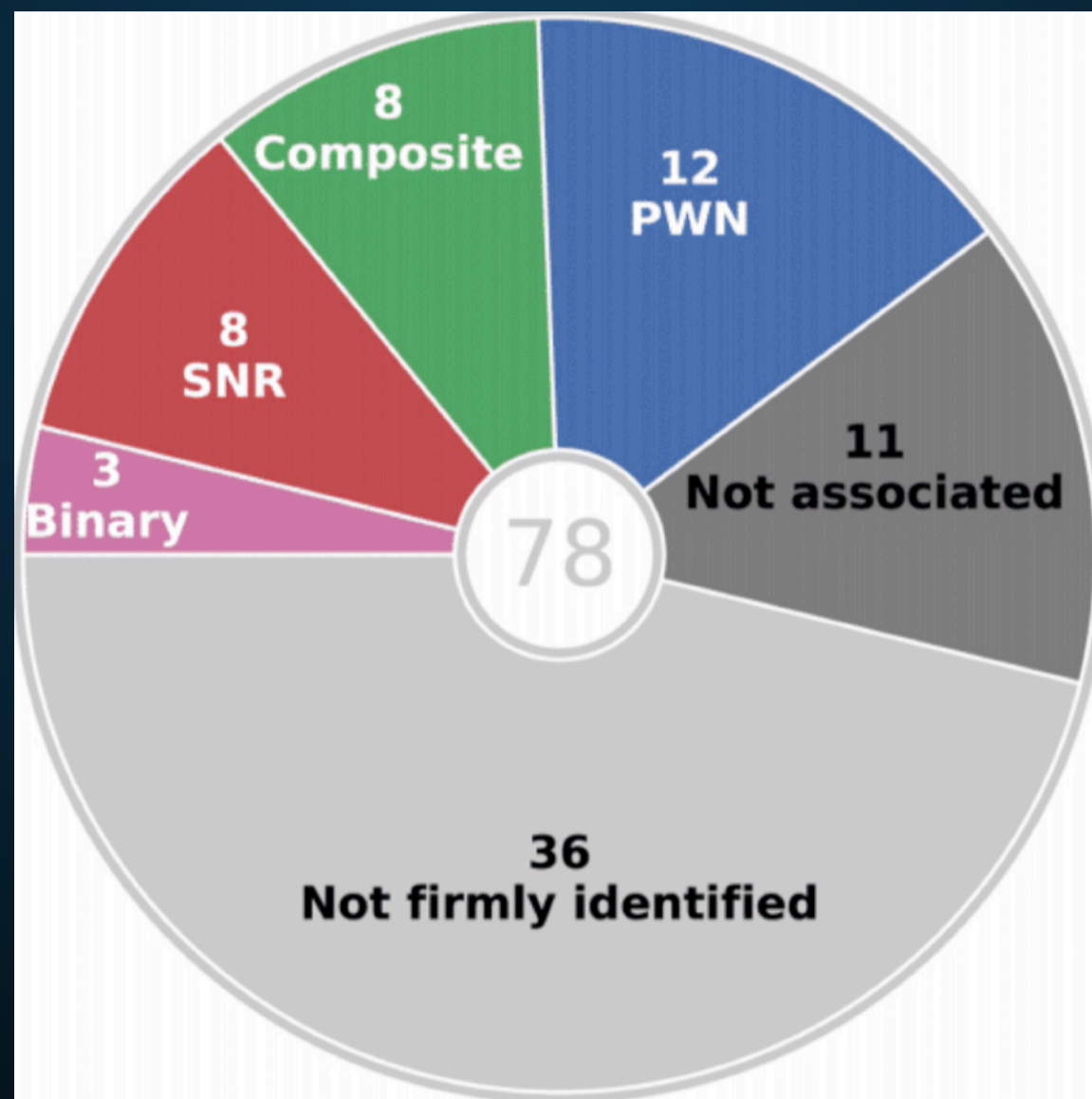
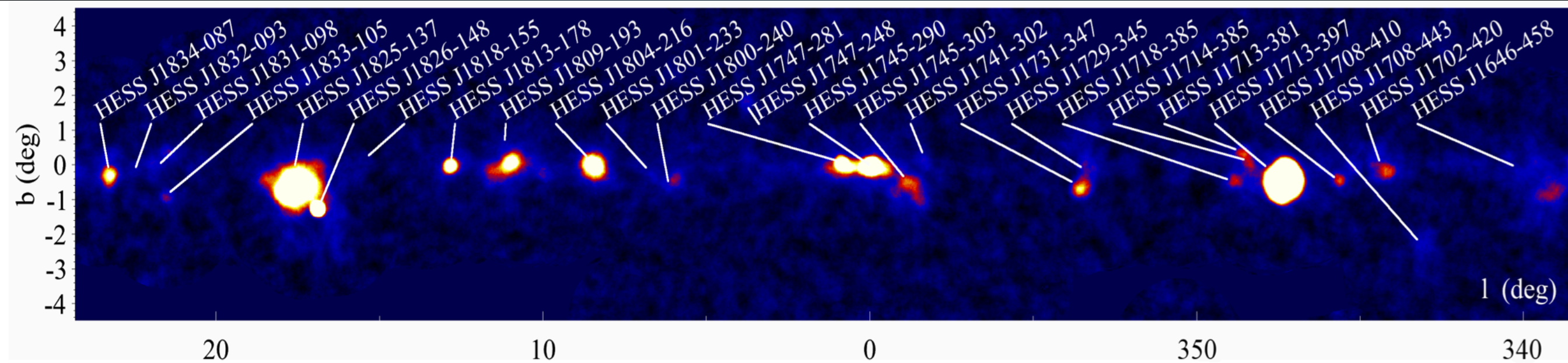
CRACKS IN THE STORY



- Milagro observations found an excess in TeV gamma-ray emission along the Galactic plane.

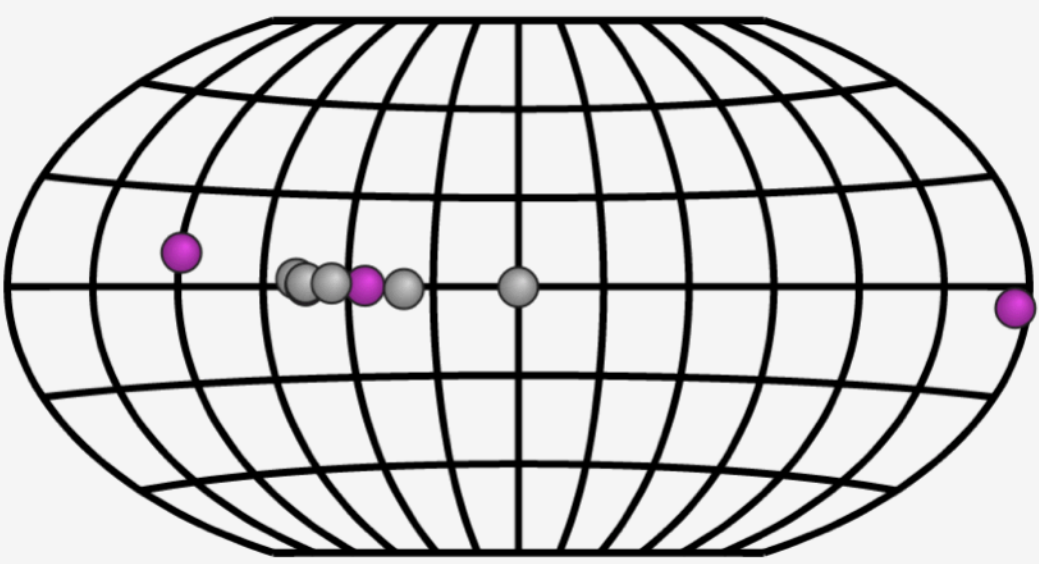
CRACKS IN THE STORY

HESS Collaboration 2018



Home

RESET - + VIEW LEGEND



Source Name: 2HWC J1953+294
Source Type: Gal | UNID | PWN
Distance: 1.0 kpc
GLON: 65.8535
GLAT: 1.0685

Select Catalogs Map Projections Map Tools

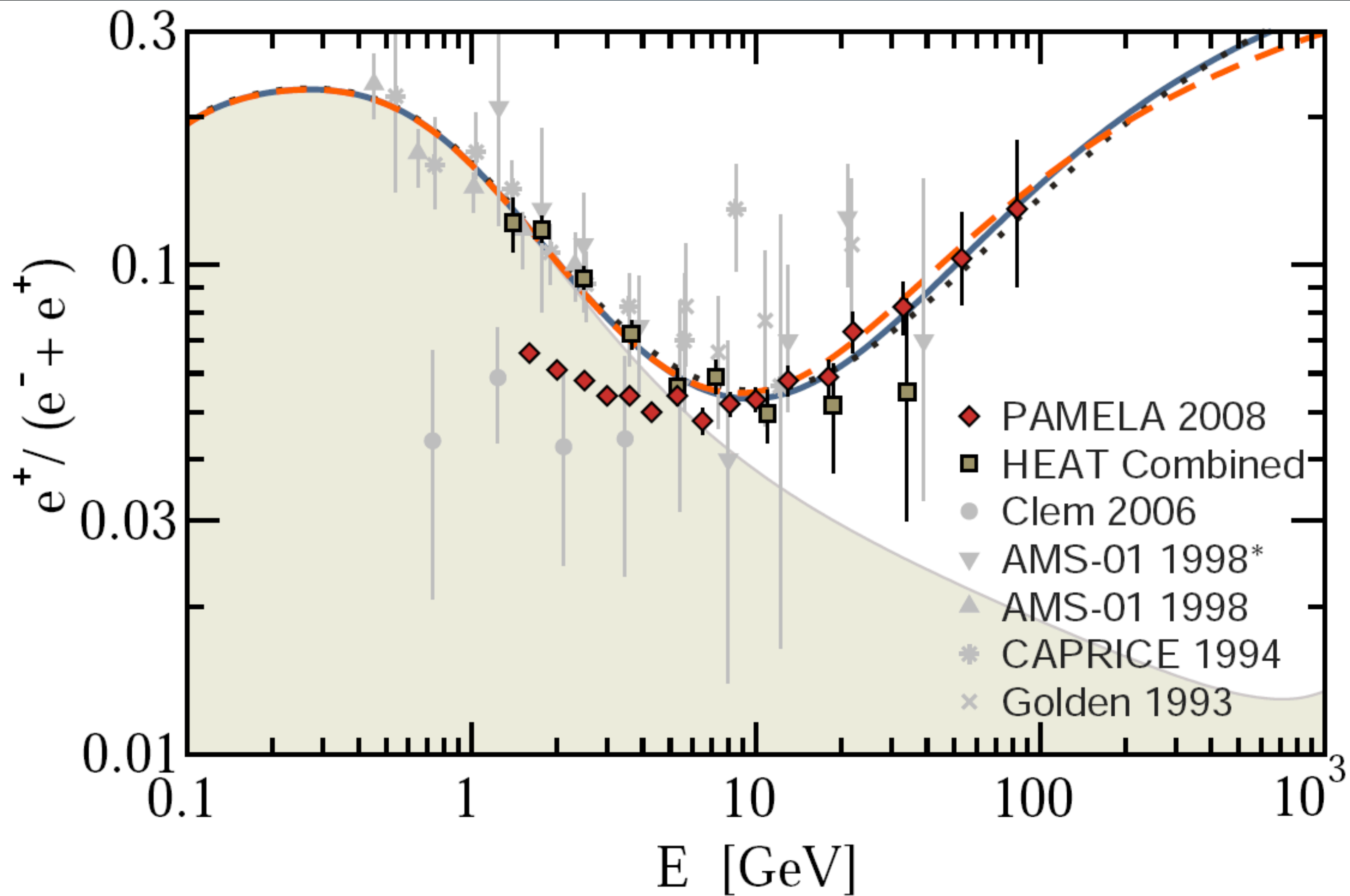
RegExp Search

x PWN x UNID x VERITAS AND AND

Reset Table Columns Sync To Map Filter Selected

Name	RA	Dec	Type Tags ▲	Distance	Catalog
SNR G054.1+00.3	19 30 32	+18 52 12	Gal,SNR,P...	4.9 kpc	Default Catalog
Crab	05 34 31.1	+22 00 52	Gal,SNR,P...	2.0 kpc	Default Catalog
MGRO J2019+37	20 18 35.03	+36 50 00.0	Gal,SNR,P...	z=0.0	Default Catalog
CTA 1	00 06 26	+72 59 01.0	Gal,SNR,P...	1.4 kpc	Default Catalog
2HWC J1953+294	19 53 02.4	+29 28 48	Gal,UNID,P...	1.0 kpc	Default Catalog
MGRO J1908+06	19 07 54	+06 16 07	UNID	z=0.0	Default Catalog
VER J2019+368	20 19 25	+36 48 14	UNID	z=0.0	Default Catalog
VER J1746-289	17 46 19.71	-28 57 58.4	UNID	z=0.0	Newly Announced
VER J2019+407	20 20 04.8	+40 45 26	UNID	z=0.0	Default Catalog
VER J2016+371	20 16 00	37 12 00	UNID		Newly Announced

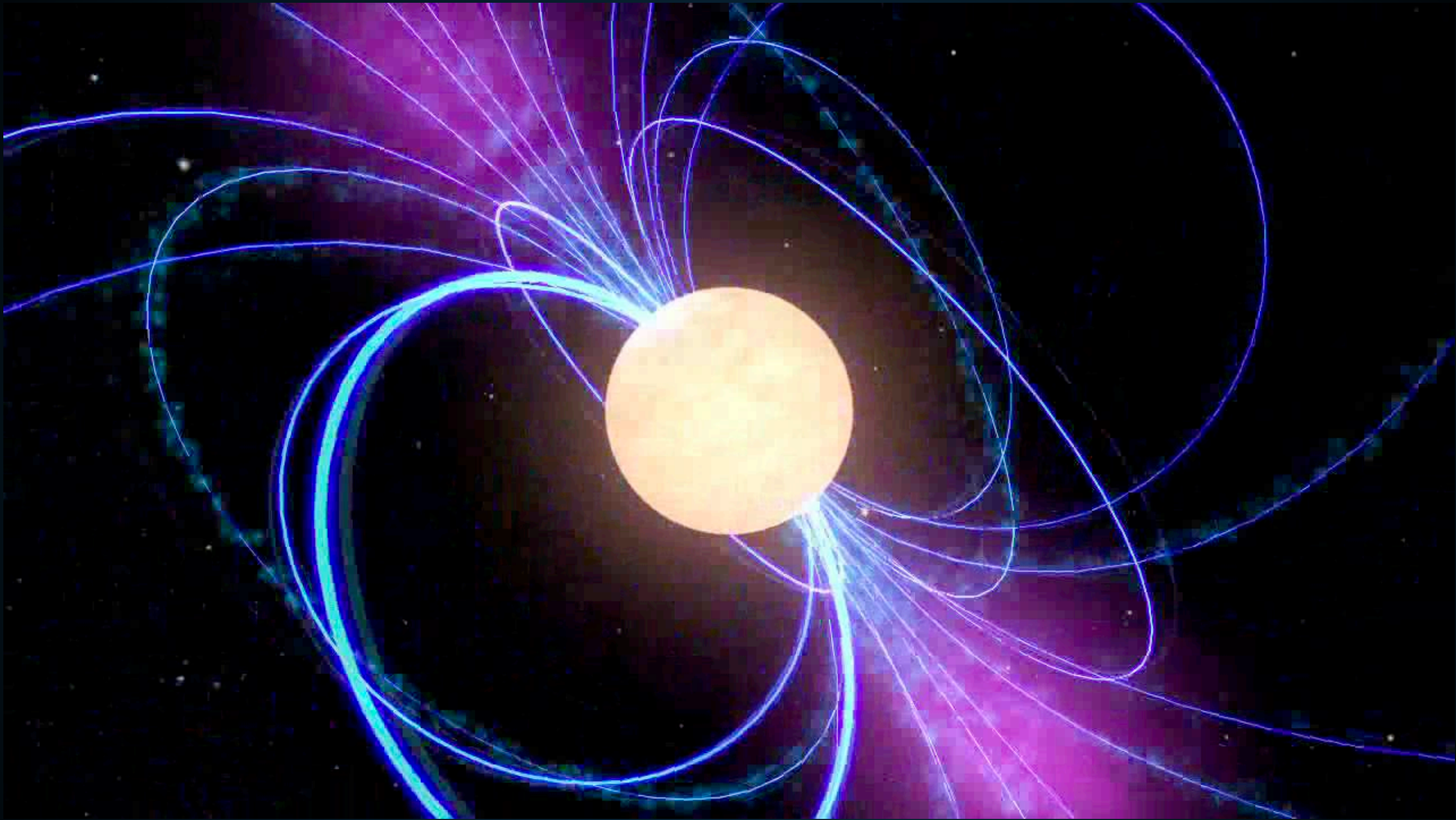
CRACKS IN THE STORY



- **In this talk, I will argue that electrons and positrons dominate the Milky Way's energetics at TeV energies:**
 - **1.) Pulsars dominate the diffuse TeV gamma-ray emission.**
 - **2.) Pulsars produce the majority of the bright TeV sources.**
 - **3.) Pulsars are responsible for the rising positron fraction.**

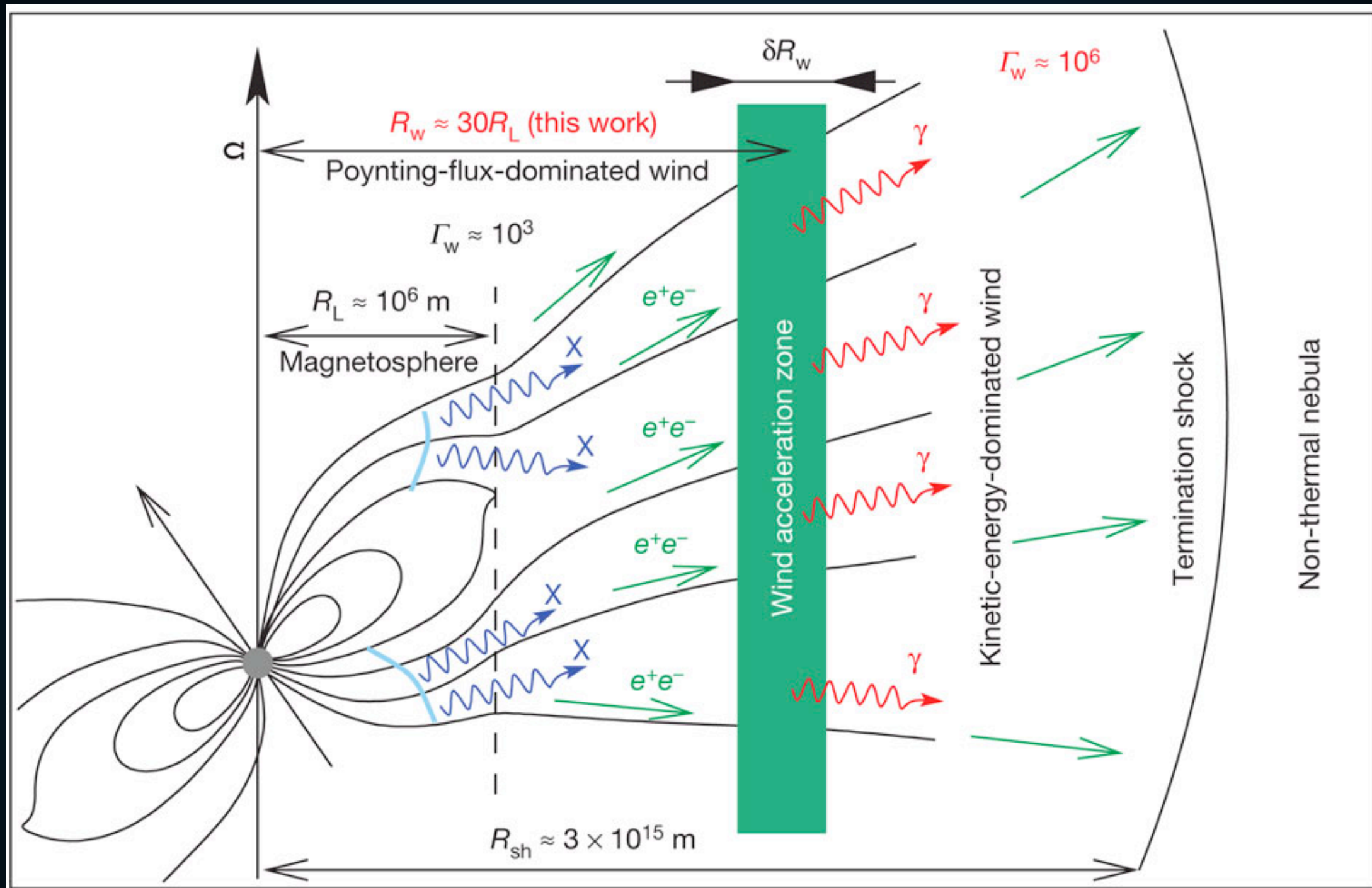
What do we know about pulsars?

PULSARS AS ASTROPHYSICAL ACCELERATORS



- **Rotational Kinetic Energy of the neutron star is the ultimate power source of all emission in this problem.**

PRODUCTION OF ELECTRON AND POSITRON PAIRS



- **Electrons boiled off of the pulsar surface produce e^+e^- pairs.**
- **Final e^+e^- Spectrum is model dependent.**

REACCELERATION IN THE PULSAR WIND NEBULA



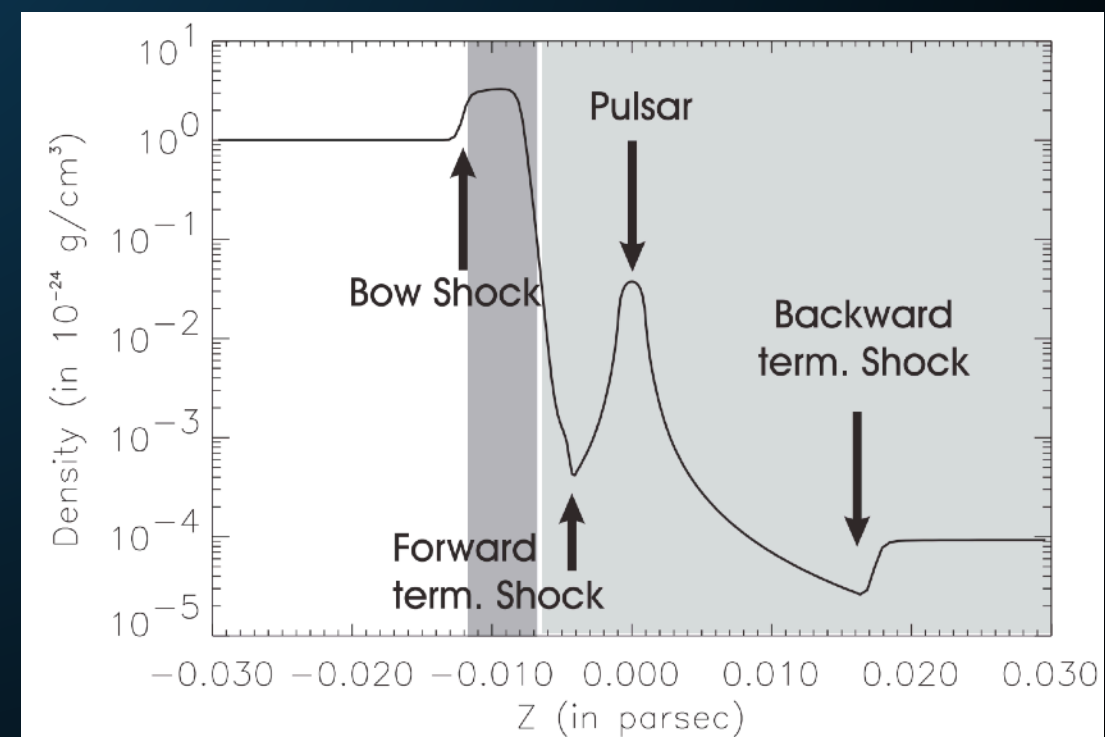
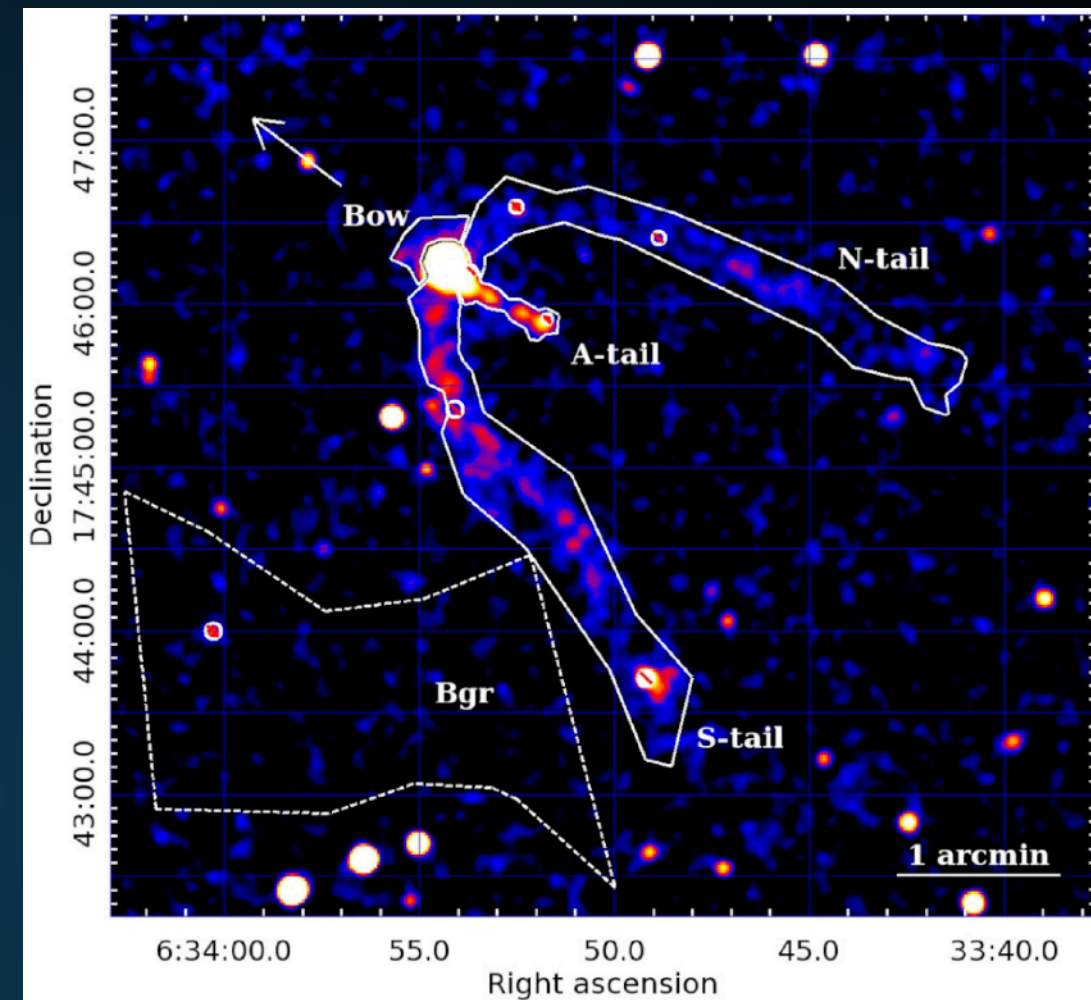
Blandford & Ostriker (1978)
Hoshino et al. (1992)
Coroniti (1990)
Sironi & Spitkovsky (2011)

- **PWN termination shock:**
 - **Voltage Drop > 30 PV**
 - **e^+e^- energy > 1 PeV**
(known from synchrotron)
- **Resets e^+e^- spectrum.**
- **Many Possible Models:**
 - **1st Order Fermi-Acceleration**
 - **Magnetic Reconnection**
 - **Shock-Driven Reconnection**

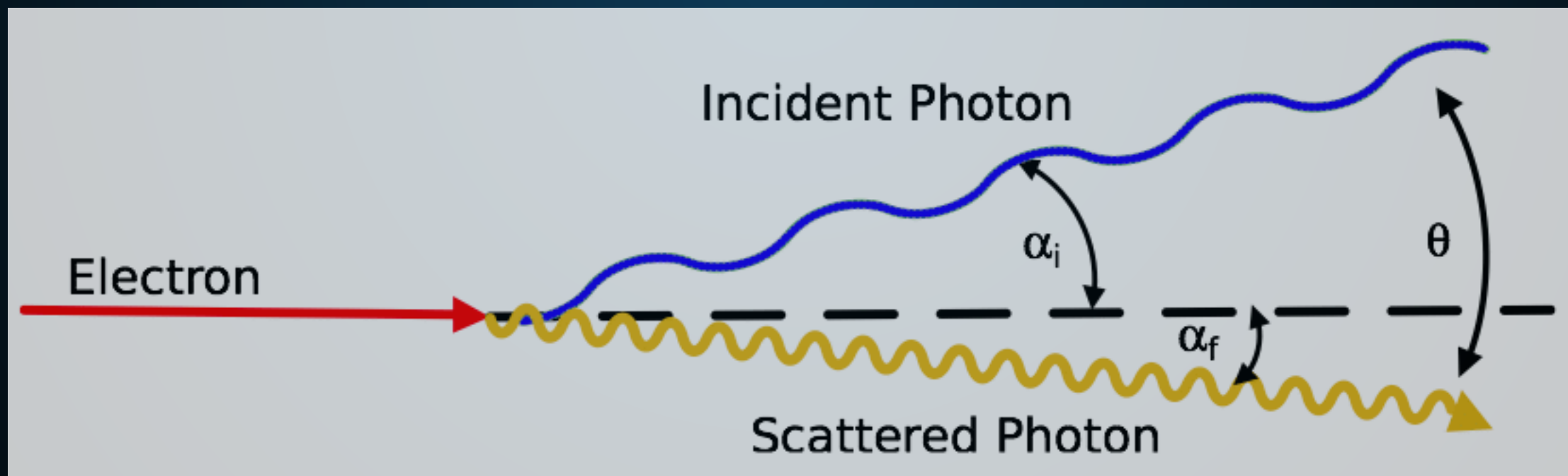
- **Extent of radio and X-Ray PWN is approximately 1 pc.**
- **Termination shock produced when ISM energy density stops the relativistic pulsar wind.**

$$R_{\text{PWN}} \simeq 1.5 \left(\frac{\dot{E}}{10^{35} \text{ erg/s}} \right)^{1/2} \times \left(\frac{n_{\text{gas}}}{1 \text{ cm}^{-3}} \right)^{-1/2} \left(\frac{v}{100 \text{ km/s}} \right)^{-3/2} \text{ pc}$$

- **NOTE: The radial extent of PWN is explained by a known physical mechanism.**



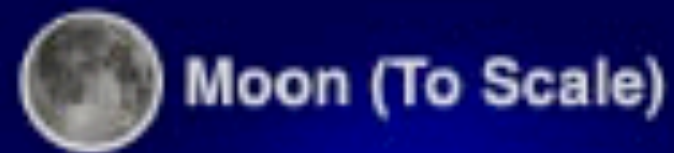
High energy electrons should also make gamma-rays.



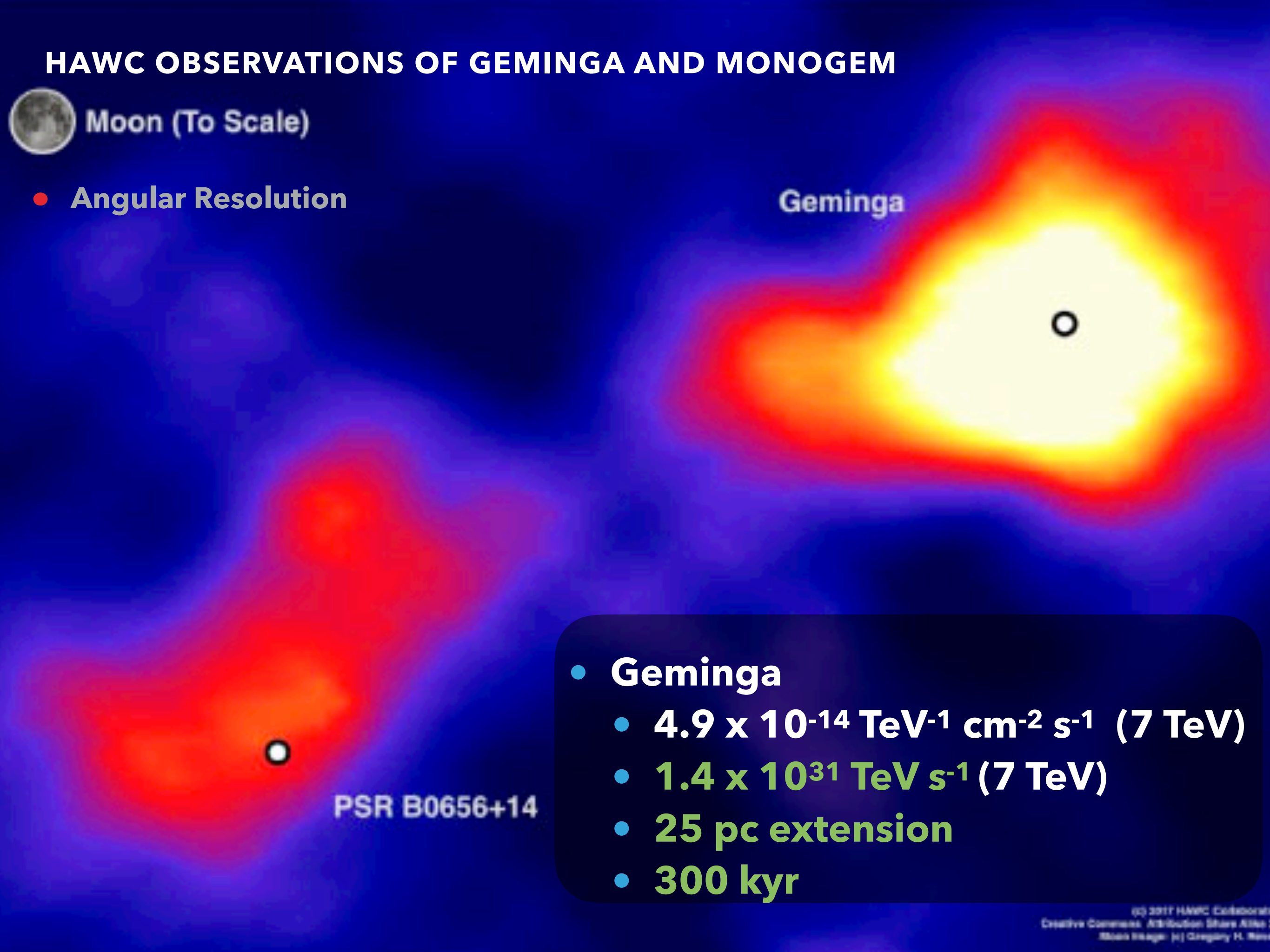
New Observations!



HAWC OBSERVATIONS OF GEMINGA AND MONOGEM



- Angular Resolution

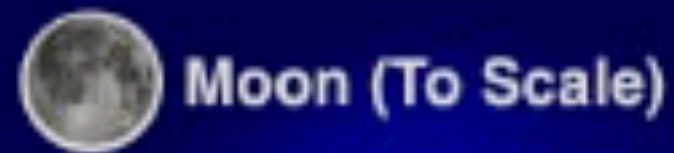


Geminga

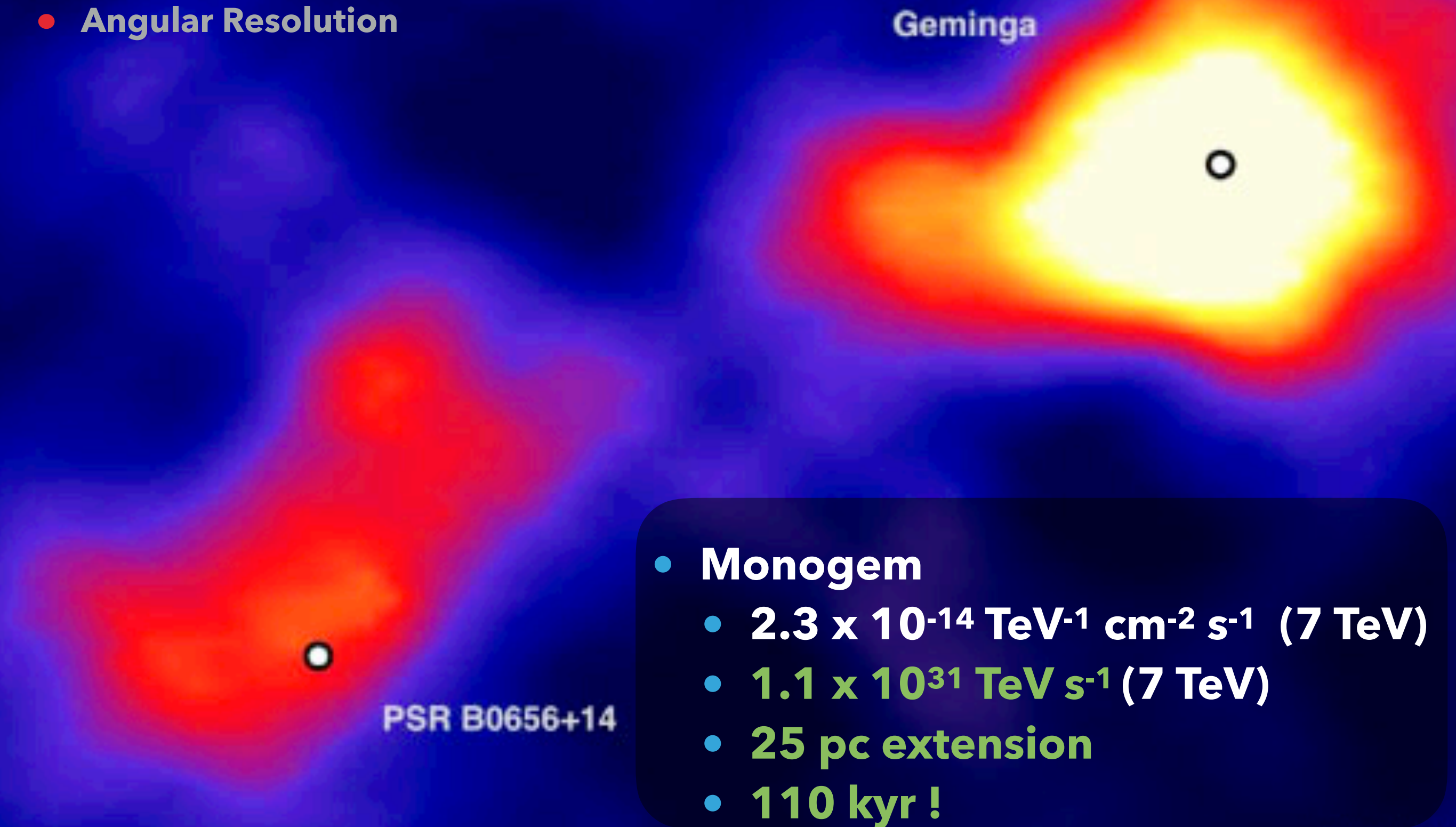
PSR B0656+14

- **Geminga**
 - $4.9 \times 10^{-14} \text{ TeV}^{-1} \text{ cm}^{-2} \text{ s}^{-1}$ (7 TeV)
 - $1.4 \times 10^{31} \text{ TeV s}^{-1}$ (7 TeV)
 - 25 pc extension
 - 300 kyr

HAWC OBSERVATIONS OF GEMINGA AND MONOGEM

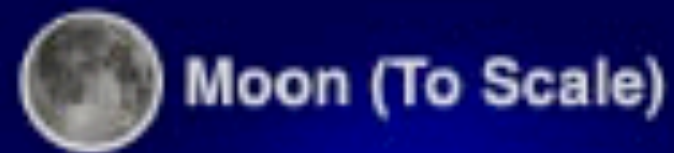


- Angular Resolution

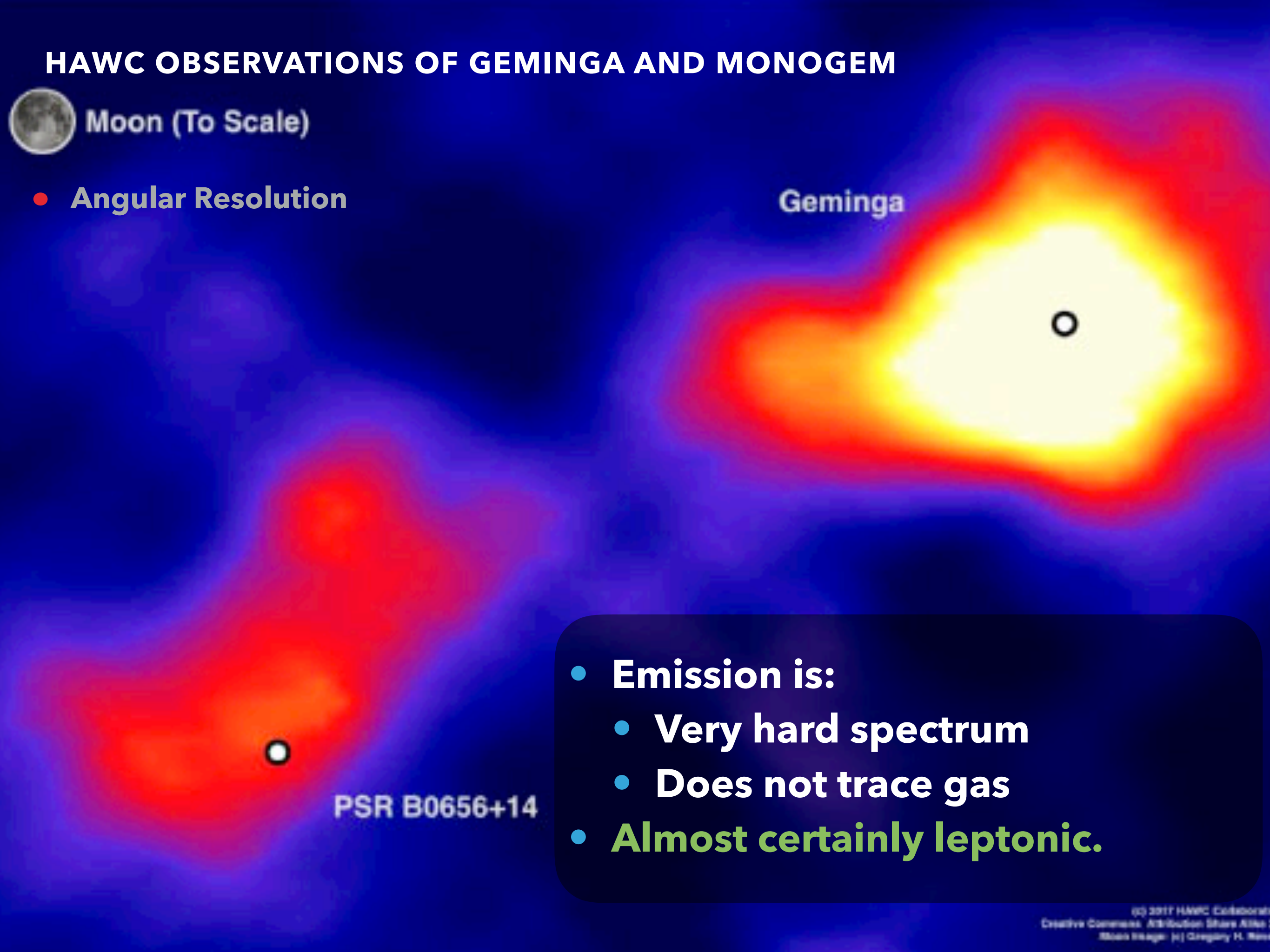


- Monogem
 - $2.3 \times 10^{-14} \text{ TeV}^{-1} \text{ cm}^{-2} \text{ s}^{-1}$ (7 TeV)
 - $1.1 \times 10^{31} \text{ TeV s}^{-1}$ (7 TeV)
 - 25 pc extension
 - 110 kyr !

HAWC OBSERVATIONS OF GEMINGA AND MONOGEM

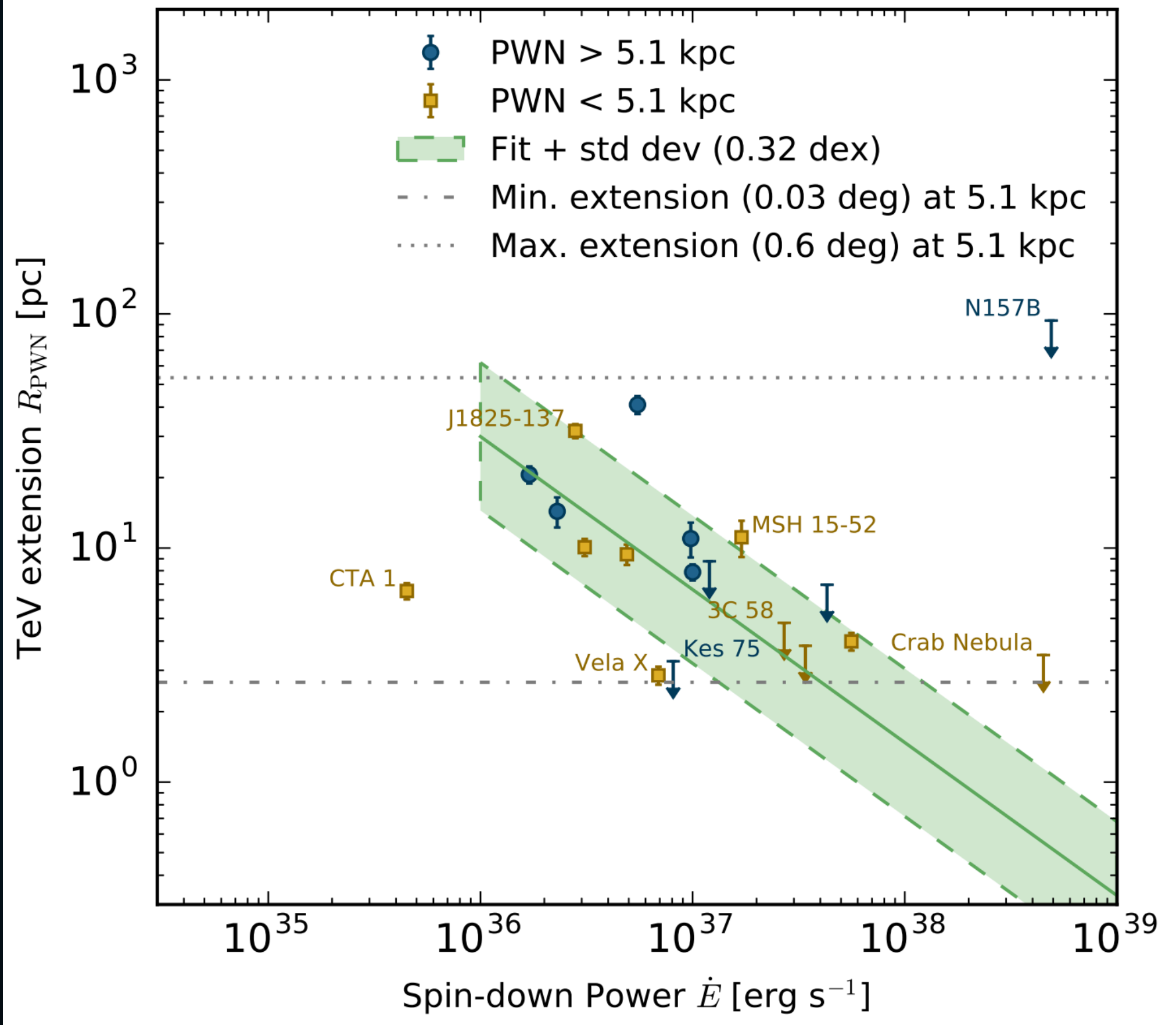


- Angular Resolution

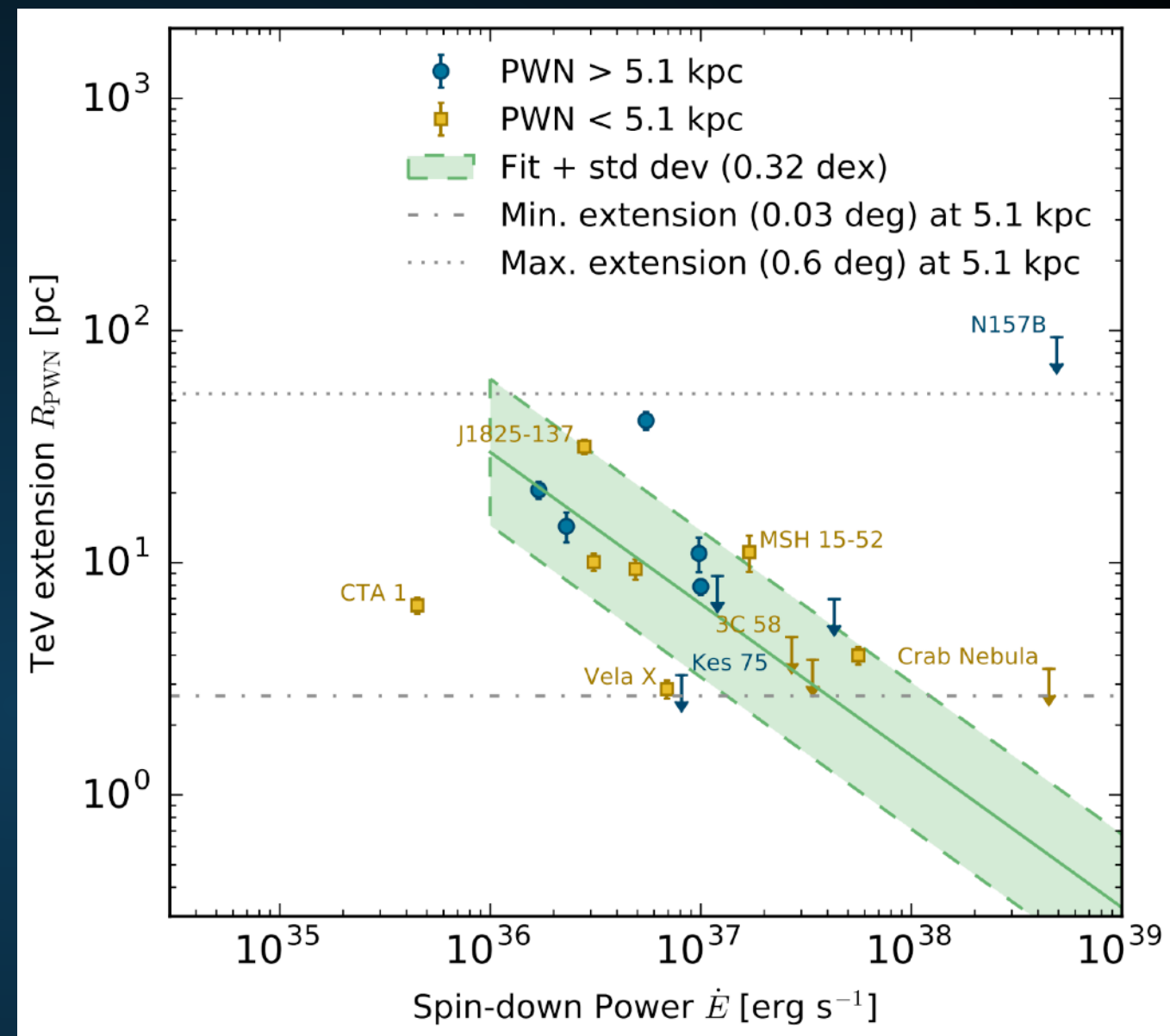


- Emission is:
 - Very hard spectrum
 - Does not trace gas
 - **Almost certainly leptonic.**



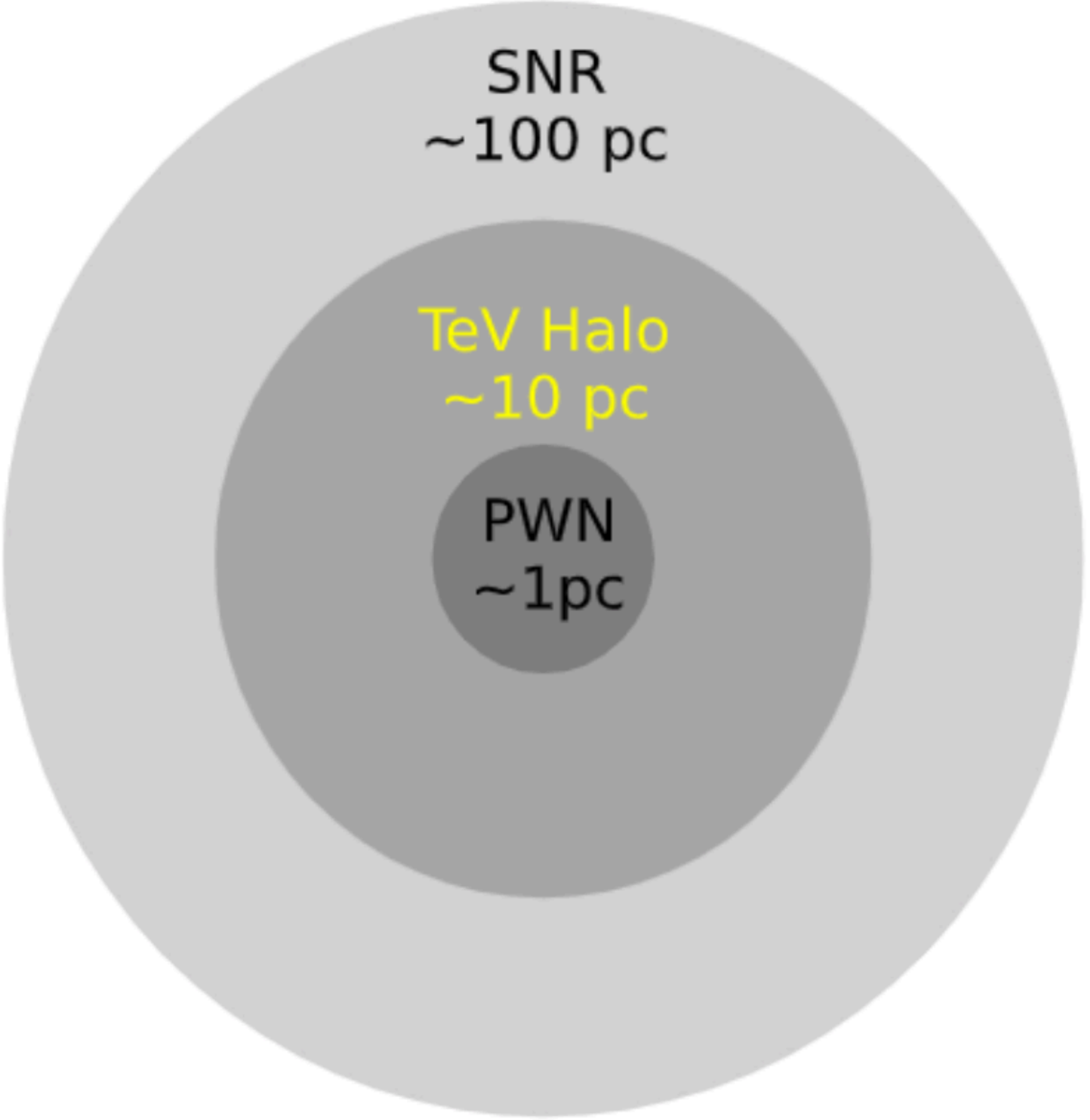


- They are much larger than the PWN.
- Especially at low-energies.



NOTE: This has the opposite energy dependence as the X-Ray PWN.

$$R_{\text{PWN}} \simeq 1.5 \left(\frac{\dot{E}}{10^{35} \text{ erg/s}} \right)^{1/2} \times \left(\frac{n_{\text{gas}}}{1 \text{ cm}^{-3}} \right)^{-1/2} \left(\frac{v}{100 \text{ km/s}} \right)^{-3/2} \text{ pc}$$



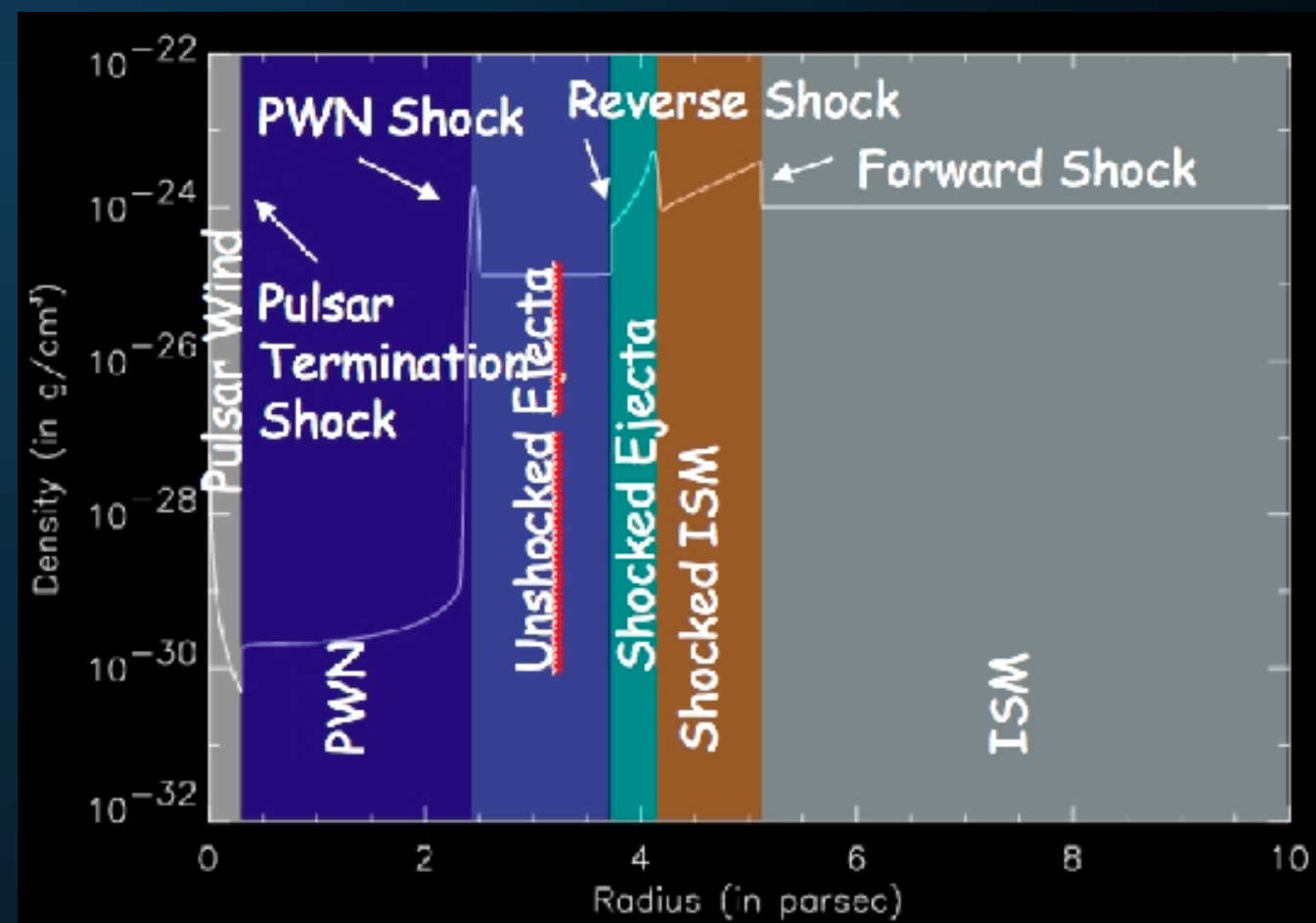
SNR
 ~ 100 pc

TeV Halo
 ~ 10 pc

PWN
 ~ 1 pc

TeV HALOS

- **TeV halos are a new feature**
 - **3 orders of magnitude larger than PWN in volume**
 - **Opposite energy dependence**
- **PWN are morphologically connected to the physics of the termination shock**
- **TeV halos need a similar morphological description.**



We'll go back to the model later...

What do TeV observations tell us about pulsars?

TEV HALOS - AN EMPIRICAL MODEL

- **Assume that every pulsar converts an equivalent fraction of its spin down power into gamma-rays, with the same spectrum as Geminga.**
- **This statement is well supported:**
 - **Observed because they are the two closest sources.**
 - **Many similar HESS Sources**

ASSUMPTION: PULSAR POPULATION MODELS

- Use a generic model for pulsar luminosities
- $B_0 = 10^{12.5} \text{ G } (+/- 10^{0.3} \text{ G})$
- $P_0 = 0.3 \text{ s } (+/- 0.15 \text{ s})$
- Spindown Timescale of $\sim 10^4 \text{ yr}$ (depends on B_0)
- Galprop model for supernova distances

PsrPopPy: An open-source package for pulsar population simulations

D. Bates^{1,2}, D. R. Lorimer^{1,3}, A. Rane¹ and J. Swiggum¹

¹Department of Physics and Astronomy, West Virginia University, Morgantown, WV, 26506 USA

²Centre for Astrophysics, School of Physics and Astronomy, The University of Manchester, Manchester M13 9PL, UK

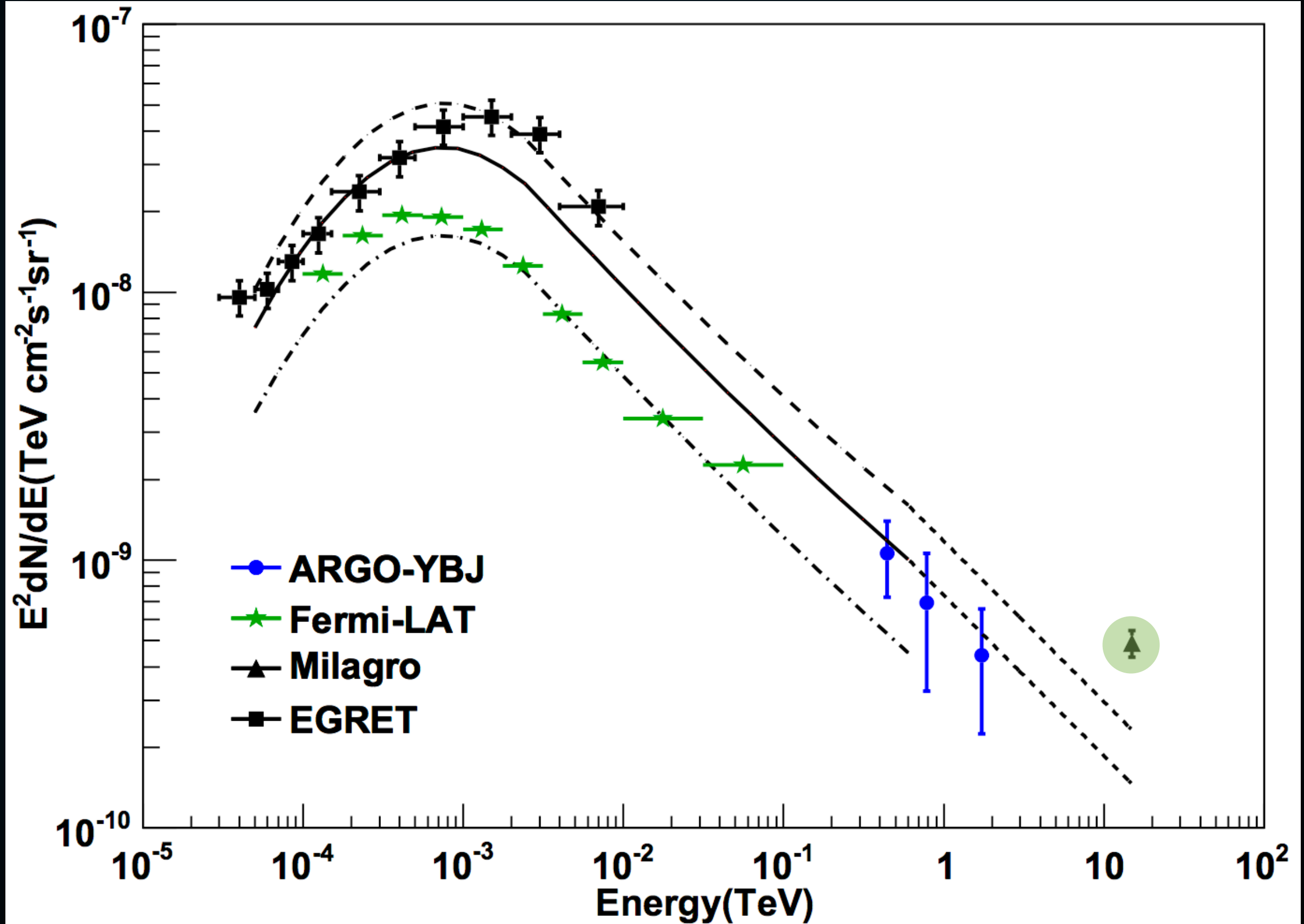
³Astronomy Observatory, PO Box 2, Green Bank, WV 24944, USA

software package for the simulation of pulsar populations. The codebase includes a variety of physical processes, which remain in their original form, and improving the simulation support.

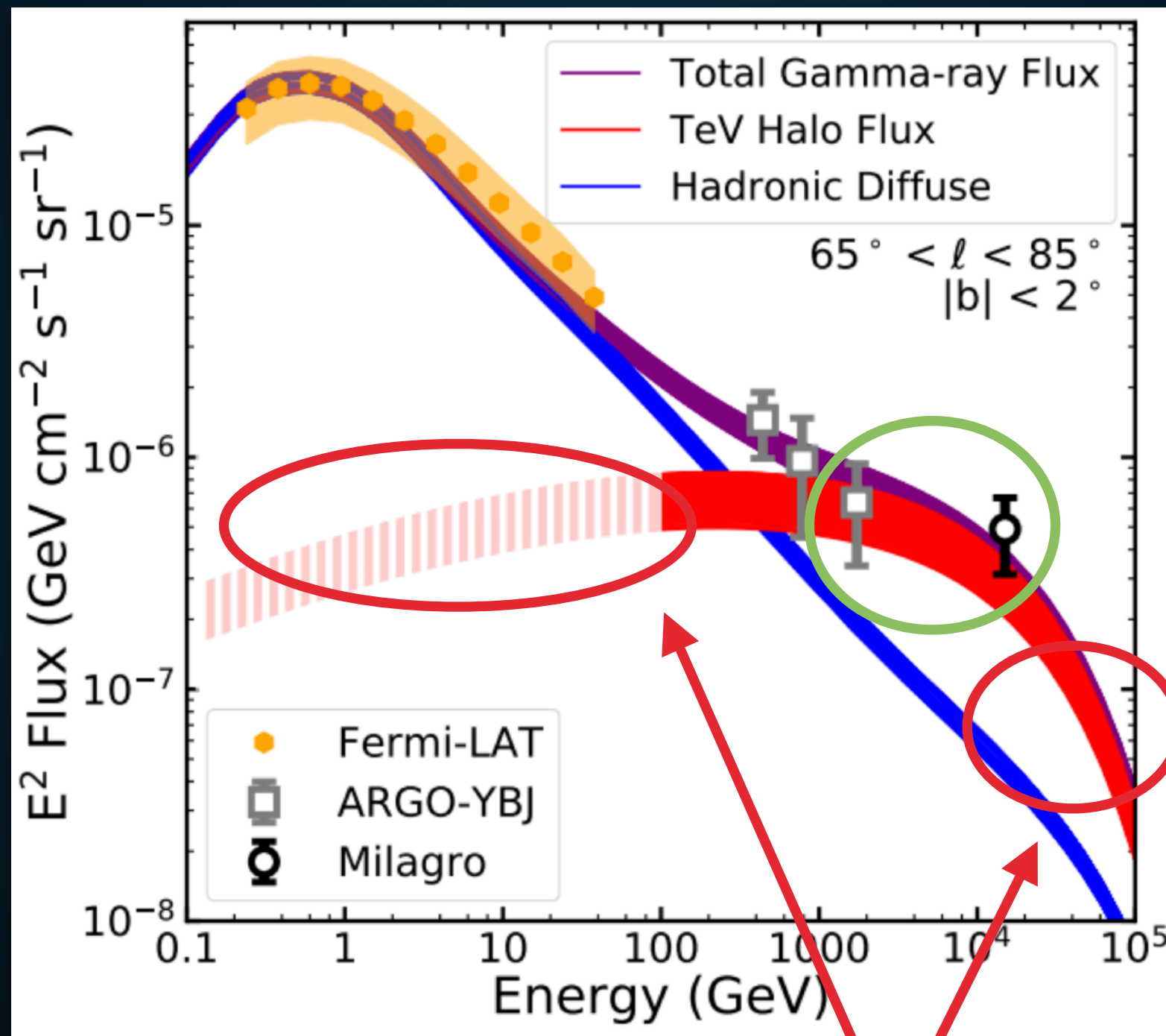
Implication I:

Most TeV emission is produced by TeV halos

IMPLICATION I: THE TEV EXCESS



- TeV halos naturally explain the TeV excess!



spectral assumption!

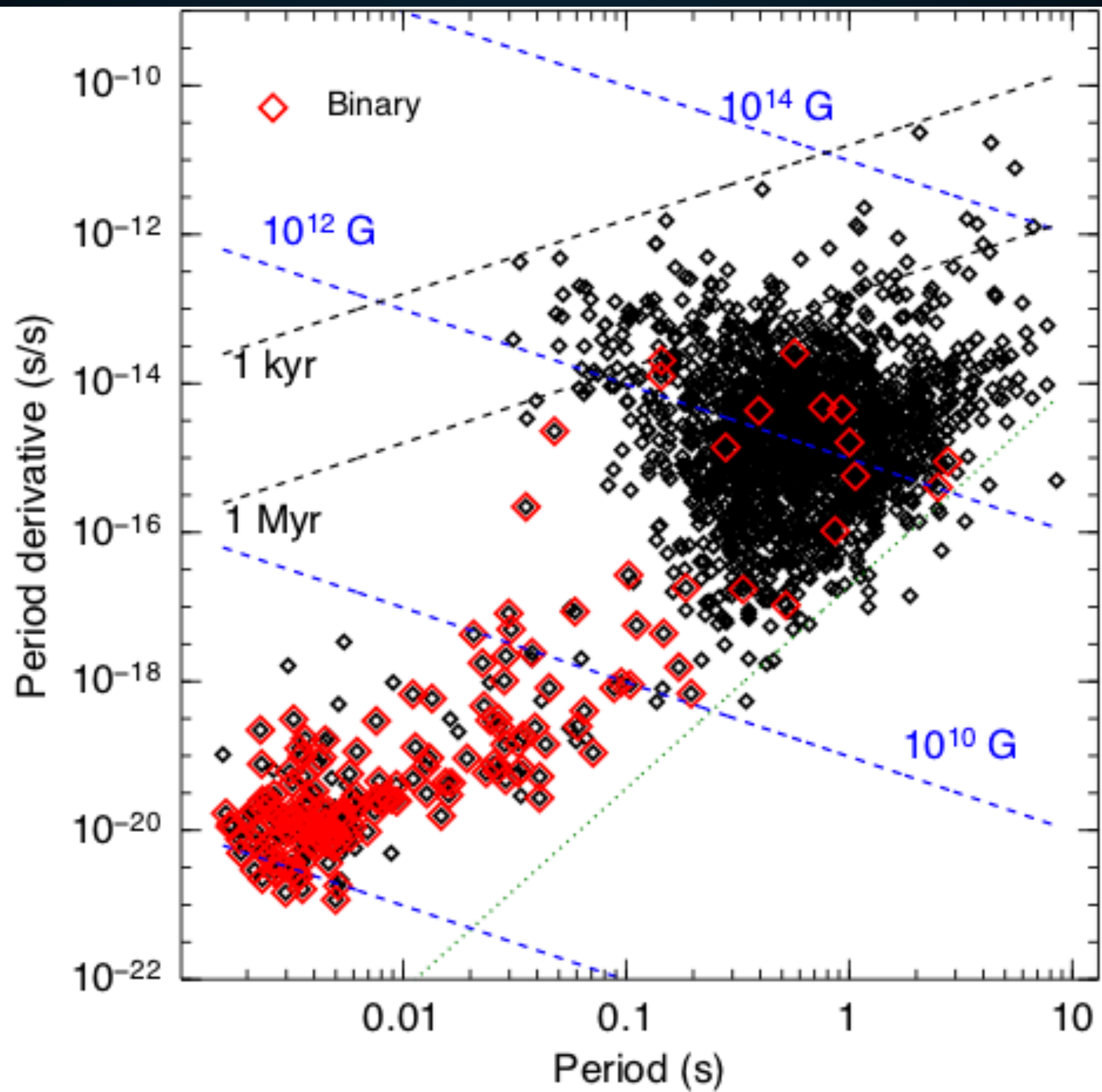
Implication II:

Most TeV gamma-ray sources are TeV halos.

TeV HALO NUMEROLOGY

- **HAWC has observed 39 sources.**
- **5 are coincident with old (>100 kyr) pulsars**
- **12 others coincident with young (<100 kyr) pulsars**
 - **TeV emission may be contaminated by SNR**

WHY DO WE CARE?

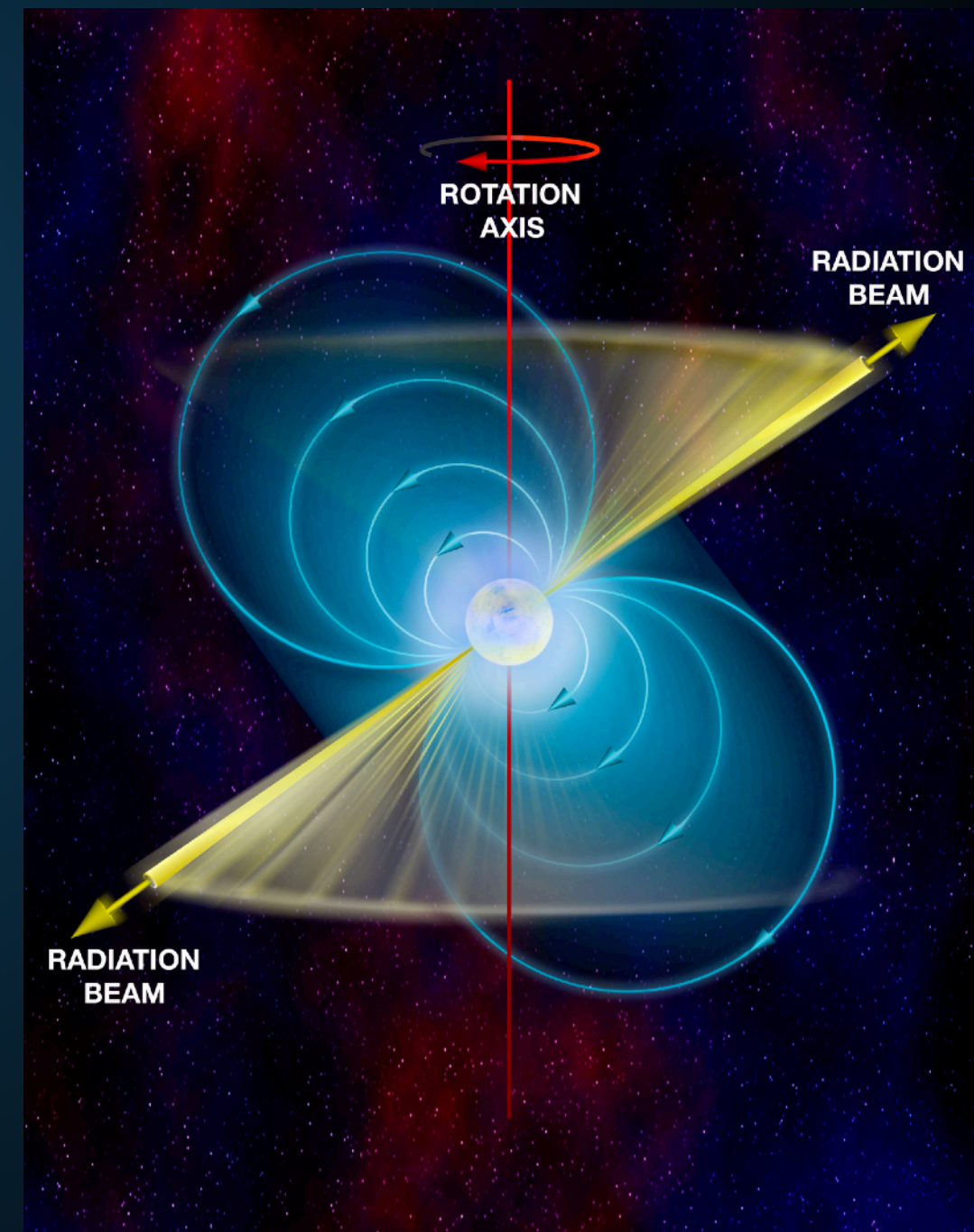


- **Radio pulsars are beamed!**

- **Beaming fraction is small**

$$f = \left[1.1 \left(\log_{10} \left(\frac{\tau}{100 \text{ Myr}} \right) \right)^2 + 15 \right] \%$$

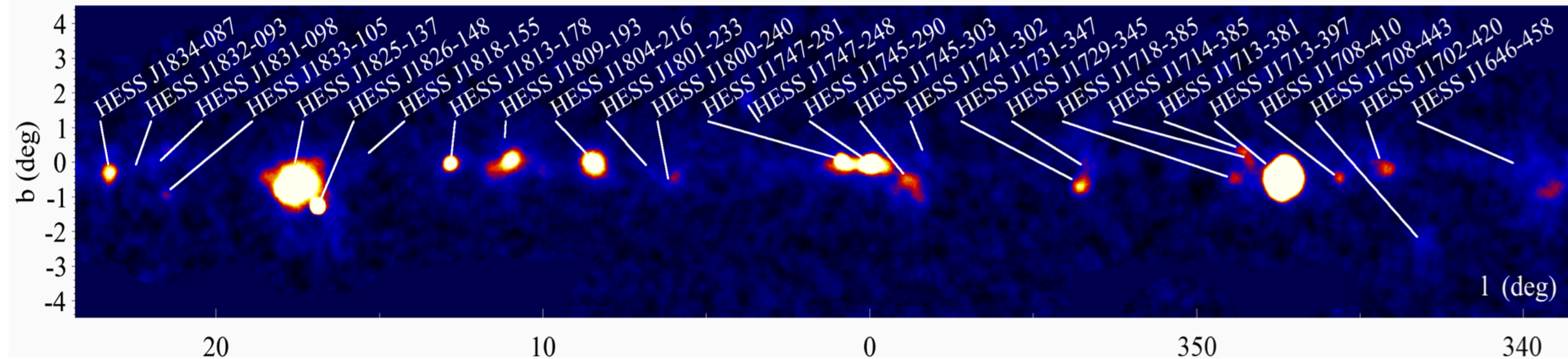
- **This varies between 15-30%.**
- **Most pulsars are unseen in radio!**



2HWC Name	ATNF Name	Distance (kpc)	Angular Separation	Projected Separation	Expected Flux ($\times 10^{-15}$)	Actual Flux ($\times 10^{-15}$)	Flux Ratio	Expected Extension	Actual Extension	Age (kyr)	Chance Overlap
J0700+143	B0656+14	0.29	0.18°	0.91 pc	43.0	23.0	1.87	2.0°	1.73°	111	0.0
J0631+169	J0633+1746	0.25	0.89°	3.88 pc	48.7	48.7	1.0	2.0°	2.0°	342	0.0
J1912+099	J1913+1011	4.61	0.34°	27.36 pc	13.0	36.6	0.36	0.11°	0.7°	169	0.30
J2031+415	J2032+4127	1.70	0.11°	3.26 pc	5.59	61.6	0.091	0.29°	0.7°	181	0.002
J1831-098	J1831-0952	3.68	0.04°	2.57 pc	7.70	95.8	0.080	0.14°	0.9°	128	0.006

2HWC Name	ATNF Name	Distance (kpc)	Angular Separation	Projected Separation	Expected Flux ($\times 10^{-15}$)	Actual Flux ($\times 10^{-15}$)	Flux Ratio	Expected Extension	Actual Extension	Age (kyr)	Chance Overlap
J1930+188	J1930+1852	7.0	0.03°	3.67 pc	23.2	9.8	2.37	0.07°	0.0°	2.89	0.002
J1814-173	J1813-1749	4.7	0.54°	44.30 pc	243	152	1.60	0.11°	1.0°	5.6	0.61
J2019+367	J2021+3651	1.8	0.27°	8.48 pc	99.8	58.2	1.71	0.28°	0.7°	17.2	0.04
J1928+177	J1928+1746	4.34	0.03°	2.27 pc	8.08	10.0	0.81	0.11°	0.0°	82.6	0.002
J1908+063	J1907+0602	2.58	0.36°	16.21 pc	40.0	85.0	0.47	0.2°	0.8°	19.5	0.26
J2020+403	J2021+4026	2.15	0.18°	6.75 pc	2.48	18.5	0.134	0.23°	0.0°	77	0.01
J1857+027	J1856+0245	6.32	0.12°	13.24 pc	11.0	97.0	0.11	0.08°	0.9°	20.6	0.06
J1825-134	J1826-1334	3.61	0.20°	12.66 pc	20.5	249	0.082	0.14°	0.9°	21.4	0.14
J1837-065	J1838-0655	6.60	0.38°	43.77 pc	12.0	341	0.035	0.08°	2.0°	22.7	0.48
J1837-065	J1837-0604	4.78	0.50°	41.71 pc	8.3	341	0.024	0.10°	2.0°	33.8	0.68
J2006+341	J2004+3429	10.8	0.42°	80.07 pc	0.48	24.5	0.019	0.04°	0.9°	18.5	0.08

- Correcting for the beaming fraction implies that 56^{+15}_{-11} TeV halos are currently observed by HAWC.
- However, only 39 total HAWC sources.



The H.E.S.S. Galactic plane survey

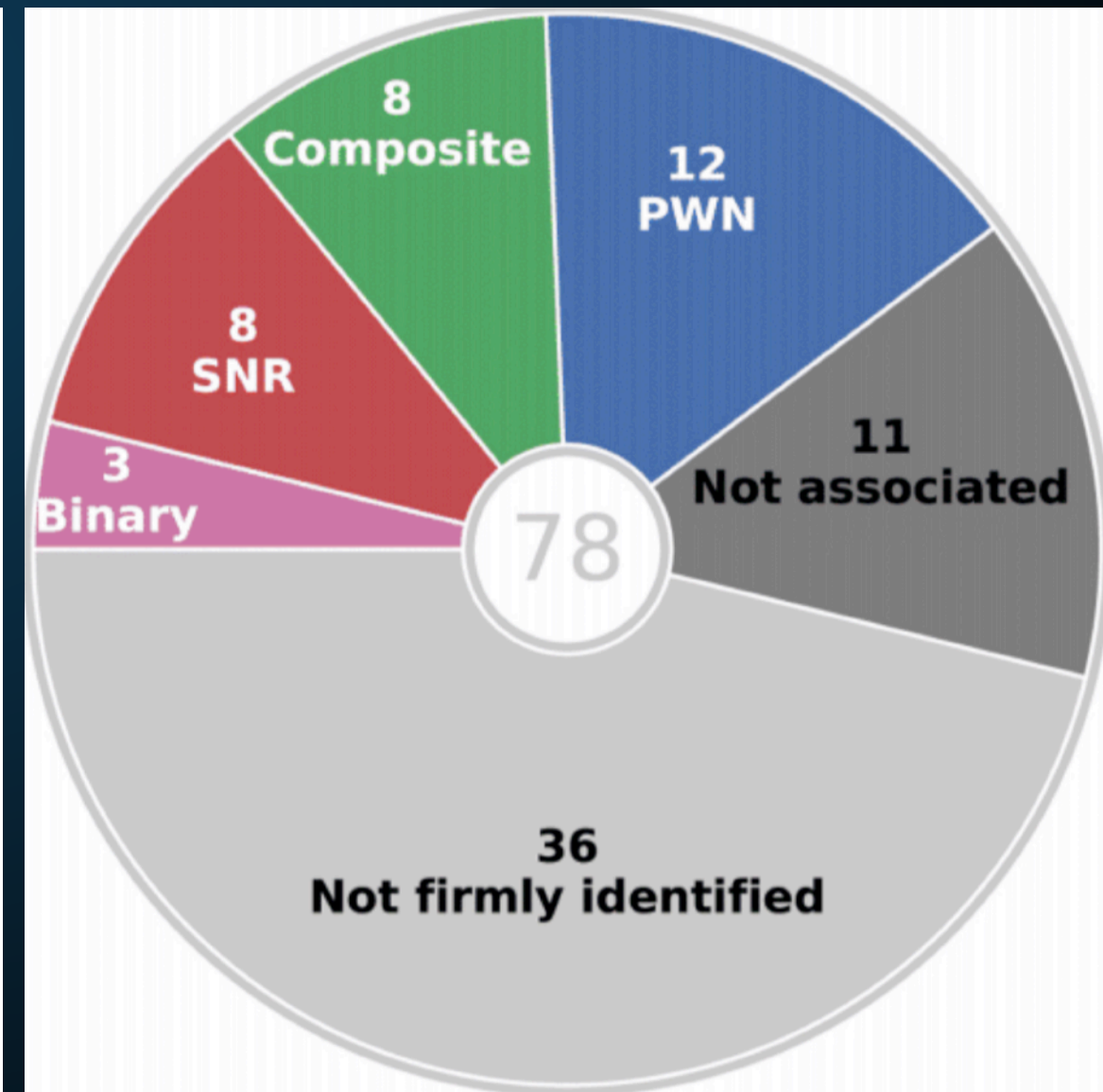
H.E.S.S. Collaboration, H. Abdalla¹, A. Abramowski², F. Aharonian^{3,4,5}, F. Ait Benkhali³, E.O. Angüner²¹, M. Arakawa⁴³, M. Arrieta¹⁵, P. Aubert²⁴, M. Backes⁸, A. Balzer⁹, M. Barnard¹, Y. Becherini¹⁰, J. Becker Tjus¹¹, D. Berge¹², S. Bernhard¹³, K. Bernlöhr³, R. Blackwell¹⁴, M. Böttcher¹, C. Boisson¹⁵, J. Bolmont¹⁶, S. Bonnefoy³⁷, P. Bordas³, J. Bregeon¹⁷, F. Brun¹⁸, P. Brun¹⁸, M. Bryan⁹, M. Büchele³⁶, T. Bulik¹⁹, M. Capasso²⁹, S. Carrigan^{3,48}, S. Caroff³⁰, A. Carosi²⁴, S. Casanova^{21,3}, M. Cerruti¹⁶, N. Chakraborty³, R.C.G. Chaves^{17,22}, A. Chen²³, J. Chevalier²⁴, S. Colafrancesco²³, B. Condon²⁶, J. Conrad^{27,28}, I.D. Davids⁸, J. Decock¹⁸, C. Deil³, J. Devin¹⁷, P. deWilt¹⁴, L. Dirson², A. Djannati-Atai³¹, W. Domainko³, A. Donath³, L.O'C. Drury⁴, K. Dutson³³, J. Dyks³⁴, T. Edwards³, K. Egberts³⁵, P. Eger³, G. Emery¹⁶, J.-P. Ernenwein²⁰, S. Eschbach³⁶, C. Farnier^{27,10}, S. Fegan³⁰, M.V. Fernandes², A. Fiasson²⁴, G. Fontaine³⁰, A. Förster³, S. Funk³⁶, M. Füßling³⁷, S. Gabici³¹, Y.A. Gallant¹⁷, T. Garrigoux¹, H. Gast^{3,49}, F. Gaté²⁴, G. Giavitto³⁷, B. Giebels³⁰, D. Glawion²⁵, J.F. Glicenstein¹⁸, D. Gottschall²⁹, M.-H. Grondin²⁶, J. Hahn³, M. Haupt³⁷, J. Hawkes¹⁴, G. Heinzelmann², G. Henri³², G. Hermann³, J.A. Hinton³, W. Hofmann³, C. Hoischen³⁵, T.L. Holch⁷, M. Holler¹³, D. Horns², A. Ivascenko¹, H. Iwasaki⁴³, A. Jacholkowska¹⁶, M. Jamroz³⁸, D. Jankowsky³⁶, F. Jankowsky²⁵, M. Jingo²³, L. Jouvin³¹, I. Jung-Richardt³⁶, M.A. Kastendieck², K. Katarzynski³⁹, M. Katsuragawa⁴⁴, U. Katz³⁶, D. Kerszberg¹⁶, D. Khangulyan⁴³, B. Khélifi³¹, J. King³, S. Klepser³⁷, D. Klockov²⁹, W. Kluźniak³⁴, Nu. Komin²³, K. Kosack¹⁸, S. Krakau¹¹, M. Kraus³⁶, P.P. Krüger¹, H. Laffon²⁴, G. Lamanna²⁴, J. Lau¹⁴, J.-P. Lees²⁴, J. Lefaucheur¹⁵, A. Lemièr³¹, M. Lemoine-Goumard²⁶, J.-P. Lenain¹⁶, E. Leser³⁵, T. Lohse⁷, M. Lorentz¹⁸, R. Liu³, R. López-Coto³, I. Lypova³⁷, V. Marandon³, D. Malyshev²⁹, A. Marcowith¹⁷, C. Mariaud³⁰, R. Marx³, G. Maurin²⁴, N. Maxted^{14,45}, M. Mayer⁷, P.J. Meintjes⁴⁰, M. Meyer²⁷, A.M.W. Mitchell³, R. Moderski³⁴, M. Mohamed²⁵, L. Mohrmann³⁶, K. Morá²⁷, E. Moulin¹⁸, T. Murach³⁷, S. Nakashima⁴⁴, M. de Naurois³⁰, H. Ndiyavala¹, F. Niederwanger¹³, J. Niemiec²¹, L. Oakes⁷, P. O'Brien³³, H. Odaka⁴⁴, S. Ohm³⁷, M. Ostrowski³⁸, I. Oya³⁷, M. Padovani¹⁷, M. Panter³, R.D. Parsons³, M. Paz Arribas⁷, N.W. Pekeur¹, G. Pelletier³², C. Perennes¹⁶, P.-O. Petrucci³², B. Peyaud¹⁸, Q. Piel²⁴, S. Pita³¹, V. Poireau²⁴, H. Poon³, D. Prokhorov¹⁰, H. Prokoph¹², G. Pühlhofer²⁹, M. Punch^{31,10}, A. Quirrenbach²⁵, S. Raab³⁶, R. Rauth¹³, A. Reimer¹³, O. Reimer¹³, M. Renaud¹⁷, R. de los Reyes³, F. Rieger^{3,41}, L. Rinchiuso¹⁸, C. Romoli⁴, G. Rowell¹⁴, B. Rudak³⁴, C.B. Rulten¹⁵, S. Safi-Harb⁵⁰, V. Sahakian^{6,5}, S. Saito⁴³, D.A. Sanchez²⁴, A. Santangelo²⁹, M. Sasaki³⁶, M. Schandri³⁶, R. Schlickeiser¹¹, F. Schüssler¹⁸, A. Schulz³⁷, U. Schwanke⁷, S. Schwemmer²⁵, M. Seglar-Arroyo⁸, C. Settimo¹⁶, A.S. Seyffert¹, N. Shafi²³, I. Shilon³⁶, K. Shiningayamwe⁸, R. Simoni⁹, H. Sol¹⁵, F. Spanier¹, M. Spir-Jacob³¹, L. Stawarz³⁸, R. Steenkamp⁸, C. Stegmann^{35,37}, C. Steppa³⁵, I. Sushch¹, T. Takahashi⁴⁴, J.-P. Tavernier¹⁶, T. Tavernier³¹, A.M. Taylor³⁷, R. Terrier³¹, L. Tibaldo³, D. Tiziani³⁶, M. Tluczykont², C. Trichard²⁰, M. Tsiros¹⁷, N. Tsuji⁴³, R. Tufts³, Y. Uchiyama⁴³, D.J. van der Walt¹, C. van Eldik³⁶, C. van Rensburg¹, B. van Soelen⁴⁰, G. Vasileiadis¹⁷, J. Veh³⁶, C. Venter¹, A. Viana^{3,46}, P. Vincent¹⁶, J. Vink⁹, F. Voisin¹⁴, H.J. Völk³, T. Vuillaume²⁴, Z. Wadiasingh¹, S.J. Wagner²⁵, P. Wagner⁷, R.M. Wagner²⁷, R. White³, A. Wiercholska²¹, P. Willmann³⁶, A. Wörnlein³⁶, D. Wouters¹⁸, R. Yang³, D. Zaborov³⁰, M. Zacharias¹, R. Zanin³, A.A. Zdziarski³⁴, A. Zech¹⁵, F. Zefi³⁰, A. Ziegler³⁶, J. Zorn³, and N. Zywucka³⁸

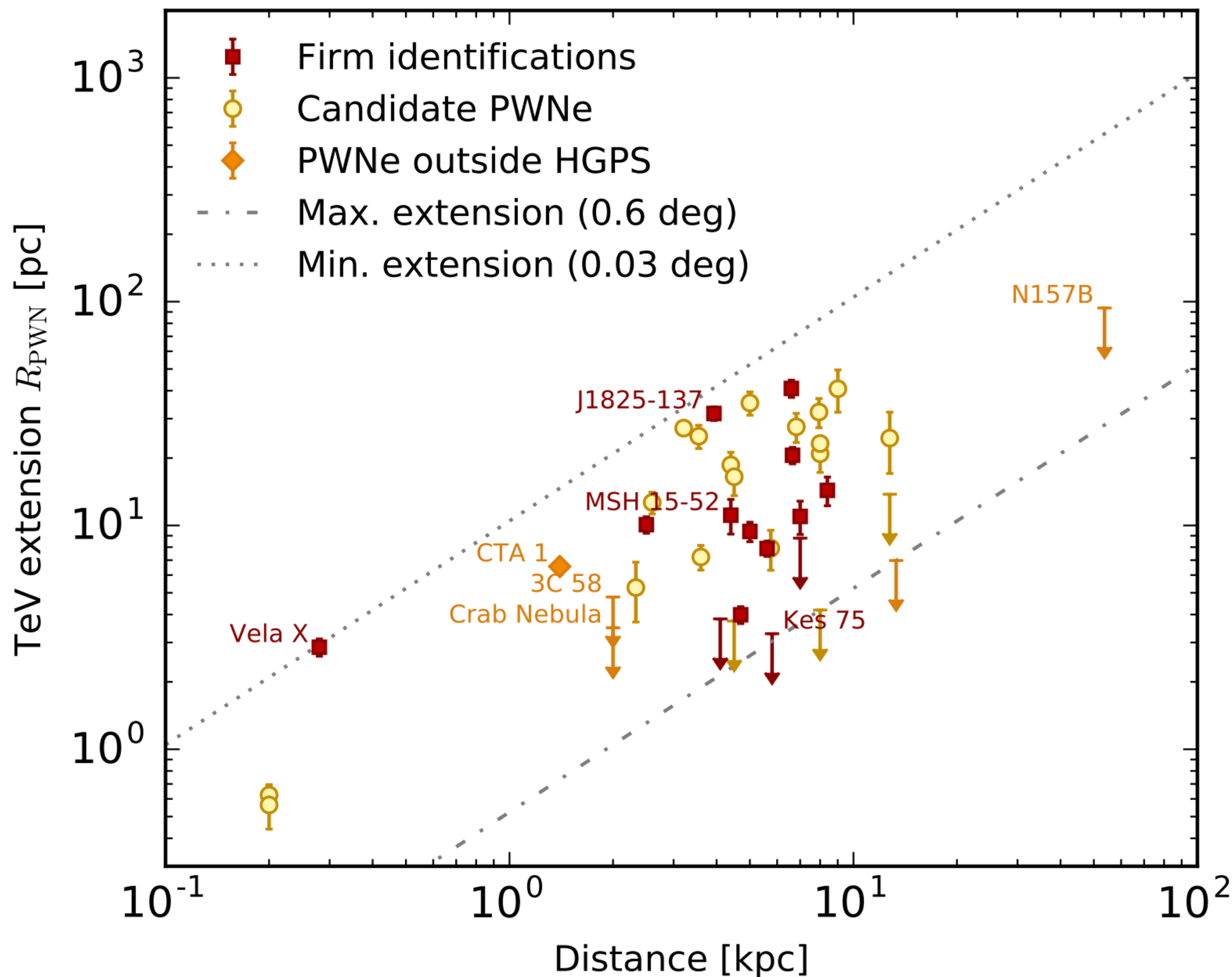
(Affiliations can be found after the references)

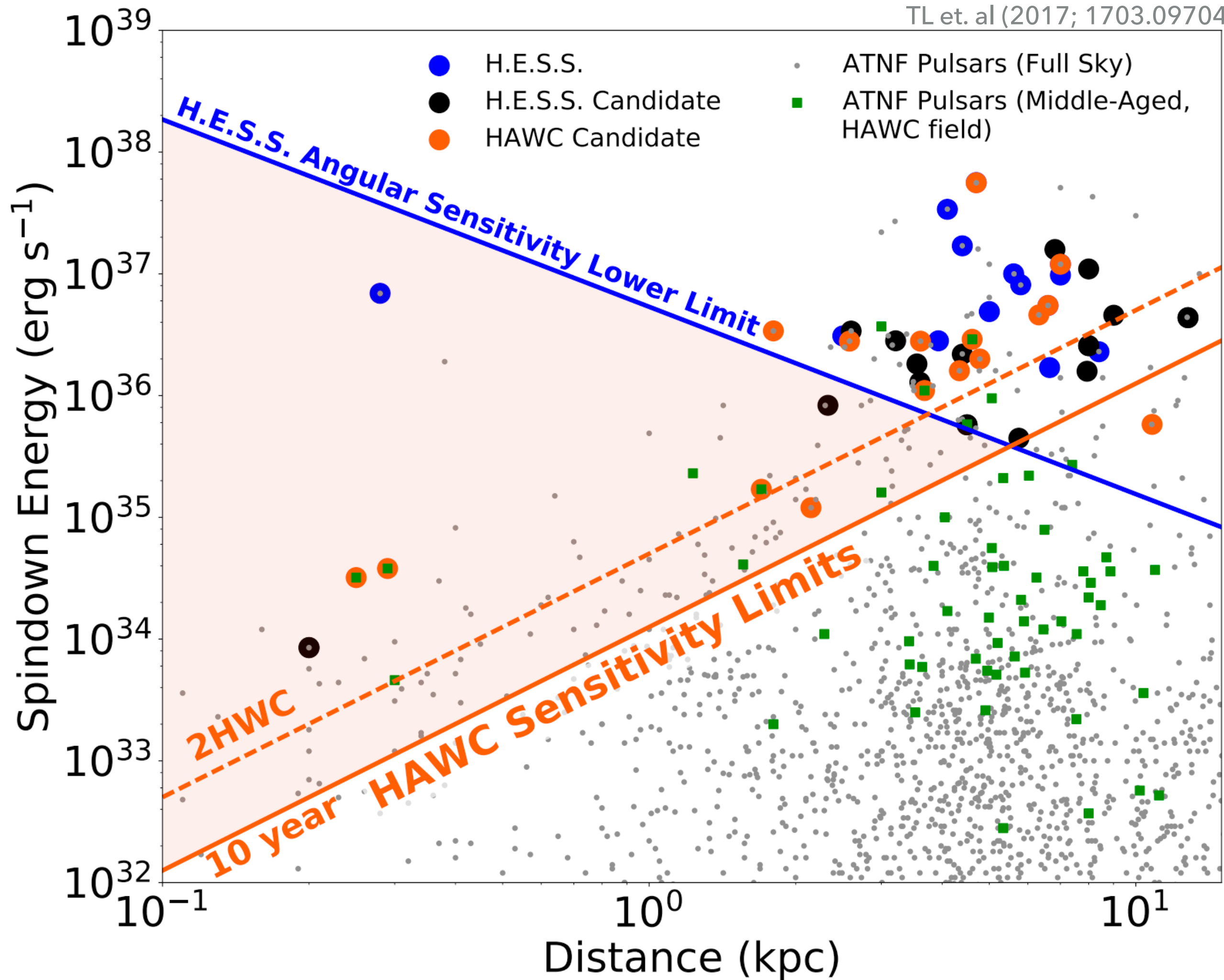
April 10, 2018

ABSTRACT

We present the results of the most comprehensive survey of the Galactic plane in very high-energy (VHE) γ -rays, including a public release of Galactic sky maps, a catalog of VHE sources, and the discovery of 16 new sources of VHE γ -rays. The High Energy Spectroscopic System (H.E.S.S.) Galactic plane survey (HGPS) was a decade-long observation program carried out by the H.E.S.S. I array of Cherenkov telescopes in Namibia from 2004 to 2013. The observations amount to nearly 2700 h of quality-selected data, covering the Galactic plane at longitudes from $\ell = 250^\circ$ to 65° and latitudes $|b| \leq 3^\circ$. In addition to the unprecedented spatial coverage, the HGPS also features a relatively high angular resolution ($0.08^\circ \approx 5$ arcmin mean point spread function 68% containment radius), sensitivity ($\lesssim 1.5\%$ Crab flux for point-like sources), and energy range (0.2 to 100 TeV). We constructed a catalog of VHE γ -ray sources from the HGPS data set with a systematic procedure for both source detection and characterization of morphology and spectrum. We present this likelihood-based method in detail, including the introduction of a model component to account for unresolved, large-scale emission along the Galactic plane. In total, the resulting HGPS catalog contains 78 VHE sources, of which 14 are not reanalyzed here, for example, due to their complex morphology, namely shell-like sources and the Galactic center region. Where possible, we provide a firm identification of the VHE source or plausible associations with sources in other astronomical catalogs. We also studied







FIRST DETECTIONS!

[[Previous](#) | [Next](#) | [ADS](#)]

HAWC detection of TeV emission near PSR B0540+23

ATel #10941; *Colas Riviere (University of Maryland), Henrike Fleischhack (Michigan Technological University), Andres Sandoval (Universidad Nacional Autonoma de Mexico) on behalf of the HAWC collaboration*

on 9 Nov 2017; 23:11 UT

Credential Certification: Colas Riviere (riviere@umd.edu)

Subjects: Gamma Ray, TeV, VHE, Pulsar

[Tweet](#)

[Recommend 5](#)

The High Altitude Water Cherenkov (HAWC) collaboration reports the discovery of a new TeV gamma-ray source HAWC J0543+233. It was discovered in a search for extended sources of radius 0.5° in a dataset of 911 days (ranging from November 2014 to August 2017) with a test statistic value of 36 (6σ pre-trials), following the method presented in [Abeysekara et al. 2017, ApJ, 843, 40](#). The measured J2000.0 equatorial position is RA= 85.78° , Dec= 23.40° with a statistical uncertainty of 0.2° . HAWC J0543+233 was close to passing the selection criteria of the 2HWC catalog ([Abeysekara et al. 2017, ApJ, 843, 40](#), see [HAWC J0543+233 in 2HWC map](#)), which it now fulfills with the additional data.

HAWC J0543+233 is positionally coincident with the pulsar PSR B0540+23 ($\dot{E} = 4.1 \times 10^{34}$ erg s $^{-1}$, dist = 1.56 kpc, age = 253 kyr). It is the third low \dot{E} ot, middle-aged pulsar announced to be detected with a TeV halo, along with Geminga and B0656+14. It was predicted to be one of the next such detection by HAWC by [Linden et al., 2017, arXiv:1703.09704](#).

Using a simple source model consisting of a disk of radius 0.5° , the measured spectral index is -2.3 ± 0.2 and the differential flux at 7 TeV is $(7.9 \pm 2.3) \times 10^{-15}$ TeV $^{-1}$ cm $^{-2}$ s $^{-1}$. The errors are statistical only. Further morphological and spectral analysis as well as studies of the systematic uncertainty are ongoing.

[[Previous](#) | [Next](#) | [ADS](#)]

HAWC detection of TeV source HAWC J0635+070

ATel #12013; *Chad Brisbois (Michigan Technological University), Colas Riviere (University of Maryland), Henrike Fleischhack (Michigan Technological University), Andrew Smith (University of Maryland) on behalf of the HAWC collaboration*

on 6 Sep 2018; 14:47 UT

Credential Certification: Colas Riviere (riviere@umd.edu)

Subjects: Gamma Ray, TeV, VHE, Pulsar

[Tweet](#)

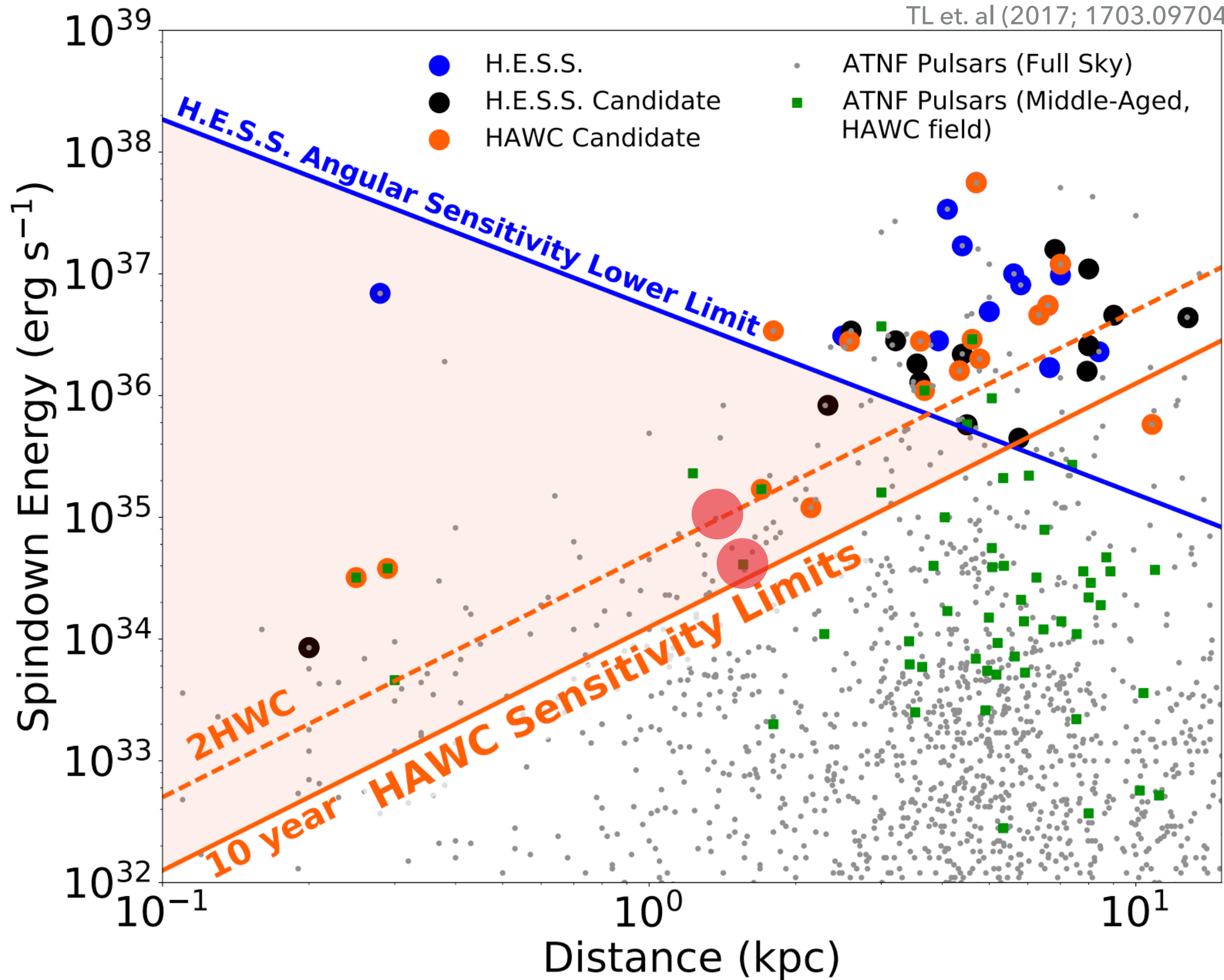
[Recommend 2](#)

The High Altitude Water Cherenkov (HAWC) collaboration reports the discovery of a new TeV gamma-ray source HAWC J0635+070. It was discovered in a search for extended sources covering 1128 days of HAWC observations with a test statistic value of 27 ($>5\sigma$ pre-trials), following the method presented in [\[Abeysekara et al. 2017, ApJ, 843, 40\]](#). Its significance in the 2HWC data set excluded it from being included in the catalog ($\sim 3.5\sigma$ pre-trials), but with the addition of ~ 600 more days of data it now satisfies that criterion. The best-fit J2000.0 equatorial position is RA= $98.71 \pm 0.20^\circ$, Dec= $7.00 \pm 0.22^\circ$, with a Gaussian 1-sigma extent of $0.65^\circ \pm 0.18^\circ$.

The spectral energy distribution is well-fit by a power law with spectral index -2.15 ± 0.17 . The differential flux at 10 TeV is $(8.6 \pm 3.2) \times 10^{-15}$ TeV $^{-1}$ cm $^{-2}$ s $^{-1}$. All errors are statistical only; further morphological and spectral analysis as well as studies of the systematic uncertainty are ongoing.

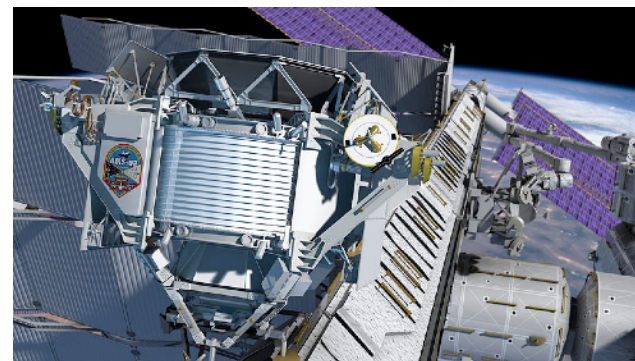
Given its spectrum and morphology, we believe HAWC J0635+070 may be the TeV halo of the pulsar PSR J0633+0632 ($\dot{E} = 1.2 \times 10^{35}$ erg s $^{-1}$, dist = 1.35 kpc, age = 59 kyr, unknown proper motion [[Manchester et al., 2005, AJ, 129](#)]). The gamma-ray spectrum and morphology is compatible with a "Geminga-like" TeV Halo [[Abeysekara et al. 2017, Science, 358, 911](#); [Linden et al., 2017, PRD, 96, 103016](#)]. We encourage follow-up observations at other wavelengths.

- **HAWC has detected two additional TeV halos**
- **Total Count:**
 - **Middle-Aged: 6**
 - **Younger: 13**



**Implication III: The positron excess is
due to pulsar activity**

Positron fraction



10^{-1}

1

10

10^2

positron, electron energy [GeV]

- AMS
- △ FERMI
- PAMELA
- AMS-01
- HEAT
- ▼ CAPRICE98
- ▲ CAPRICE94
- TS93

PULSARS PRODUCE THE POSITRON EXCESS

- **What were the uncertainties in pulsar models?**

- **I: The e^+e^- production efficiency?**

Profumo (0812.4457); Malyshev et al. (0903.1310)

%. A quantitative discussion of plausible values for f_{e^\pm} was recently given in Ref. [38]. We shall not review their discussion here, but Ref. [38] argues (see in particular their very informative App. B and C) that in the context of a standard model for the pulsar wind nebulae, a reasonable range for f_{e^\pm} falls between 1% and 30%.

- **II: The e^+e^- spectrum.**

- **III: The propagation of e^+e^- to Earth.**

PULSARS PRODUCE THE POSITRON EXCESS

- **What were the uncertainties in pulsar models?**

- **I: The e^+e^- production efficiency?**

- **II: The e^+e^- spectrum.**

Hooper et al. (0810.1527)

part of their energy adiabatically because of the expansion of the wind. The energy spectrum injected by a single pulsar depends on the environmental parameters of the pulsar, but some attempts to calculate the average spectrum injected by a population of mature pulsars suggest that the spectrum may be relatively hard, having a slope of $\sim 1.5-1.6$ [18]. This spectrum, however, results from a complex interplay of individual pulsar spectra, of the spatial and age distributions of pulsars in the Galaxy, and on the assumption that the chief channel for pulsar spin down is magnetic dipole radiation. Due to the related uncertainties, variations from this injection spectra cannot be ruled out. Typically, one concentrates the attention on pulsars of age $\sim 10^5$ years because younger pulsars are likely to still

- **III: The propagation of e^+e^- to Earth.**

TEV HALOS ANSWER THE KEY QUESTIONS!

Name	Tested radius [$^{\circ}$]	Index	$F_7 \times 10^{15}$ [$\text{TeV}^{-1} \text{cm}^{-2} \text{s}^{-1}$]	TeVCat
2HWC J0631+169	-	-2.57 ± 0.15	6.7 ± 1.5	Geminga
”	2.0	-2.23 ± 0.08	48.7 ± 6.9	Geminga
2HWC J0635+180	-	-2.56 ± 0.16	6.5 ± 1.5	Geminga

- We assume a power-law electron injection spectrum with an exponential cutoff

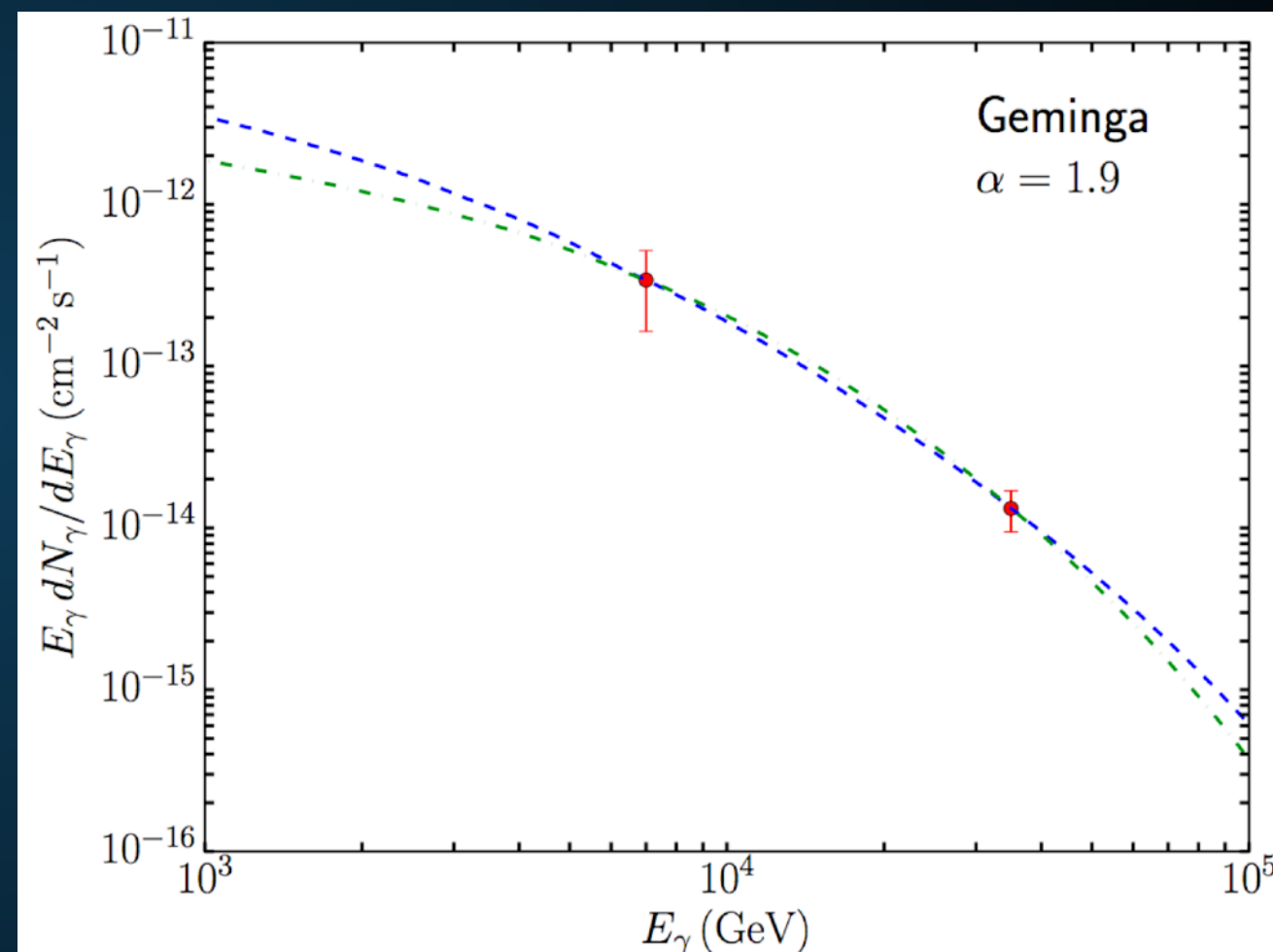
- Best Fit:

$$-1.9 < \alpha < -1.5$$

$$E_{\text{cut}} \cong 50 \text{ TeV}$$

$$\sim 3\text{--}9 \times 10^{33} \text{ erg s}^{-1} !$$

9-27% of the total pulsar spin-down power!



PULSARS PRODUCE THE POSITRON EXCESS

- **What were the uncertainties in pulsar models?**

- I: The e^+e^- production efficiency?

- II: The e^+e^- spectrum.

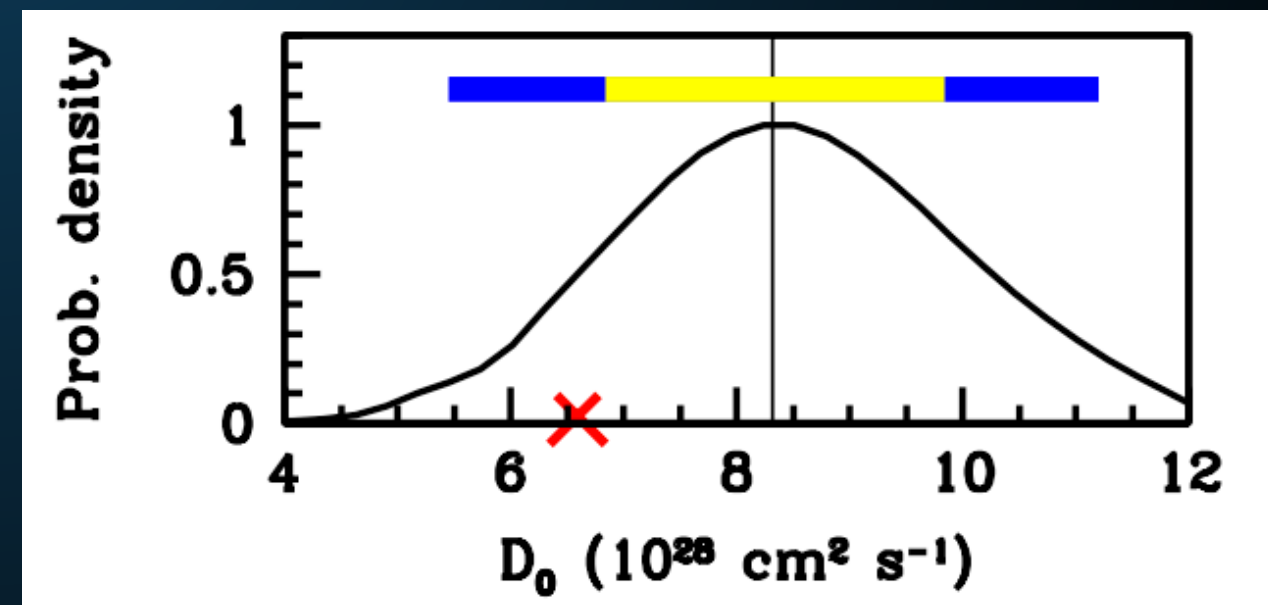
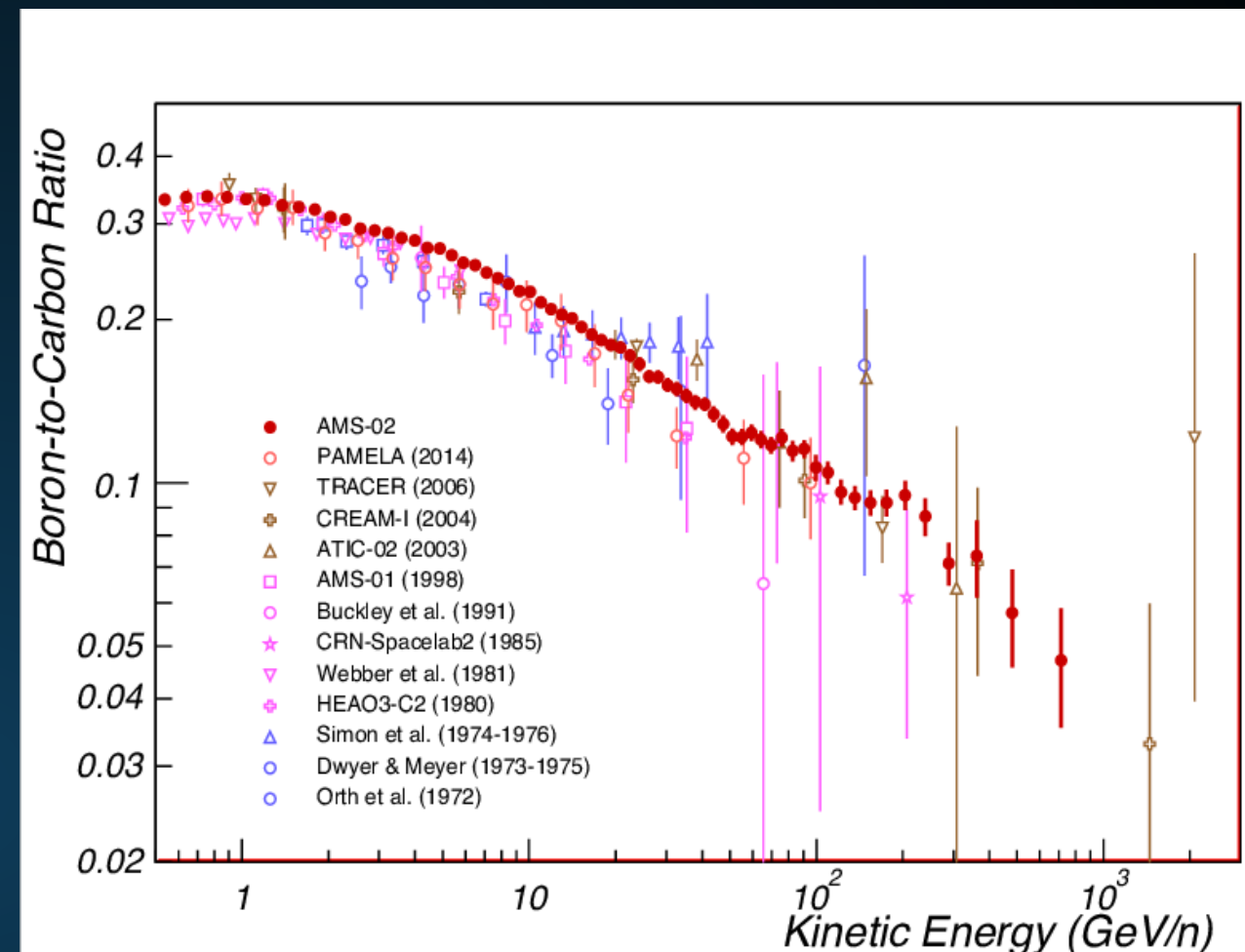
- III: The propagation of e^+e^- to Earth.

Malyshev et al. (0903.1310)

The observed spectrum on Earth of electrons and positrons injected by pulsars is also strongly dependent on propagation effects. In particular, the observed cutoff in the flux of electrons from a pulsar can be much smaller than the injection cutoff due to energy losses (“cooling”) during propagation. We define the cooling break, $E_{\text{br}}(t)$, as the maximal energy electrons can have after propagating for time t . Since – as stated above – the typical

Cosmic-ray propagation is the last key.

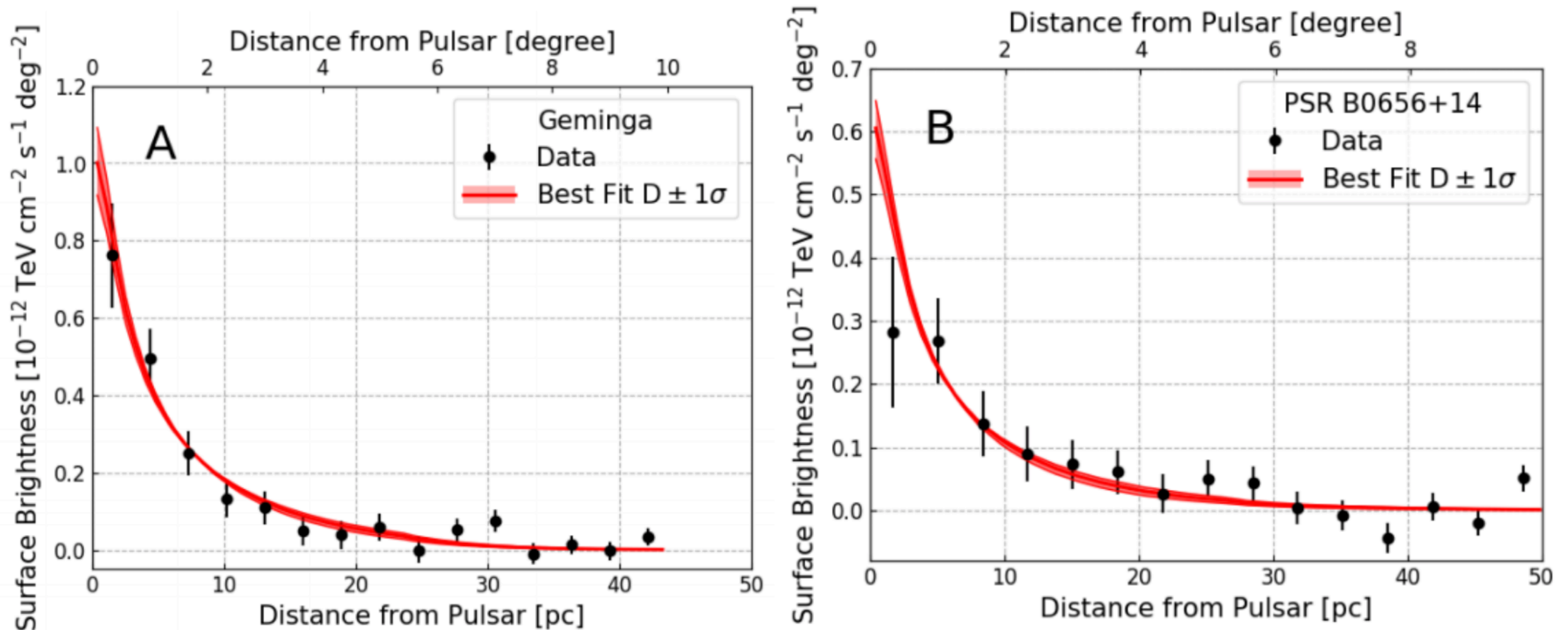
- **Cosmic-Ray primary to secondary ratios tell us about:**
 - **The average grammage encountered by cosmic-rays before they escape the galaxy (e.g. B/C)**
 - **The average time cosmic-rays propagate before they escape (eg. $^{10}\text{Be}/^9\text{Be}$).**
 - **Diffusion: $5 \times 10^{28} \text{ cm}^2 \text{ s}^{-1}$.**



Fool me once.... shame on, shame on you...

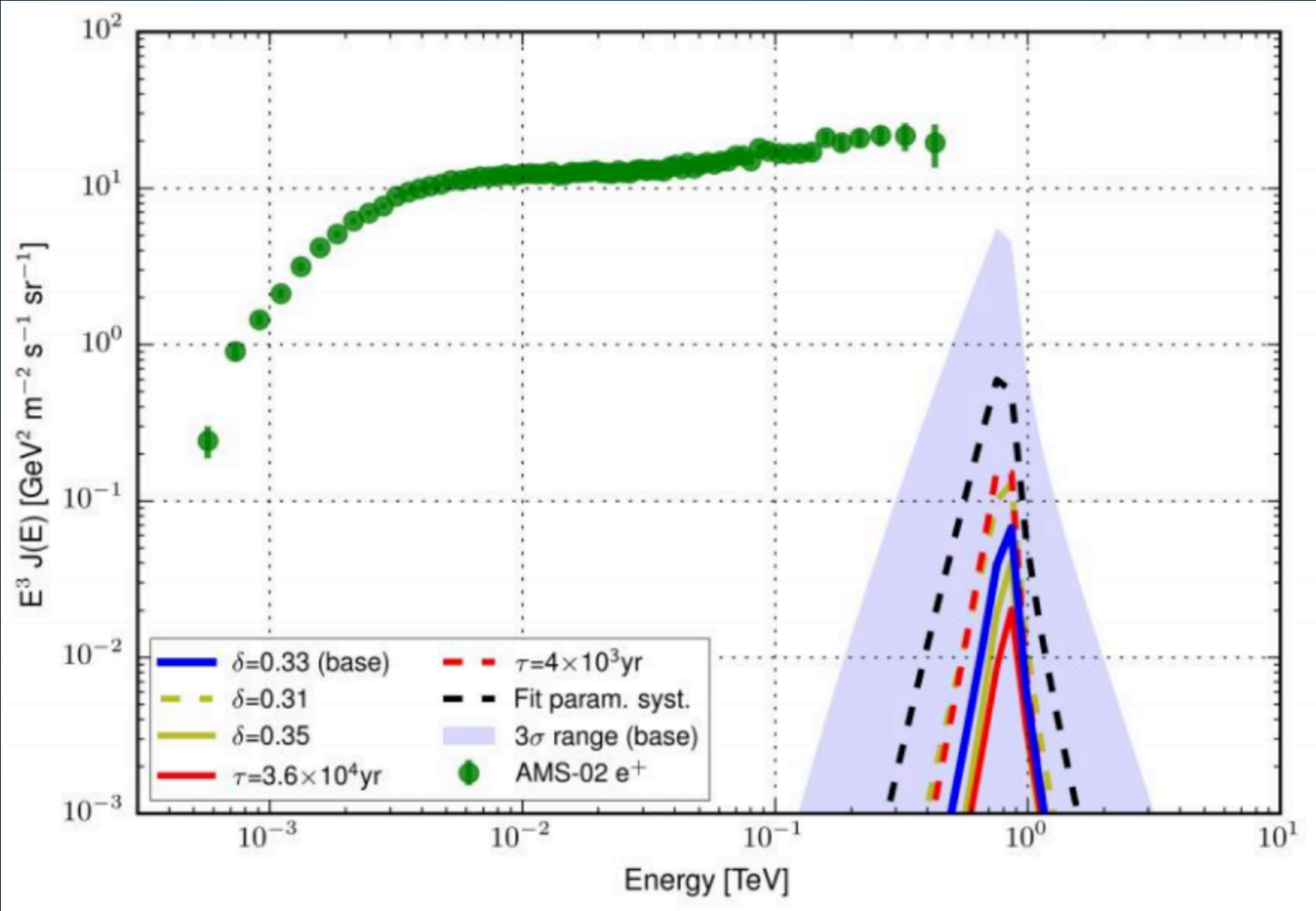
Fool me..... you can't get fooled again!

HAWC OBSERVATIONS

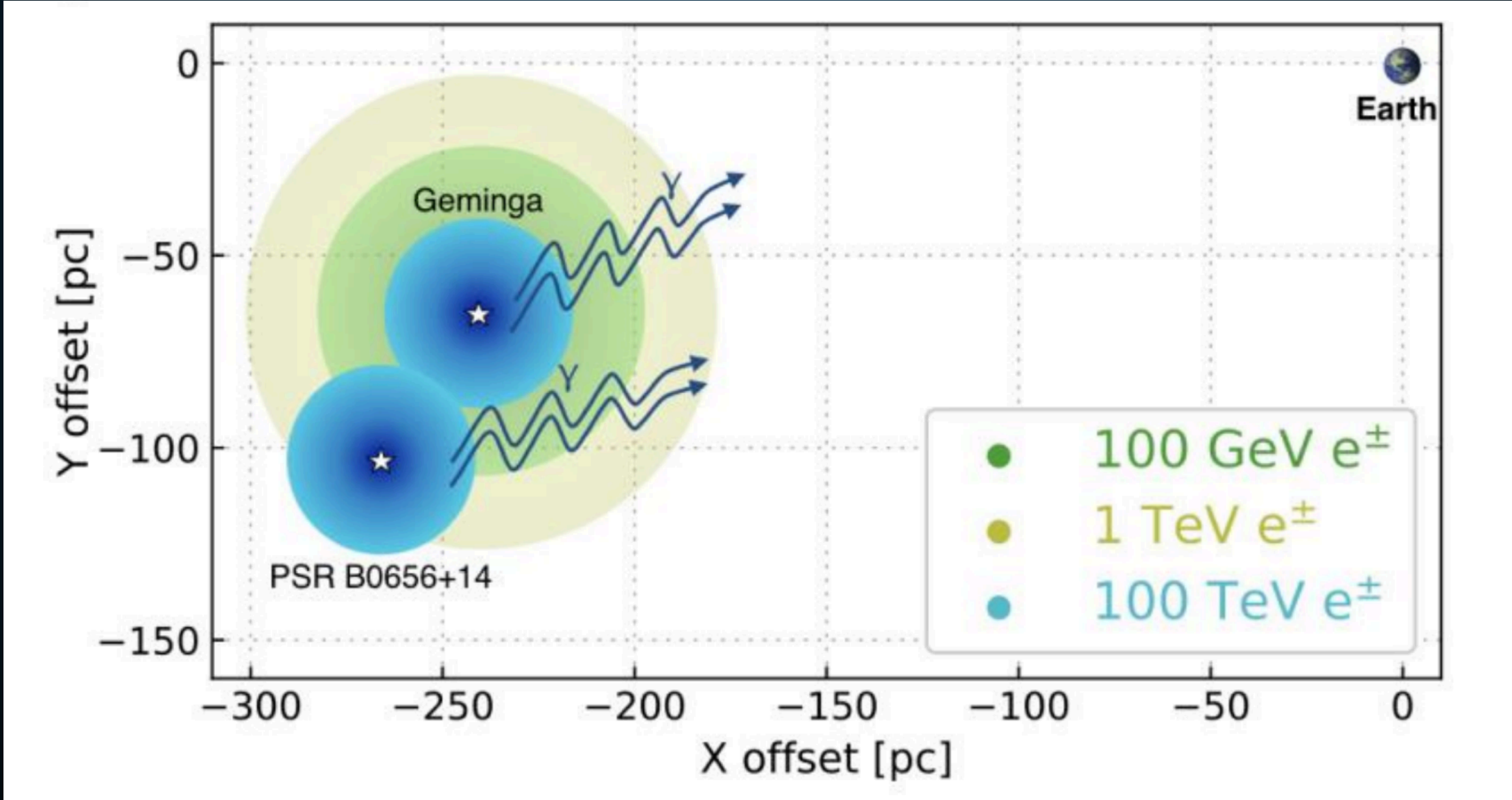


- Morphology of each pulsar fit by diffusion.
- Diffusion coefficient near the pulsar is quite small.

Pulsar Parameters		Geminga	PSR B0656+14
(Right ascension, declination) (J2000 source location)	[degrees]	(98.48, 17.77)	(104.95, 14.24)
τ_c (characteristic age)	[years]	342,000	110,000
D_{100} (Diffusion coefficient of 100TeV electrons from joint fit of two PWNe)	$[\times 10^{27} \text{ cm}^2/\text{sec}]$	4.5 ± 1.2	4.5 ± 1.2

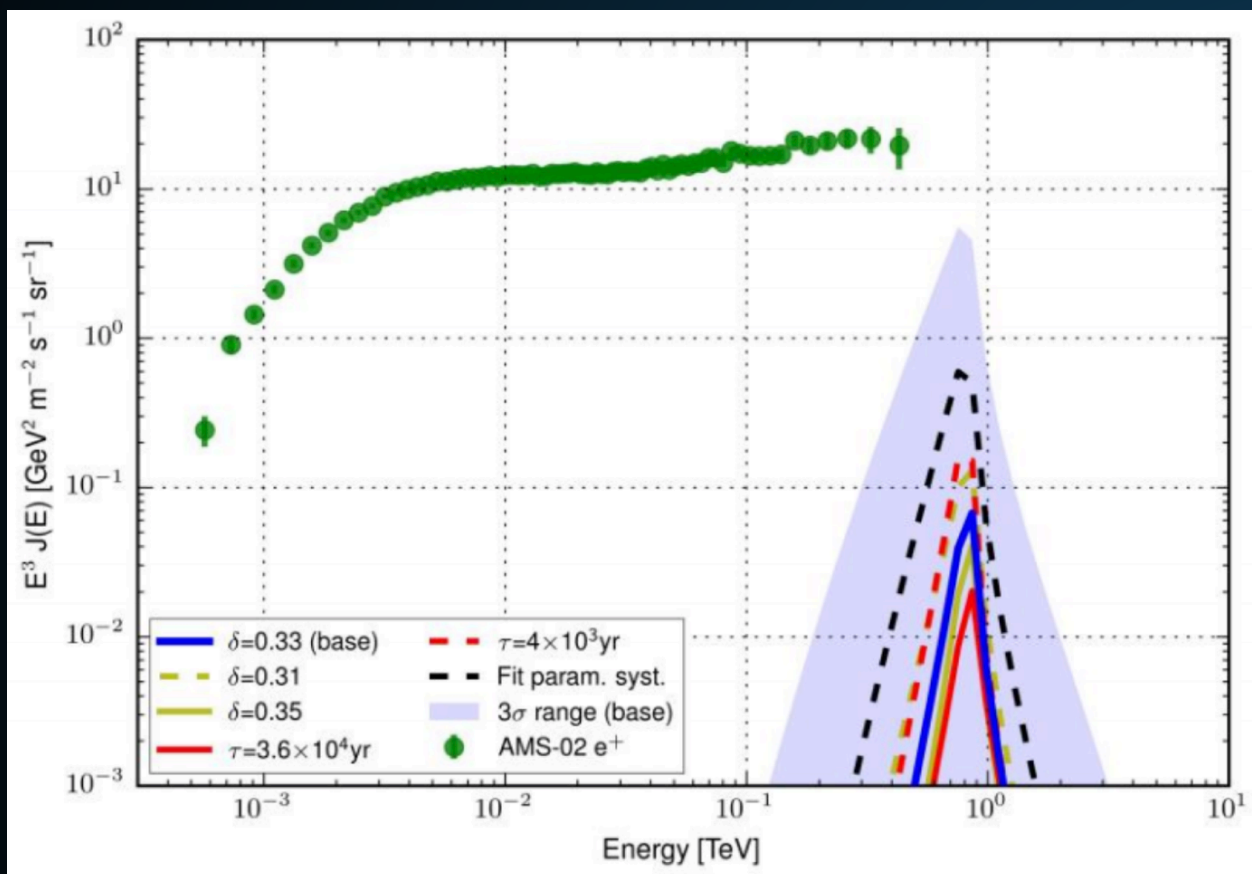


Pulsar Parameters		Geminga	PSR B0656+14
(Right ascension, declination) (J2000 source location)	[degrees]	(98.48, 17.77)	(104.95, 14.24)
τ_c (characteristic age)	[years]	342,000	110,000
D_{100} (Diffusion coefficient of 100TeV electrons from joint fit of two PWNe)	$[\times 10^{27} \text{ cm}^2/\text{sec}]$	4.5 ± 1.2	4.5 ± 1.2



TWO POSSIBLE ASSUMPTIONS

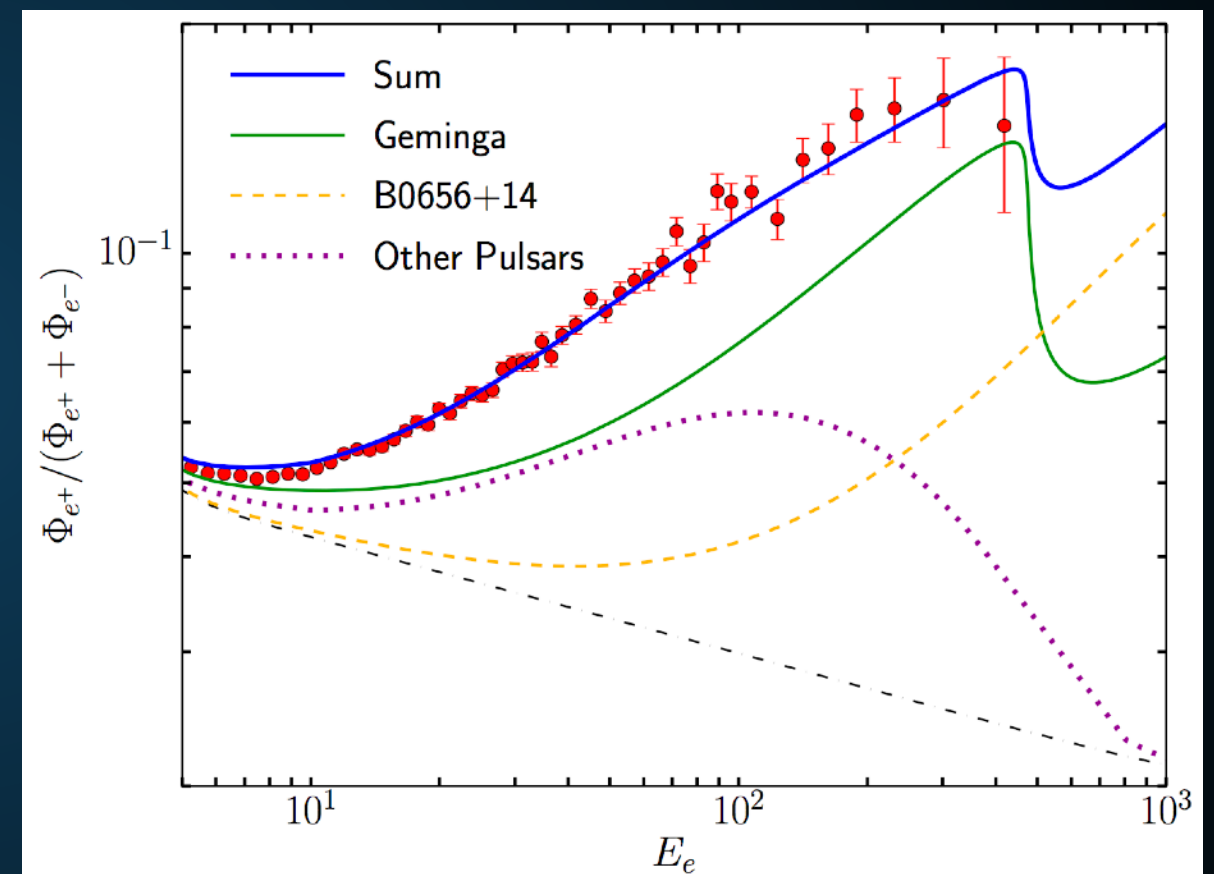
Extrapolate Low-Diffusion Constant
UP to Earth:



100 GeV positrons do not make it to
Earth

HAWC Collaboration (Science; 1711.06223)

Extrapolate the High Diffusion
Constant DOWN to Earth:



100 GeV positrons do make it to Earth

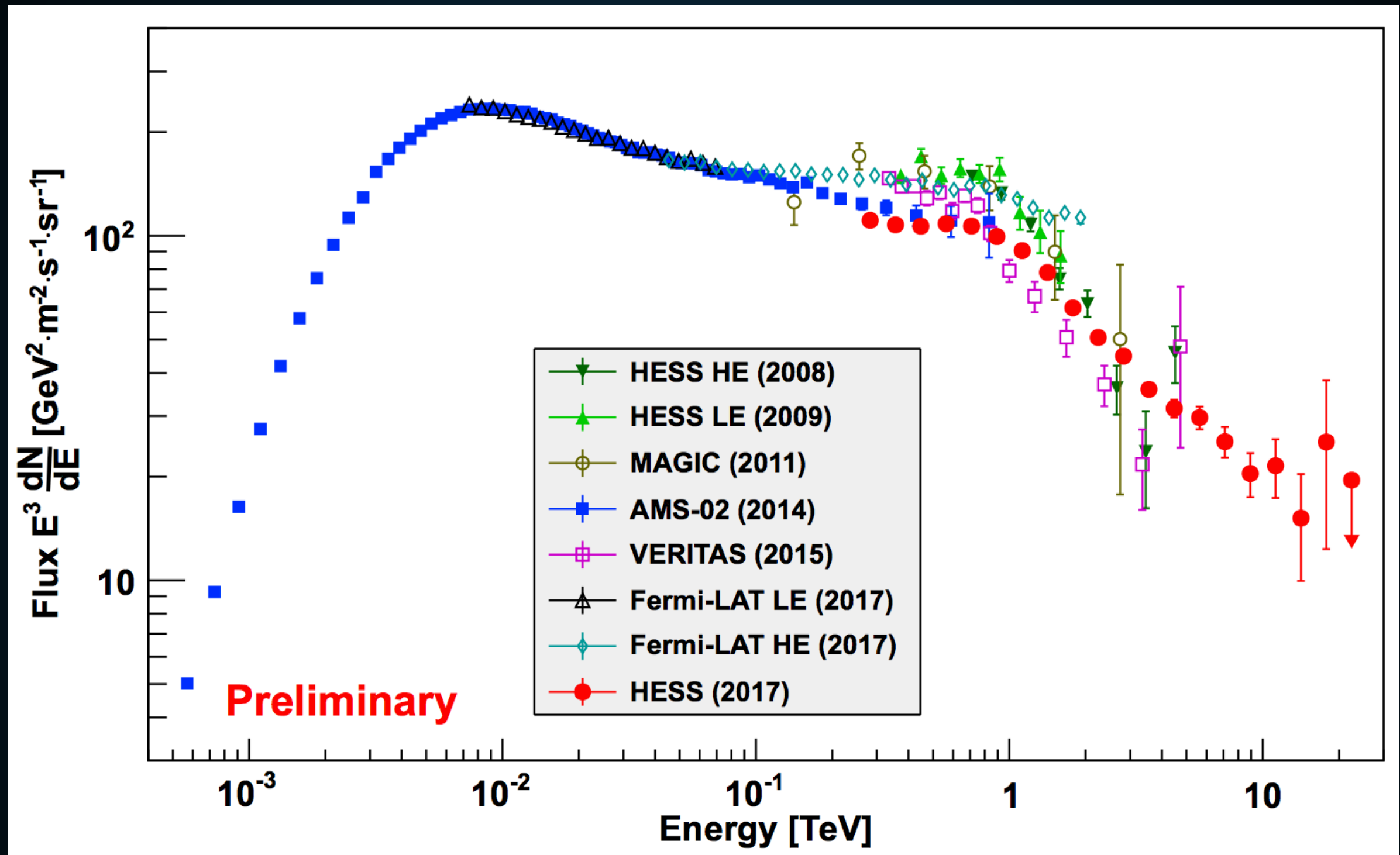
Hooper et al. (1702.08436)

Profumo et al. (1803.09731)

Fang et al. (1803.02640)

CAN THE LOCAL DIFFUSION CONSTANT BE LOW?

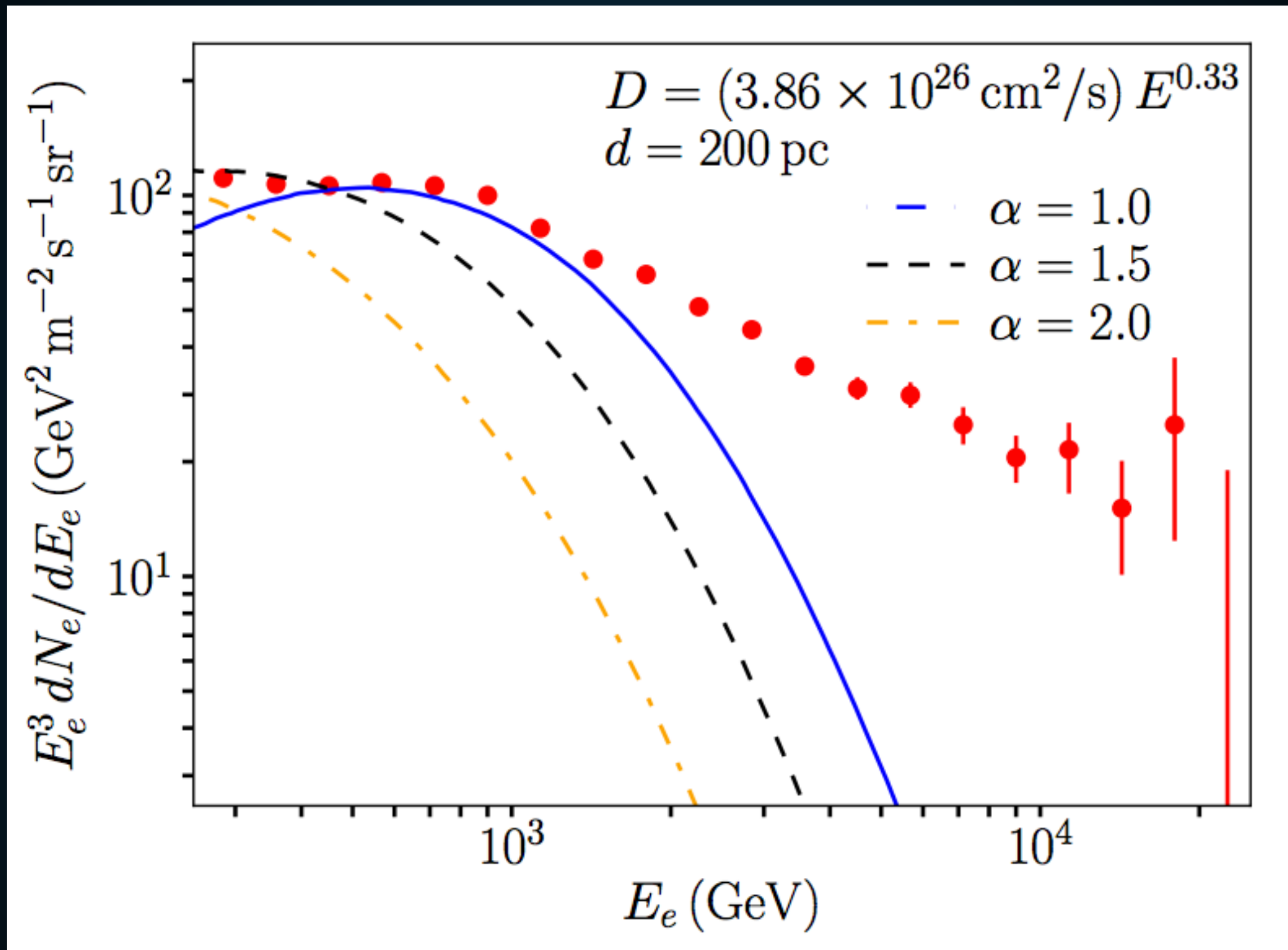
Hooper & Linden (1711.07482)



- Recently the HESS telescope detected 20 TeV electrons near Earth.

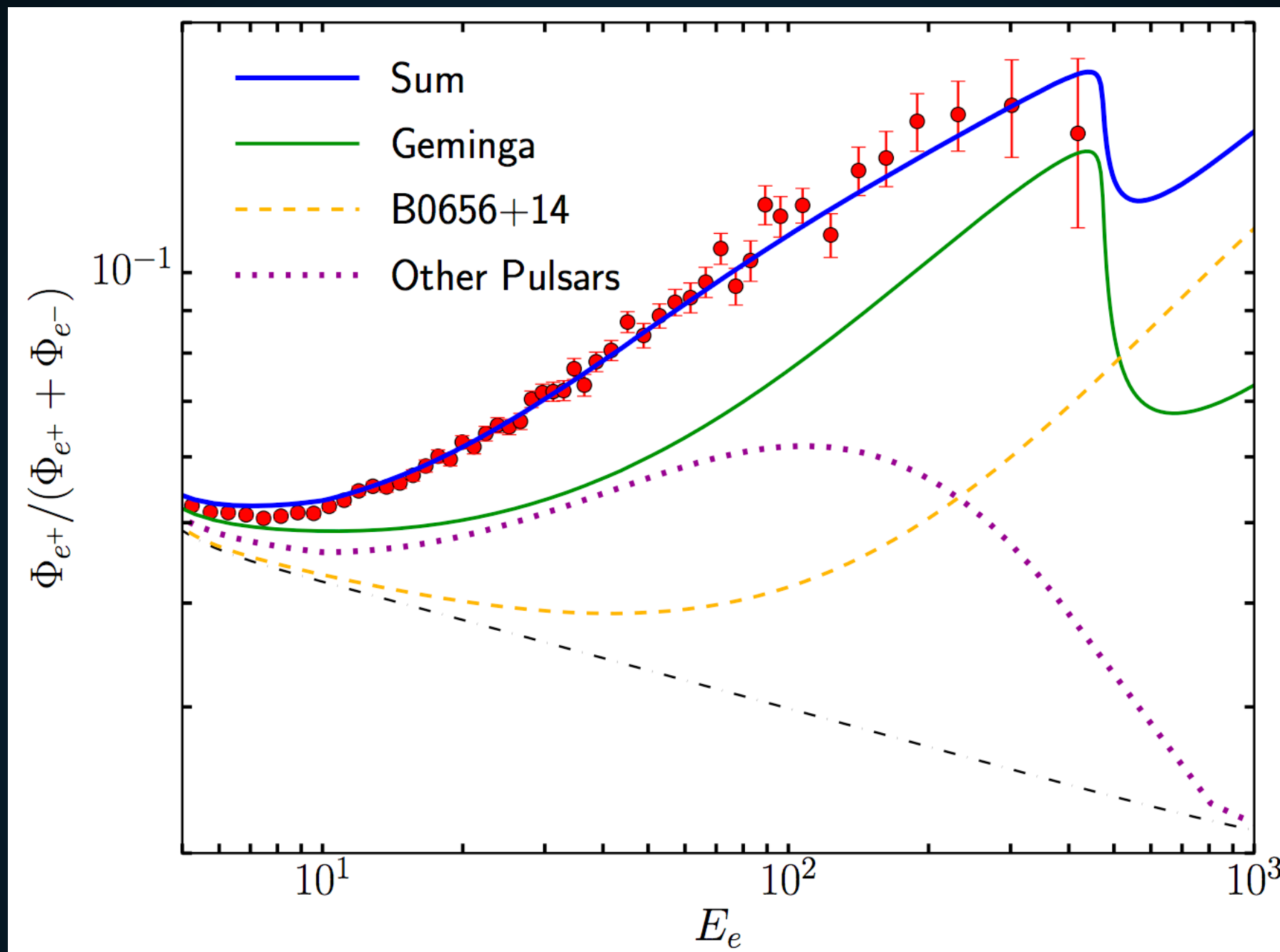
CAN THE LOCAL DIFFUSION CONSTANT BE LOW?

Hooper & Linden (1711.07482)



- If diffusion near Earth is low, then there is no source for these particles.

THE POSITRON FRACTION FROM TEV HALOS



- Reasonable models can be exactly fit to the excess.

***Braking index slightly changed to fit model to data.**

ASSUMPTIONS

TeV Gamma-Ray Luminosity Roughly Proportional to Spindown Power

= Pulsars explain the Milagro TeV Excess

+ High Energy
electrons trapped in
TeV halos

= HAWC Sources
are TeV halos

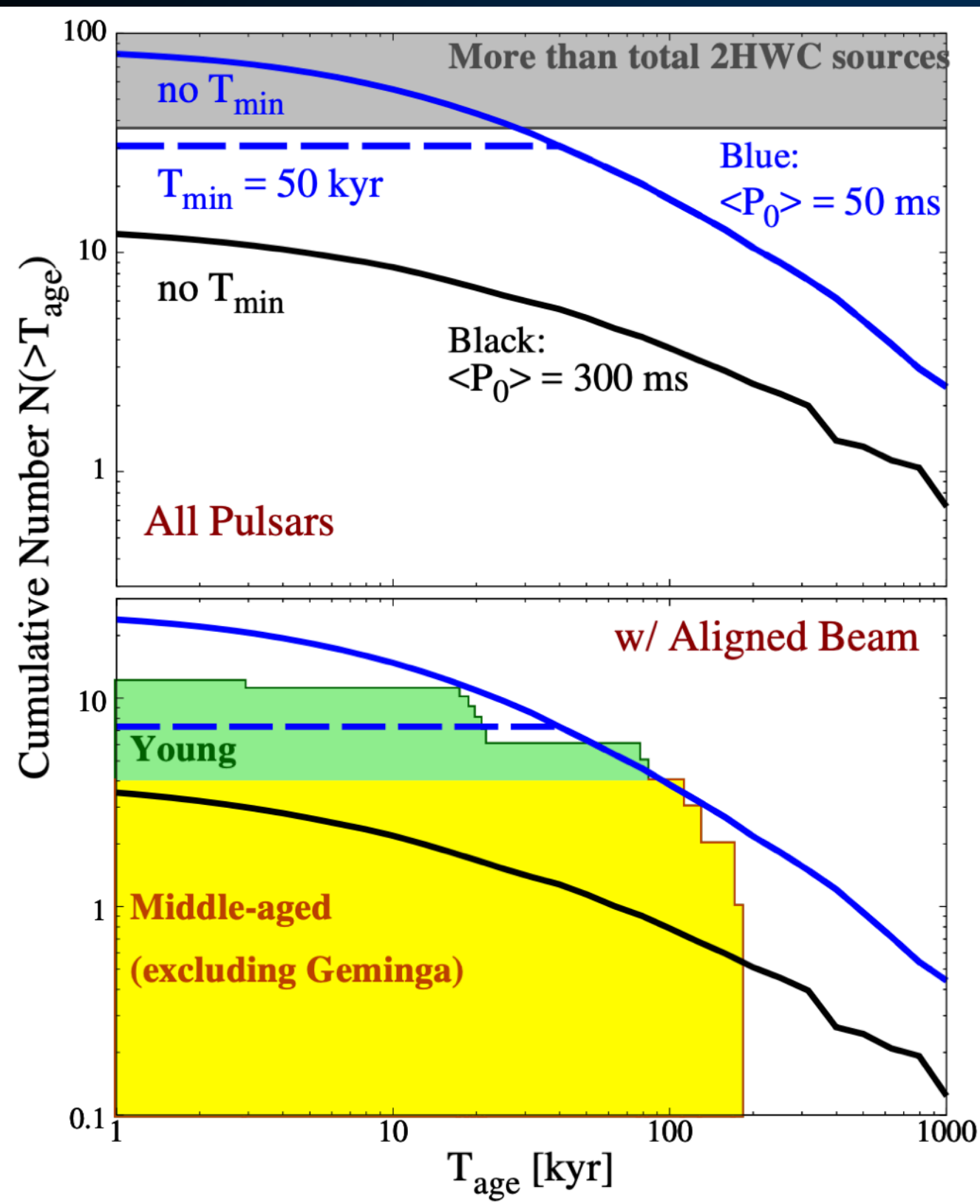
+ Low energy
electrons escape
from TeV halos

= Pulsars explain
the positron excess

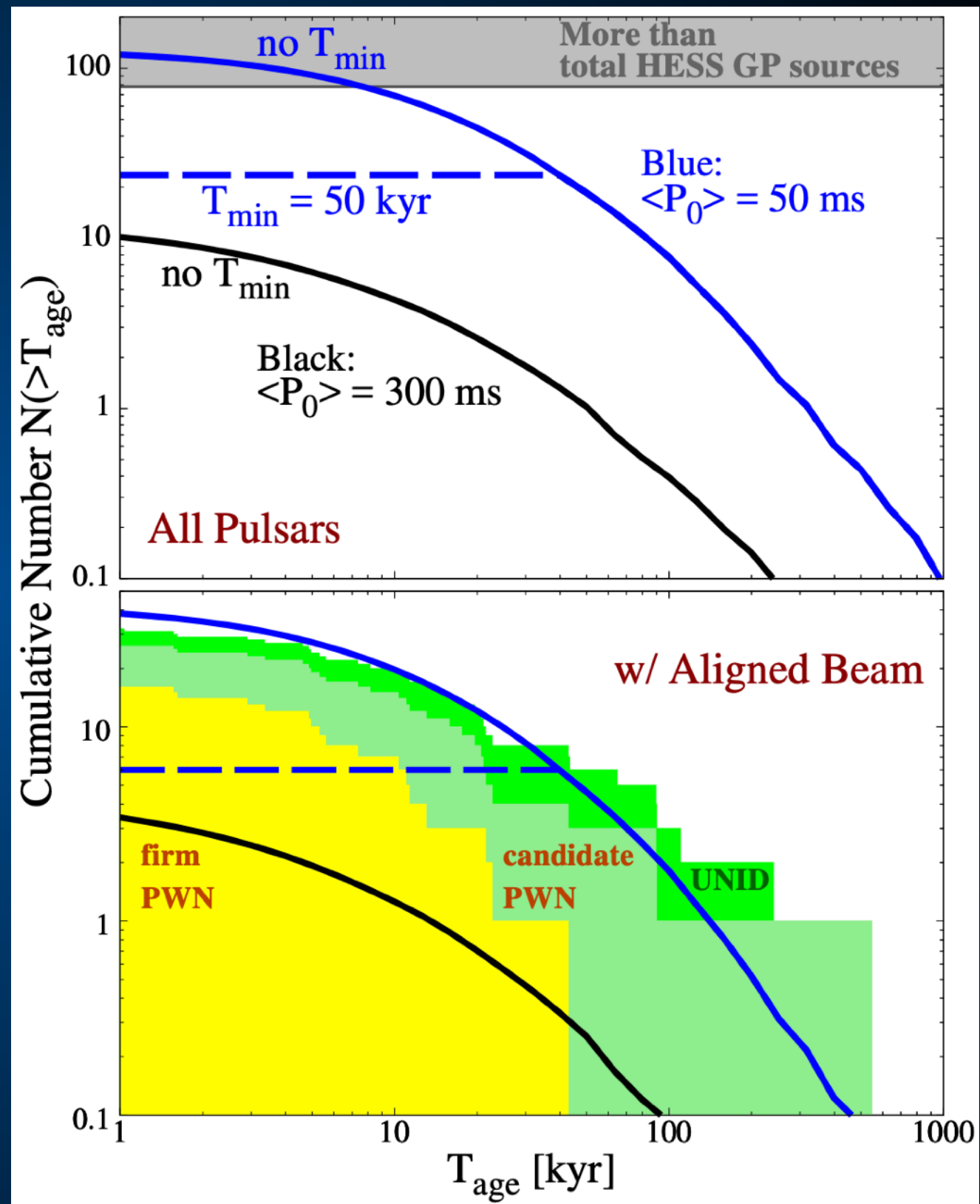


Understanding Pulsars

Sudoh, TL, Beacom (TBS)



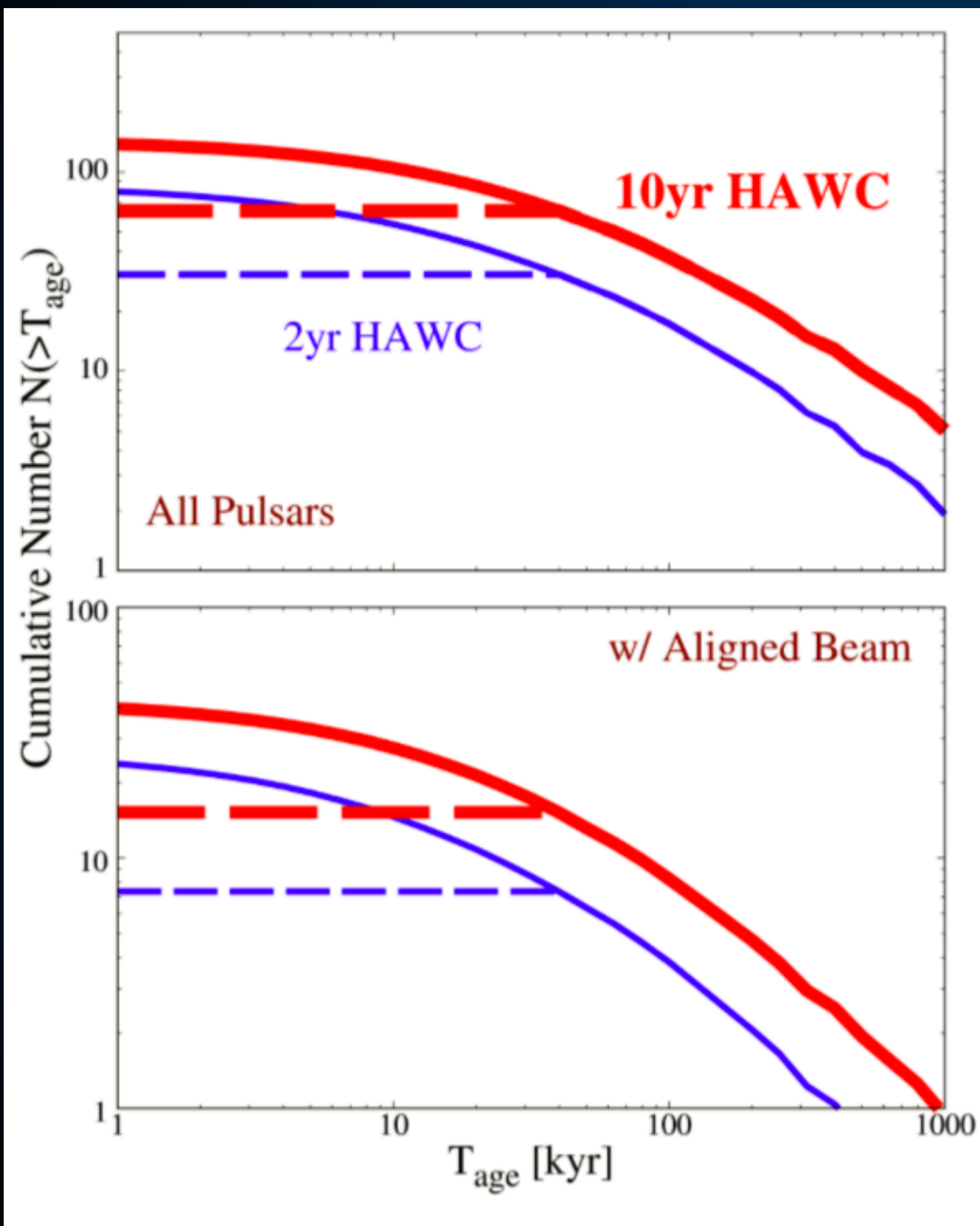
HAWC



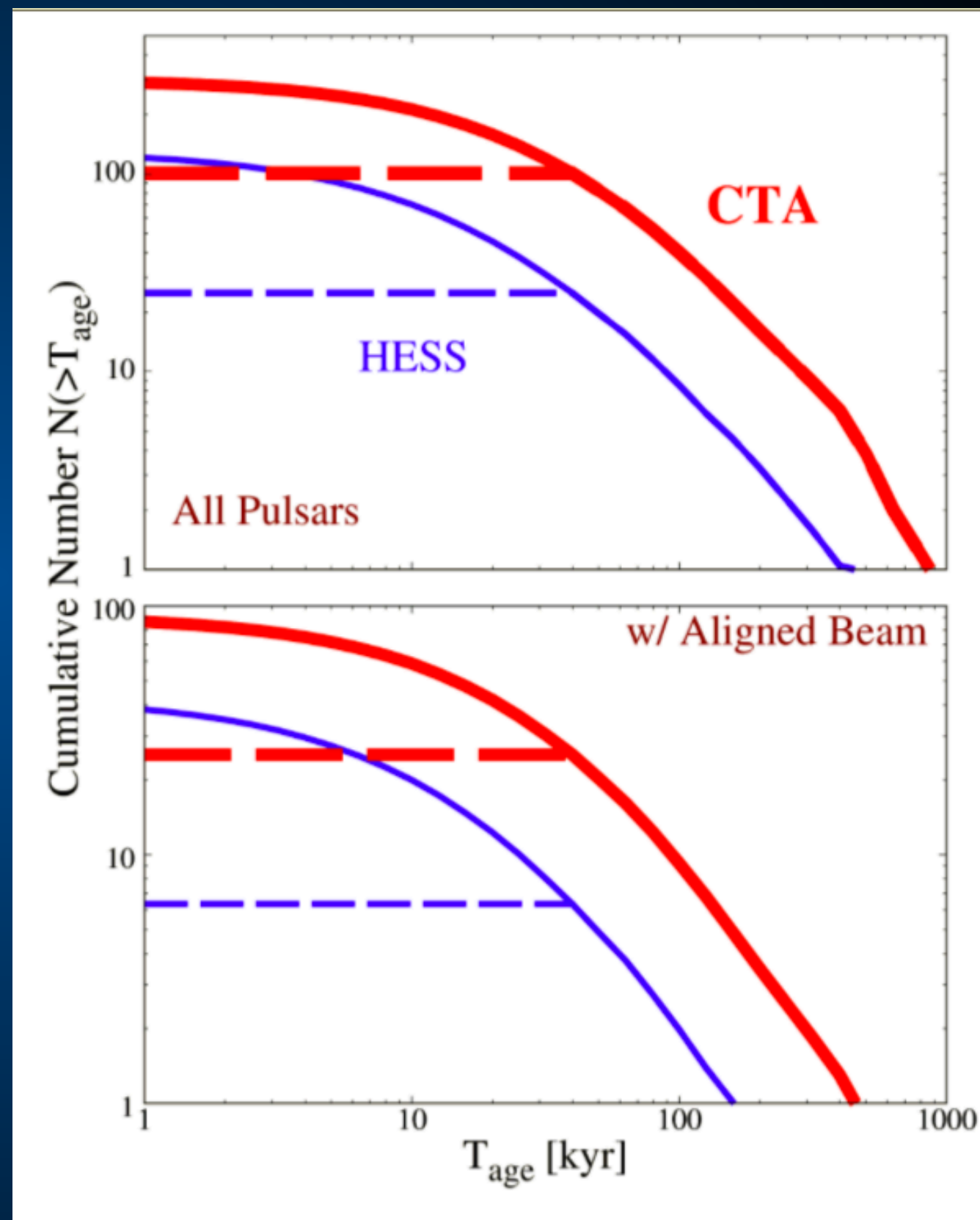
HESS

Detecting New Pulsars

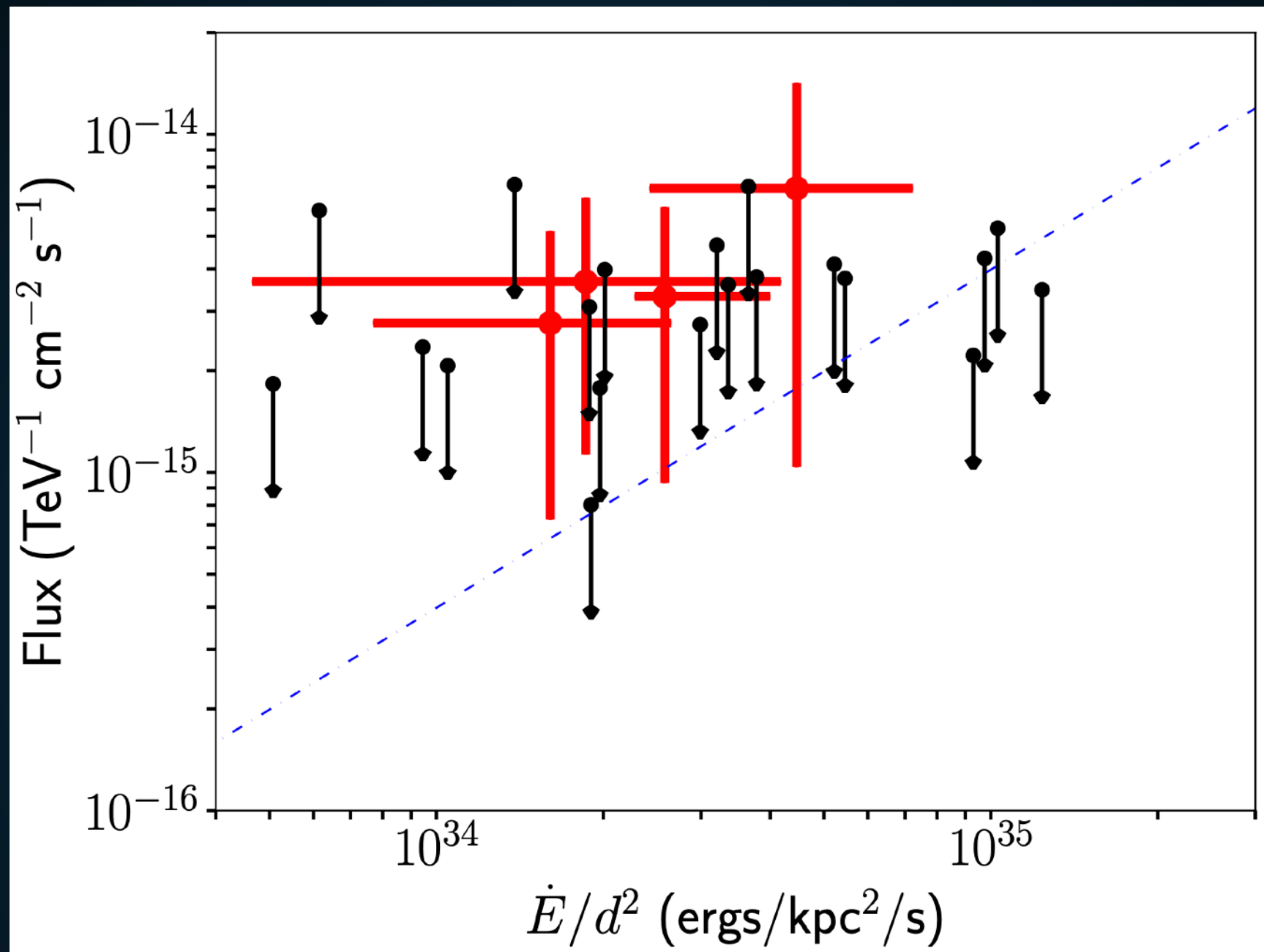
Sudoh, TL, Beacom (TBS)



HAWC (10 yr)

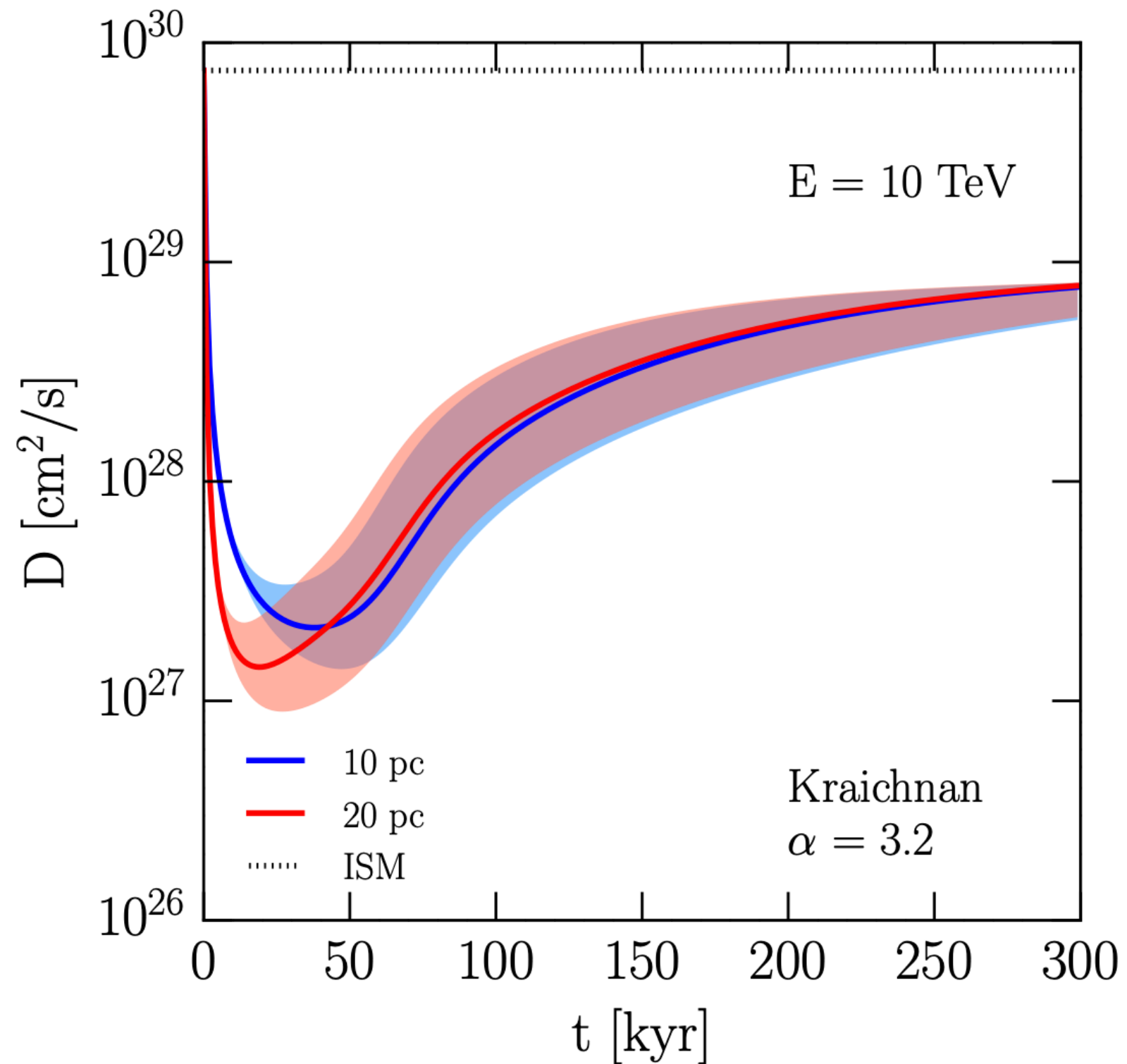


HESS/CTA



- Early evidence that millisecond pulsars also produce TeV halos.
- New opportunities to understand binary evolution.

- **First models that explain low diffusion constant.**
- **New opportunities to understand galactic magnetic fields.**



- Should observe coincident synchrotron Halo
- Possible Detection! (G327-1.1)

	Region	Area (arcsec ²)	Cts (1000)	N _H (10 ²² cm ⁻²)	Photon Index	Amplitude (10 ⁻⁴)	kT (keV)	τ (10 ¹² s cm ⁻³)	Norm. (10 ⁻³)	F ₁ (10 ⁻¹²)	F ₂	Red. χ^2
1	Compact Source	84.657	6.34	1.93 ^{+0.08} _{-0.08}	1.61 ^{+0.08} _{-0.07}	1.05 ^{+0.11} _{-0.10}	0.45	...	0.80
2	Cometary PWN	971.22	7.75	1.93	1.62 ^{+0.08} _{-0.07}	1.47 ^{+0.16} _{-0.14}	1.09
3	Trail East	537.42	2.13	1.93	1.84 ^{+0.12} _{-0.12}	0.44 ^{+0.07} _{-0.06}	0.27
4	Trail West	766.56	3.12	1.93	1.80 ^{+0.11} _{-0.11}	0.61 ^{+0.09} _{-0.08}	0.39
5	Trail 1	424.45	1.98	1.93	1.76 ^{+0.12} _{-0.12}	0.39 ^{+0.05} _{-0.05}	0.26
6	Trail 2	588.19	2.13	1.93	1.95 ^{+0.11} _{-0.11}	0.49 ^{+0.07} _{-0.06}	0.28
7	Trail 3	994.92	2.99	1.93	2.09 ^{+0.10} _{-0.10}	0.78 ^{+0.09} _{-0.08}	0.42
8	Trail 4	839.48	2.38	1.93	2.28 ^{+0.12} _{-0.12}	0.74 ^{+0.09} _{-0.09}	0.37
9	Prong East	828.58	1.66	1.93	1.72 ^{+0.14} _{-0.14}	0.30 ^{+0.06} _{-0.05}	0.27
10	Prong West	971.22	2.06	1.93	1.85 ^{+0.14} _{-0.14}	0.44 ^{+0.08} _{-0.07}	1.09
11	Diffuse PWN*	20007	27.7	1.93	2.11 ^{+0.04} _{-0.05}	6.91 ^{+0.37} _{-0.74}	0.23 ^{+0.14} _{-0.05}	0.21 ^{+0.88} _{-0.16}	6.0 ⁺¹⁶ _{-4.0}	3.68	17.7	0.82
12	Relic PWN*	26787	17.2	1.93	2.58 ^{+0.07} _{-0.10}	6.51 ^{+0.53} _{-0.71}	0.23	0.21	6.9 ⁺¹⁸ _{-5.5}	3.14	20.3	...

- New opportunities for studying TeV halo morphologies!

- **TeV observations open up a new window into understanding Milky Way pulsars.**
- **Early indications:**
 - **TeV halos produce most of the TeV sources observed by ACTs and HAWC**
 - **TeV halos dominate the diffuse TeV emission in our galaxy.**
 - **Positron Excess is due to pulsar activity**

- **Additional implications:**
 - **Young pulsar braking index**
 - **MSPs?**
 - **Galactic cosmic-ray diffusion**
 - **Source of IceCube neutrinos**
 - **TeV Dark Matter Constraints**